UNIVERSITÀ DEGLI STUDI DI PADOVA

UNIVERSITA' DEGLI STUDI DI PADOVA

Dipartimento di Ingegneria Industriale DII

Corso di Laurea Magistrale in Ingegneria Meccanica

Tesi di Laurea Magistrale

Commissioning of a test rig for the use of propane and experimental investigation of the internal heat transfer and pressure drop in a horizontal tube

Relatore: Prof. Ing. Davide Del Col (DII-Università di Padova)
Correlatori: Prof. Ing. Luke Andrea (TTK Universität Kassel)
Ing. Severin Skusa (TTK Universität Kassel)

Candidato: Riccardo Confente, Matricola 1058022

Anno Accademico 2014/2015

Sommario

Il presente lavoro, con tutte le prove sperimentali annesse, è stato sviluppato e realizzato presso l'Istituto di Termodinamica dell' Università di Kassel (Germania) nell'ambito del programma di scambio Erasmus dell'Università di Padova (Italia).
Per la liquefazione del gas naturale, sono impiegati dei circuiti frigoriferi in cascata ed il più grande miglioramento che si può effettuare in questi sistemi riguarda gli scambiatori di calore, in particolare si ha come obiettivi quello di migliorare lo scambio termico e allo stesso tempo di ridurre le perdite di carico.
Pertanto, si vuole andare ad analizzare lo scambio termico di diversi idrocarburi nelle varie fasi del sistema di refrigerazione a cascata utilizzando un nuovo modello di set-up sperimentale costruito presso la Facoltà di Termodinamica dell' Università di Kassel. L'obiettivo principale di questo lavoro, riguarda l'indagine sperimentale dello scambio termico interno e delle perdite di carico in un tubo orizzontale (uno scambiatore di calore tubo in tubo) con propano come fluido di lavoro.
La struttura di questa tesi inizia dalla spiegazione dell' apparato sperimentale, focalizzandosi sui componenti e sui sensori installati nell' impianto. Successivamente, viene descritta la parte teorica e la riduzione sperimentale dei dati attraverso la spiegazione riguardo la costruzione dell' Excel file, fatta per capire quali metodi sono implementati nel file utili per il conseguimento dei risultati.
Prima di procedere con l' inizio degli esperimenti, in modo da riuscire a lavorare in sicurezza, si è proceduto a descrivere ed applicare una procedura riguardante il caricamento del propano nell' impianto e successivamente sono state effettuate delle prove di verifica riguardo eventuali perdite nel ciclo di lavoro.
Quindi, sono stati effettuati dei test riguardanti il sottoraffreddamento, il desurriscaldamento e la condensazione del propano con lo scopo di effettuare un confronto tra i risultati sperimentali e le correlazioni più rilevanti note in letteratura con l' obiettivo di valutare l'affidabilità e l' elaborazione dei dati ottenuti dai sensori dell' impianto. I test riguardanti il deflusso bifase includono la determinazione della tipologia di deflusso.
Al termine dell'analisi è possibile affermare che la riduzione dei dati da parte del file Excel è in grado di funzionare in modo corretto, chiaro e veloce e di offrire una buona interfaccia in questa fase di lavoro e soprattutto per le future fasi dell'esperimento.

Abstract

The present work, with all the practical tests needed, is developed and carried out at the Institute of Technical Thermodynamics of the University of Kassel (Germany) within the Erasmus exchange program of the University of Padua (Italy).
For the liquefaction of the natural gas, a cascade refrigeration systems are used and the biggest improvement on these systems is in the heat exchangers, in particular the targets are to enhance the heat transfer and at the same time to decrease the pressure drop. Therefore, the heat transfer of hydrocarbons in the various stages of the cascade is analyzed using a new experimental set-up model built from the Thermodynamics faculty of Kassel University.
The main focus on this commissioning is about the experimental investigation of the internal heat transfer and pressure drop in a horizontal tube (a tube shell heat exchanger) with propane as working fluid. The structure of this work starts from the experimental setup explanation, focusing on the components and sensors installed in the facility. Afterwards, the explanation of the theoretical part and data reduction with the description of the data reduction excel file are done in order to understand which methods are implemented for the results achievement.
At the beginning of the experiments a safety method about the propane filling in the facility is described and applied and the leakage tests are conducted in order to work in safety conditions.
Therefore the tests about liquid cooling , gas cooling and condensation of the propane are done with the purpose to do a comparison between the experimental results and the relevant correlations and the known literature with the aim to evaluate the reliability of the data and the reduction of it extracted from the sensors. The 2-phase tests include the determination of the 2-phase flow pattern.
At the conclusion of the analysis is possible to affirm that the data reduction excel file is able to work in the proper, clear and fast way and to offer a good interface in this stage of the project and also for the future steps of the experiment.

INDEX

Nomenclature

Latin Symbols

A, B, C	Constant of polynomial interpolation	[-]
C	General constant values	[-]
c_p	Isobaric heat capacity	$\left[\frac{W}{kg \cdot K}\right]$
D	Considered Diameter	$[m]$
f	Friction factor	$[-]$
G	Specific mass flow	$\left[\frac{kg}{s \cdot m^2}\right]$
L	Characteristic length	$[m]$
m, n	General coefficients for Nusselt correlation	$[-]$
$\dot{m}$	Mass flow	$\left[\frac{kg}{s}\right]$
p	Pressure	$[bar, mbar]$
P	Perimeter	$[m]$
q	Specific heat flow	$\left[\frac{W}{m^2}\right]$
Q	Heat	$[J]$
$\dot{Q}$	Heat flow	$[W]$
R	Thermal resistance	$\left[\frac{m^2 \cdot K}{W}\right]$
t	Temperature	$[°C]$
w	fluid speed	$\left[\frac{m}{s}\right]$
x	vapor quality	[-]
X	Martinelli parameter	[-]
z	General length	[-]

Greek Symbols

α	Heat Transfer Coefficient	$\left[\frac{\mathrm{W}}{\mathrm{m^2 \cdot K}}\right]$
β	Pitch angle of pipe	$[°]$
∂	Partial differential	[-]
Δ	General difference	[-]
ε	Void Fraction	[-]
λ	Thermal Conductivity	$\left[\frac{\mathrm{W}}{\mathrm{m \cdot K}}\right]$
μ	Dynamic Viscosity	$\left[\frac{\mathrm{Pa}}{\mathrm{s}}\right]$
ν	Specific volume	$\left[\frac{\mathrm{m^3}}{\mathrm{kg}}\right]$
ρ	Density	$\left[\frac{\mathrm{kg}}{\mathrm{m^3}}\right]$
Φ	Phase multiplicator	[-]

Subscripts

- Boundaries

in	Inlet
out	Outlet
$\mathrm{i-o}$	From inlet to outlet
int	Internal
ext	External
$1,2,3$	Reference numeration for measurement section
$1-3$	From first to third section

- Substance

g	Gas
G	Gas only
l	Liquid
L	Liquid only
th	Therminol
WF	Working fluid

- Others

fluid	Fluid reference

i, j	Cursors for sums
$loss$	Losses reference
$wall$	Wall reference

Dimensionless Numbers

Nu	Nusselt Number
Pr	Prandtl Number
Re	Reynolds Number

Abbreviations

$Corr$	Corrective
htc	Heat Transfer Coefficient
PT, RTD	Resistance temperature detector
TC	Thermocouple

1 Introduction

The European situation in terms of primary energy consumption, sees the natural gas as the second main energy resource with the $33{,}1\%$. In Italy natural gas plays an important role ($37{,}9\%$), since the electricity production is based on this resource. Even in nations where the resource consumption share is more balanced, like in Germany, natural gas is the second resource used with the $22{,}2\%$ (all energy shares from BP statistical review 2014 [1]). More than 85% of the German natural gas demand is covered by the foreign imports. In addition to the established transport of natural gas through pipelines, also the transporting of the natural gas by sea in LNG (liquefied natural gas) form is becoming increasingly important.

For LNG option, the natural gas is liquefied and transported as liquid to the destination, where a regasification plant introduces it to the gas-net. Pro of this technology is the difference in specific volume between the gas and liquid state that allows to transport 600 time more natural gas in liquefied form (LNG), the less dependency on the European gas market and in order to gather the gas in the period with less demand.

For the liquefaction of the natural gas, a cascade refrigeration systems are used. Therefore, the heat transfer of hydrocarbons in the various stages of the cascade is analyzed using a new experimental set-up model built from the Thermodynamics faculty of Kassel University.

For this, the single-phase and two-phase heat transfer for the forced convection of hydrocarbons (pure substances, mixtures and inert gases) is studied experimentally in a horizontal pipe.

Finally, the experimental results and the empirical correlations from the literature are compared.

The peculiarity of this facility is that it is run by a multiphase pump in order to use two different fluids as working fluids, one liquid and one gaseous, at the same time. Both liquid and gas phase are flowing in two different paths before entering in the test pipe and in this way it is possible to perform tests in these particular conditions. The final target of this test rig is to perform tests on an enhanced pipe with propane condensing inside it, but in order to perform the tests in the proper way the commissioning of the test facility has to be carried out.

Recapitulating, the first step of the project was to run the facility with isopropanol (liquid) and nitrogen (gas) and with the test section equipped with a $3/4$" pipe.
The second step (aim of this work) is to run the plant with propane.
The third step is to change the test pipe with a 1" pipe in order to check the consistency of the values recorded in this new configuration and it the case study at the present moment.
The fourth one is to substitute the pipe with an internal enhanced pipe of 1", which is the final goal of the project.
For safety reasons due to the risks of the fluids involved, the test system is built in a housing.
The present work, with all the practical tests needed, is developed at the Institute of Technical Thermodynamics of the University of Kassel (Germany) within the Erasmus exchange program of the University of Padua (Italy).

2 Experimental Setup

The aim of this chapter is to explain how the test rig is built and show the main components of the cycle in order to understand how the internal heat transfer coefficient is experimental calculated and how the test rig is built.

2.1 Facility description

The facility built by the Thermodynamic department of the Kassel University is representing by two principal parts:

- Primary cycle (which includes the test section)
- Secondary cycle

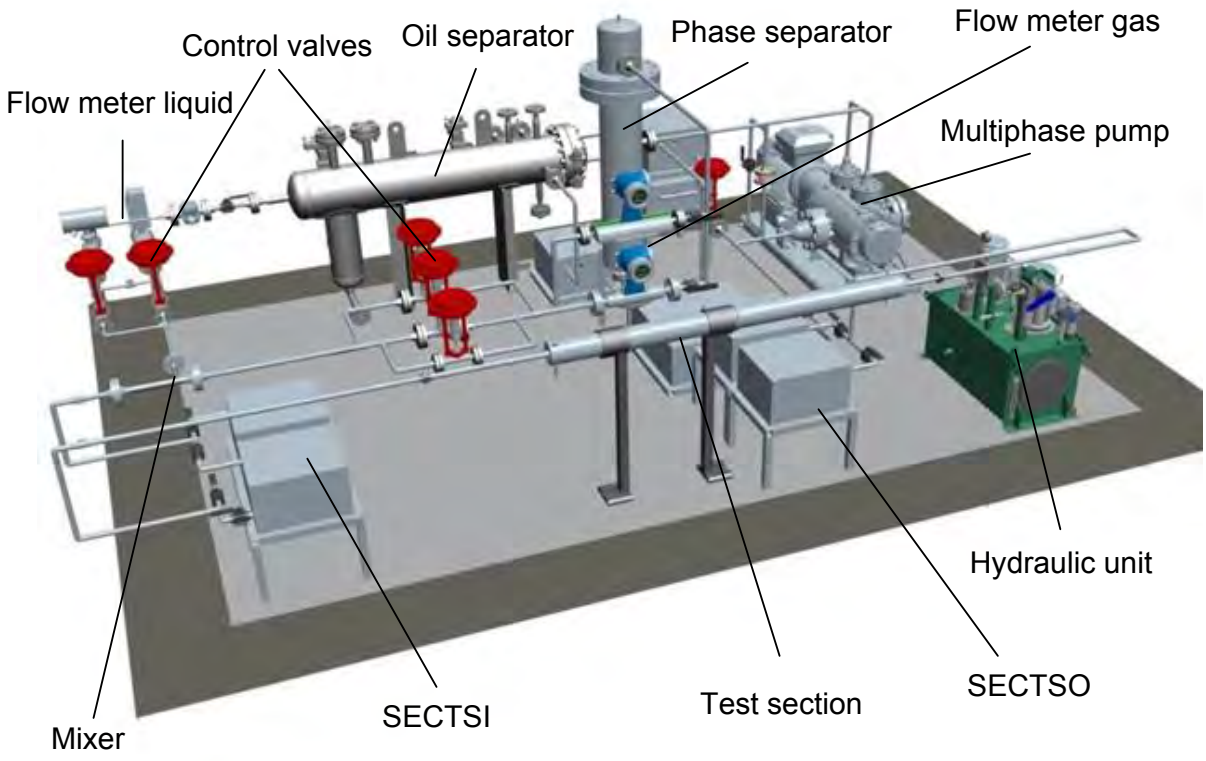

Figure 1: General view of the test rig [2]

Figure 2: Photo of the facility [2]

2.1.3 Primary cycle

Primary cycle is the main important part that leads the working fluid in different parts of the facility trough a multiphase pump (1). Here is installed is a screw pump that has the aims to set the pressure of the cycle and to prevail the pressure lost that the fluid come across in the different sections of the plant; to ensure that it works in a correct way, two conditions have to be evaluate:

1) The content of the gas fraction at the inlet of the pump has to be limited below than 94%; this content is deducible thanks to the flow meters installed in the primary cycle.
2) The pressure drop between suction and supply sections has to be lower than 10 bar to avoid mechanical stress and this difference is measured by two absolute pressure sensors AP1 and AP2.

The pump rotational range is between 400 rpm and 1500 rpm.

After this device, working fluid is leads into the droplet separator (2) that allow the separation between the liquid and gas phase with the aim to manage in two different lines, (liquid and gas line) liquid and gas flow like shown in Figure 3.

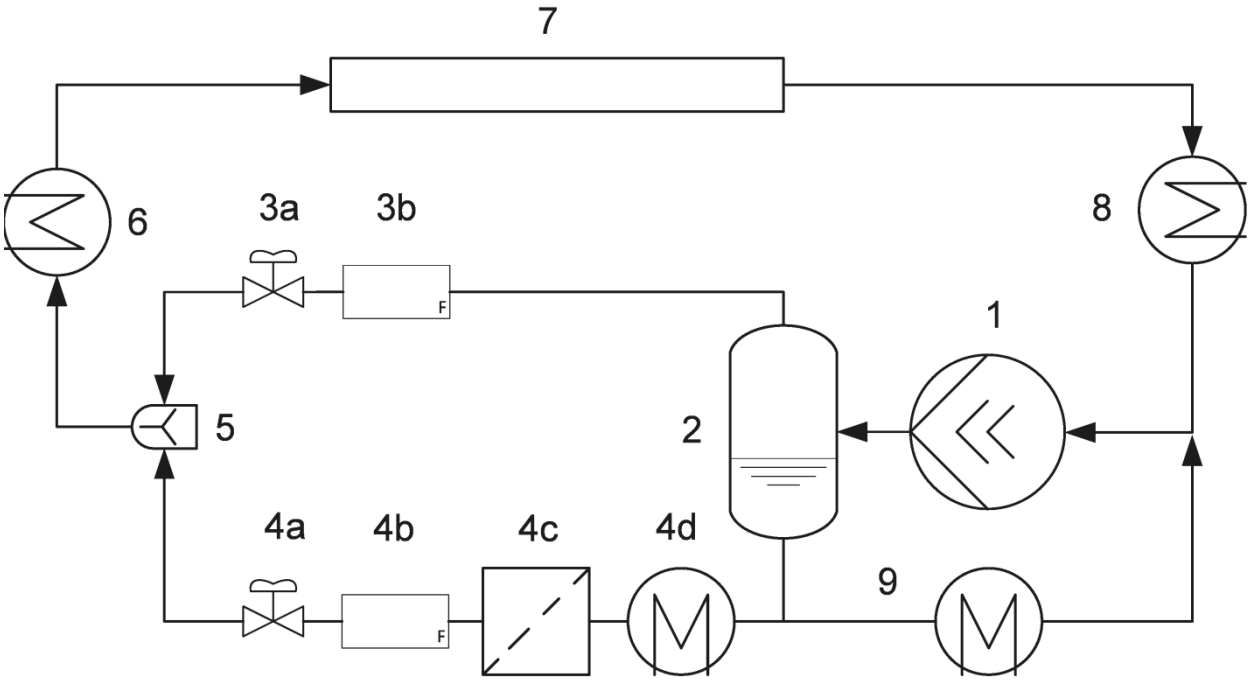

Figure 3: simplify view of the cycle

The liquid flow splits in two side, one side leads the liquid in the by-pass line, which is equipped with an heat exchanger that control the pressure in the separator (and therefore at the inlet of the test section) because it is in saturation conditions and a variation of temperature by the exchanger correspond to a variation of the pressure and this line has also the aim to preserve the integrity of the multiphase pump and the possibility to adjust the liquid mass flux in the test section with a valve (RV6).

The other side leads to the test section and carries the fluid to the Oil separator unit (*4c*) that provide to separate the oil from the liquid flow.

Oil is used as lubricant in the pump and also this process is important because the oil presence in the working fluid can influence the heat transfer measurements.

After the oil separator, the liquid goes in two parallel pipes connected with two Coriolis flow meters (4b) - (*Mass 2100-6 and Mass 2100-15*) able to measure mass flow in different (but partially overlapped) ranges. After these flow meters there are

two valves (4a) - (RV4, RV5) that allow a remote control of the mass flow from the LabVIEW software.
About gas line, this line start at the top of the droplet separator and after that the gas flow splits in 2 parallel pipes connected with two flow meters (3b) - (*Promass 83A04* and *Promass 83F25*) and through 3 parallel lines equipped with three needle valves (3c) - (*RV1*, *RV2* and *RV3*) with the same purpose of the previous.
The liquid and gas line are finally connect into a static mixer with the desired vapour quality.

2.1.4 Test section and SECTS

Test section (7) is the most important part of the facility and it is a horizontal tube-shell heat exchanger connected with a secondary cycle (SECTS).
Before to enter to the heat exchanger, pressure and inlet temperature of the working fluid are measured by an absolute pressure sensor (*AP5,6*) and a temperature sensor (*RTD12*, 119 millimetres upstream the pipe inlet).
In order not to disturb the working fluid flow inside the measurement sections in the test section there are no sensors.
The outlet temperature and the pressure loss are then measured after the exit of the test section with a second temperature sensor and a differential pressure sensor (*RTD15*, 32 centimeters downstream the pipe outlet and *DP01* between inlet and outlet).
In the test section there are 3 measurement sections; the first section is locate after 780 millimetres from the inlet, the second at a distance 1900 millimetres and the third at the distance of 3020 millimetres.
Each measurement section is equipped with 8 thermocouple (*TC1-24*) glued in grooves, 0,5x0,5 millimeter large and 30 millimeter long, collocated around the external wall of the pipe with a distance of 45 degrees one from the other as shown in Figure 4:

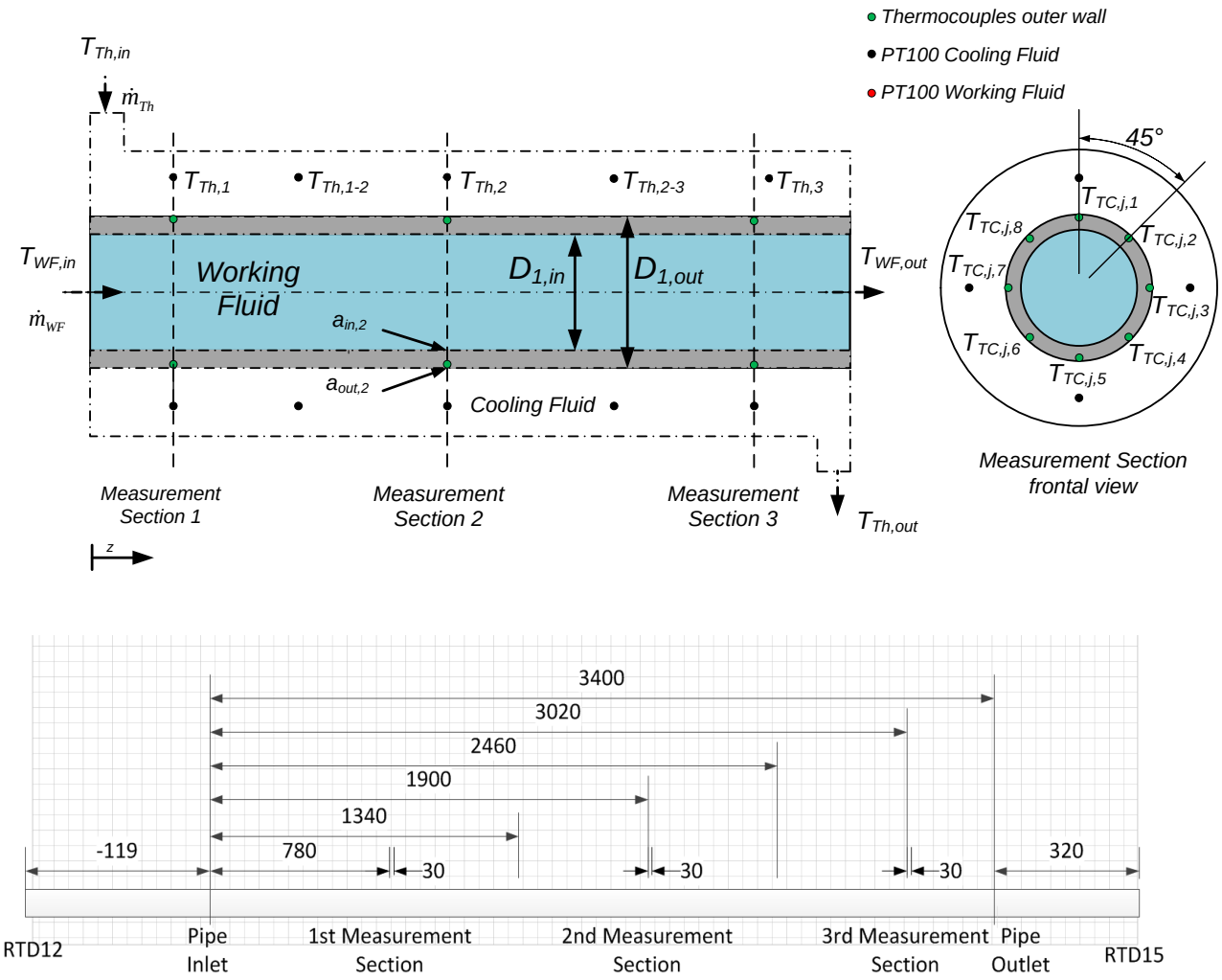

Figure 4: Schematic view of the longitudinal and cross-section in the test section [3]

In the other side of the exchanger, Test section cycle (SECTS) is the secondary cycle coupled with this one.

This cycle is equipped with therminol as secondary fluid and the set-temperature of it is controlled by the Huber machine 635 W

The secondary working fluid flows in direct-flow to the primary working fluid but is possible to change the flow pattern of the fluid as counter-flow. Before entering the heat exchanger, inlet temperature of the secondary working fluid is measured by the temperature sensor *RTD13*. The working fluid is led to flow homogeneously in the ring cross-section.

Along the outer pipe there are five measurement sections consisting of four temperature sensors for each section (*RTD24 (1-4) - 26(1-4)*) at a distance of 90 degrees along the circumference. The sensors are installed in the outer pipe and positioned in the middle of the therminol flow. These measurement sections allow getting the value of the secondary fluid along the tube and this configuration is important in order to calculate the local heat transfer coefficient (eq. 3.35).
Finally, downstream the test rig the outlet temperature is measured by the temperature sensor RTD14 and return pipe connects the outlet of the test section with the cooling machine closing the cycle.

2.1.5 Secondary Cycles

Secondary cycles are mainly composed of a heating machine, a pump, a heat exchanger and a thermostat that controls the temperature of the secondary fluid in order to manage the temperature of the working fluid inside the primary cycle.
In total three Cycles are installed:

- Test Section Inlet Cycle (*SECTSI*), placed before the entrance of the test section, provides heat to the working fluid in order to rise the inlet temperature, especially to provide overheated gas for the test. In two phase applications it can be used to control the gas quality of the working fluid
- Test Section Cycle (*SECTS*)
- Test Section Outlet Cycle (*SECTSO*) is connected to a heat exchanger downstream the test section used to complete the condensation in phase transition tests and is connected to one of the two heat exchangers in the bypass with aim to set the pressure upstream the test section by means of a pressure change in the separator.

2.2 Sensors characteristic

There are a lot of kinds of sensor installed in the facility and is important to describe the principal characteristic of them in order to have a better general overview.

Basically the test rig is equipped with 3 types of sensors and all of the needed sensors to calculate the htc are presented in this part:

1. Temperature sensors
2. Pressure sensors
3. Flow sensors

Each sensor is connected to a multiplexer in order to transduce the signal from the test by the measurement computer to significant value visible thanks to the LabVIEW software.

2.2.3 Temperature sensors

There are 2 kind of temperature sensors installed in the test rig:

- TC (thermocouple): these thermocouples are constituted with Chromel and Alumel alloys. The main characteristic of them is that are adapted to work in oxidant environment and with a high range of temperature; furthermore, these are active sensors, so they do not need electrical alimentation.
  The sensible part of the sensor is covered with concentric layers; the outer one is Inconel and the inner one is Magnesium oxide and since that the thermocouples are placed and glued in grooves, for the calculation of htc, a wall correction have to be done to take into account this fact.
- RTD (resistance temperature detector): these sensors are PT100, or rather a platinum electrical resistance that measures 100 Ohm at a temperature of 0 °C.
  They work in a more limited range of temperature in comparison with Thermocouple but have a more linear behavior which allows them to be calibrated easily.
  Contrary to what explained before for the TC, these are passive sensors, so they need electrical alimentation.

2.2.4 Pressure sensors

There are 2 kind of pressure sensors installed in the test rig with different aims:

- Absolute pressure transducer: this sensor are used obviously for the pressure measurements in the test rig but is very important at the inlet of the test section in order to understand and calculate the fluids property with these conditions of temperature and pressure.
  Furthermore it is used to ensure the orderly functioning and integrity of the multiphase pump.
- Differential pressure transducer: this sensor has the aim to analyze the pressure drop during the test section in order to get the right fluid property and therefore to extract a reliable heat transfer coefficient value.

Here installed are strain gauges pressure sensors, a diaphragm in contact with the fluid which is deformed by the pressure and the deformation can be measured by strain gauged element.

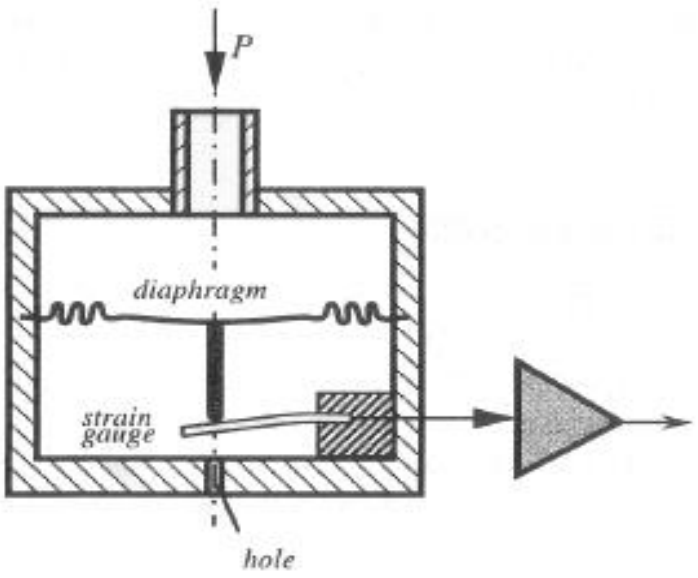

Figure 5: Schematic view of the sensor working principle [4]

2.2.5 Flow sensors

There are two types of flow meters in the test rig: Coriolis and Rotameter flow sensors.

- Coriolis sensors: These sensors are an inertial flow meter that measures directly the mass flow through the variation of the angular momentum induced in the fluid by the sensor. These sensors are used to measure the gas and liquid mass flow in the divided phase segment of the rig.

- Rotameter sensors: this is a variable area meter and is used here to measure the bypass flow; it is equipped with conic shape weight inside the sensor that is pushed up by the pressure of the flow and pulled down by gravity. The position at the equilibrium defines the volumetric flow in the pipe.

Figure 6: Schematic view of the sensor. 1) tube 2) conic shape weight [4]

Table 2.1: Data sheets of the sensors involved in the measurement [3]

SENSOR	RANGE MIN	RANGE MAX	UNIT	ACCURACY
TC			°C	$\pm$ 0,1 °C of m.v.
RTD			°C	$\pm$ 0,05 °C of m.v.
AP1	0	30	bar	$\pm$ 0,2 % of e. v
AP2	0	100	bar	$\pm$ 0,2 % of e. v
AP5,6	5	85	bar	$\pm$ 0,106 % of e. v.
DP01	0	1000	mbar	$\pm$ 0,040 % of e. v
Promass 83A04	0	90	kg/h	$\pm$ 0,1 % m.v. off 22,5 kg/h
Promass 83F25	0	3600	kg/h	$\pm$ 0,1 % m.v. off 540 kg/h
Mass2100-6	0	563,2	kg/h	$\pm$ 0,05 % m.v. off 30 kg/h
Mass2100-15	0	2914	kg/h	$\pm$ 0,05 % m.v off 80 kg/h
Mass Flux Cooling B	0	10000	kg/h	$\pm$ 0,1 % m.v. off 105 kg/h
Rotameter	0	5,5	m³ / h	$\pm$ 1,6 % m.v. off 3,065 m^3/h

2.3 Safety system

First of all, it´ s indispensable to do a foreword about the propane; EN 378-1:2005 (CEN/TC 182) offers a classification about the property and the safety for the most important fluids used in in the thermodynamics field.

PROPANE – R290

Table 2: Property of the propane [5]

Formula	Safety group	LFL [kg/m^3]	ODP	GWP (100 years)
CH3CH2CH3	A3	0,038	0	3

- Safety group: the first letter concern to a toxicity index; the applicability range vary between A (best case) and B (worst case).
  The second number concern to a flammability index; the applicability range vary between 1 (best case) to 3 (worst case).
- LFL (lower flammability limit): represent the minimum concentration of a substance in the air able to propagate the flame
- ODP: Ozone Depletion Potential
- GWP: global warming potential

Therefore, is deducible that when a facility works with propane, the leakages are an important issue, since propane is a very dangerous fluid and with the aim to work in safety.

The test rig is built in a housing as shown in Figure 7 (components in housing are ATEX certified) which is connected to an active carbon filter designed to absorb the filling amount of the test rig (<10 min in unlikely event of leakage); filter is linked with a ventilation system that ensures that no propane gets out of housing.

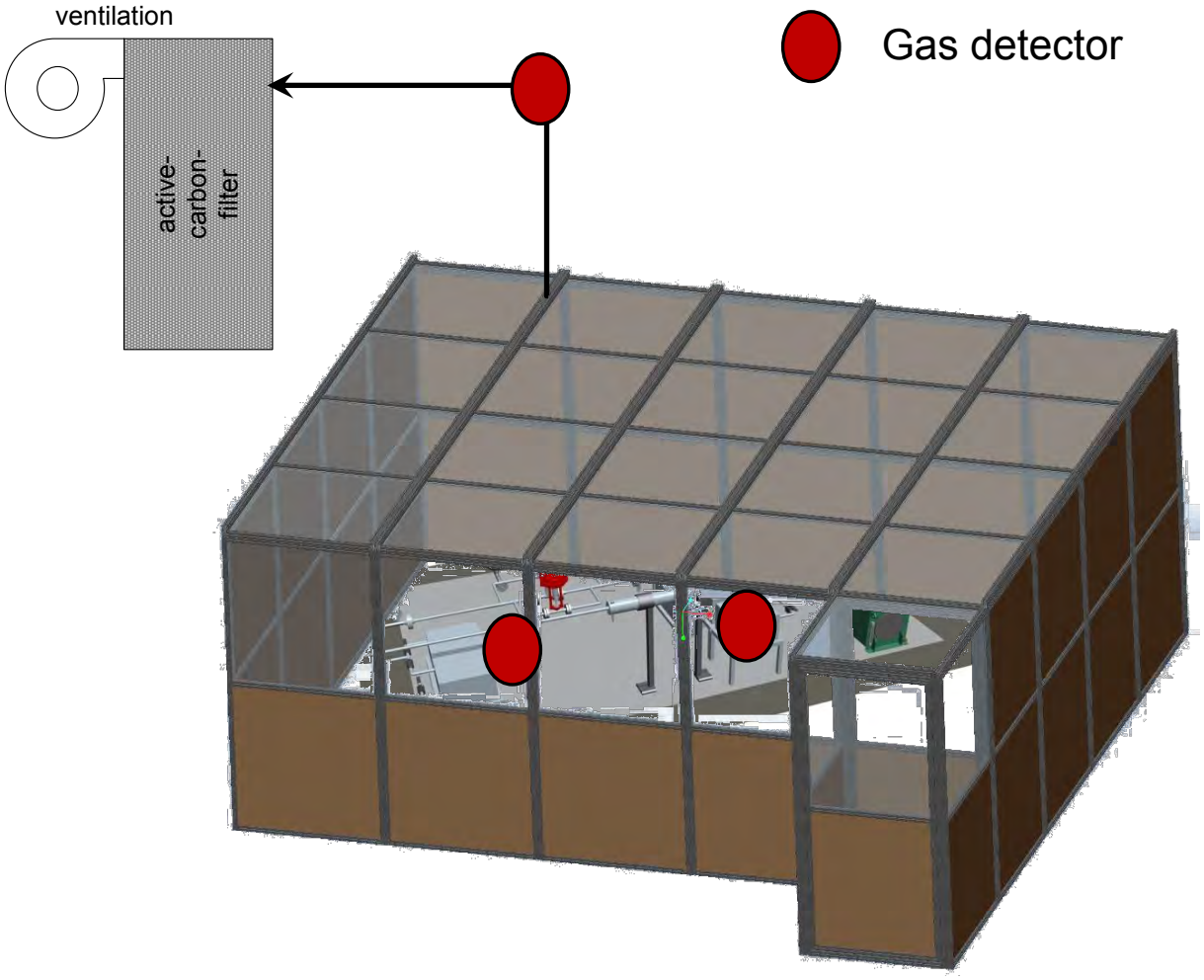

Figure 7: Housing of the test rig [2]

Furthermore, in the facility there are 3 kinds of sensors in order to recognize the leakages of the propane and to inform the previous system about this situation; in fact, if the sensors detects a leakage amount close to the value reported in the norm EN 378-1:2005 (CEN/TC 182), a signal is send at the ventilation system that provide to run at full speed in order to create a depression in the environment around the cycle; at the same time ball valves SDV NC allows to close the flux inside the test rig with exception of SDV 7 NC that create a by-pass for the pump with the purpose of don't increase the pressure in the test rig.

3 Data reduction and theoretical part

The aim of this part is to explain how the data reduction is built, put into focus the main topics like the calculation of temperature through the test section the calculation of the heat transfer coefficient and the pressure drops.
These topics are implemented in the data reduction excel file that will be show in detail in the next chapter.

3.1 Temperature determination of the working fluid

Since in the working fluid side of the heat exchanger there are no temperature sensors in order to not influence the experimental results, 3 different methods are explain with the aim to calculate the temperature tendency through the test section.

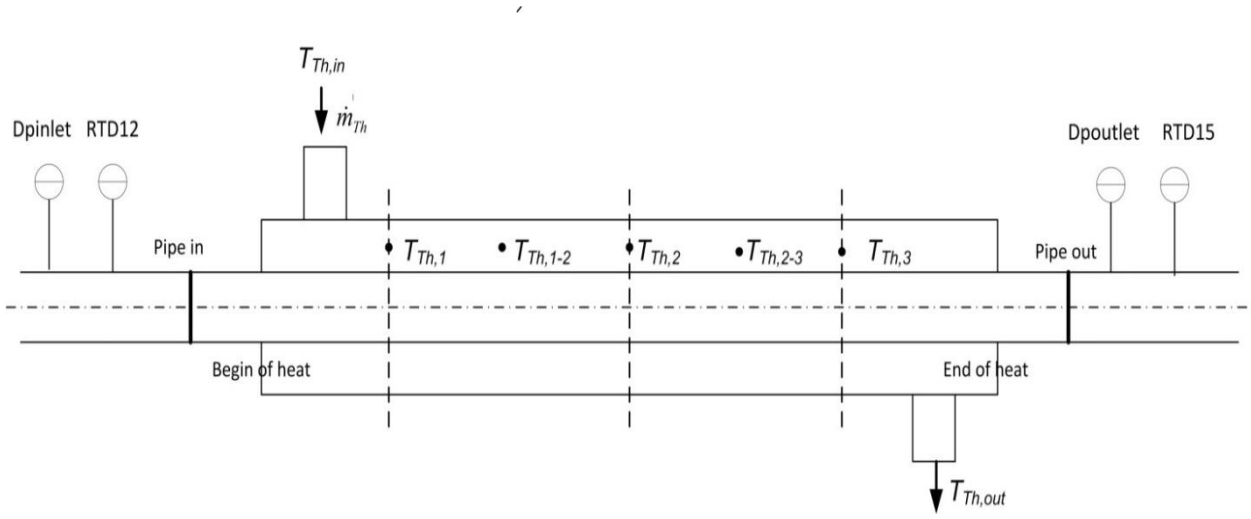

Figure 8: Test section information

1. Propane linear temperature:

The first method considers an adiabatic process upstream and downstream the heat exchanger; in other words, the temperature until the beginning of the heat exchanger is constant and measured by the RTD12 sensor.
In the same way the temperature downstream the heat exchanger is constant and measured by the RTD15 sensor. Between this length the idea is to connect these 2 values with a straight line and to extract through a proportion the corresponding temperature values in each measurement section.
This method is applicable in each case (liquid/gas cooling and condensation).

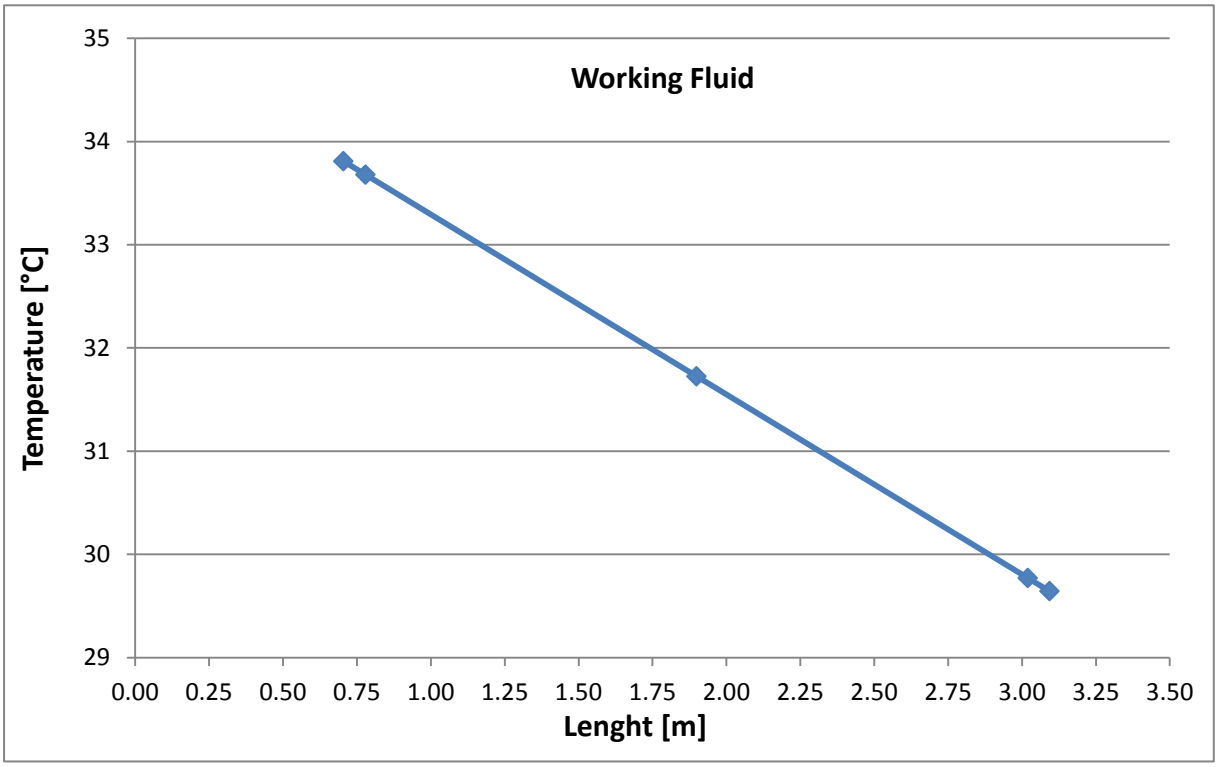

Figure 9: Example of Propane linear temperature for liquid cooling

2. Propane in-out:

The energy balance of the heat exchanger results as

$$\dot{Q}_{WF,1-2} = \dot{Q}_{th,1-2} \qquad 3.1$$

With:

$$\dot{Q}_{th1,2} = \dot{m}_{th} \cdot c_{p,th} \cdot \left(T_{th,2} - T_{th,1}\right) \quad 3.2$$

$$\dot{Q}_{WF1,2} = \dot{m}_{WF} \cdot c_{p,WF} \cdot \left(T_{WF,1} - T_{WF,2}\right) \quad 3.3$$

From this heat balance it is possible to extract the value of $T_{WF,2}$ for each measurement section and the start value $T_{WF,1}$ is the temperature value from the RTD12 sensor.
This method is applicable only in liquid/gas cooling case because in condensation the duty of the propane is:

$$\dot{Q}_{WF1,2} = \dot{m}_{WF} \cdot r_{,WF} \cdot (\Delta x) \quad 3.4$$

The vapour quality through the test section is calculated from the balance with the oil and the heat balance does not make sense.

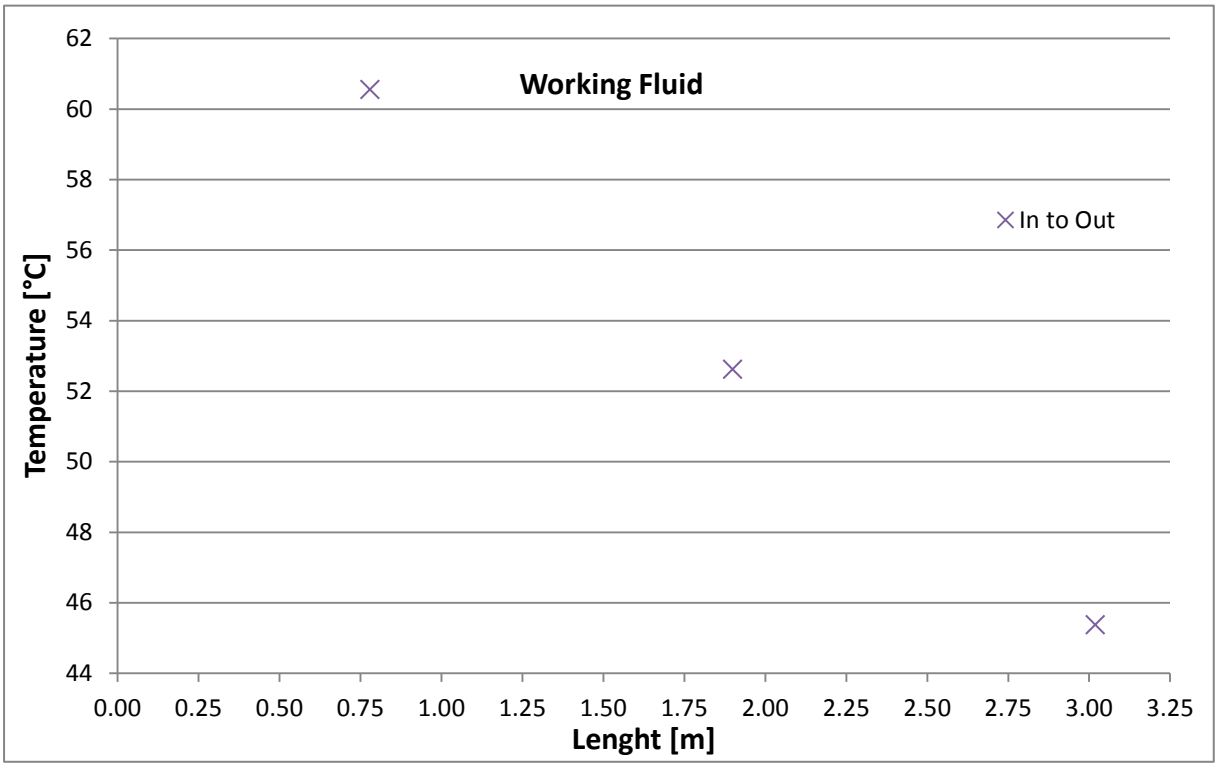

Figure 10: Example of Propane in-out for gas cooling

3. Propane out-in:

The only difference between this and the previous method is the start value and the direction of the calculation; in this case the start value is the temperature value measured by RTD15 sensor and the balance is done in the other way.

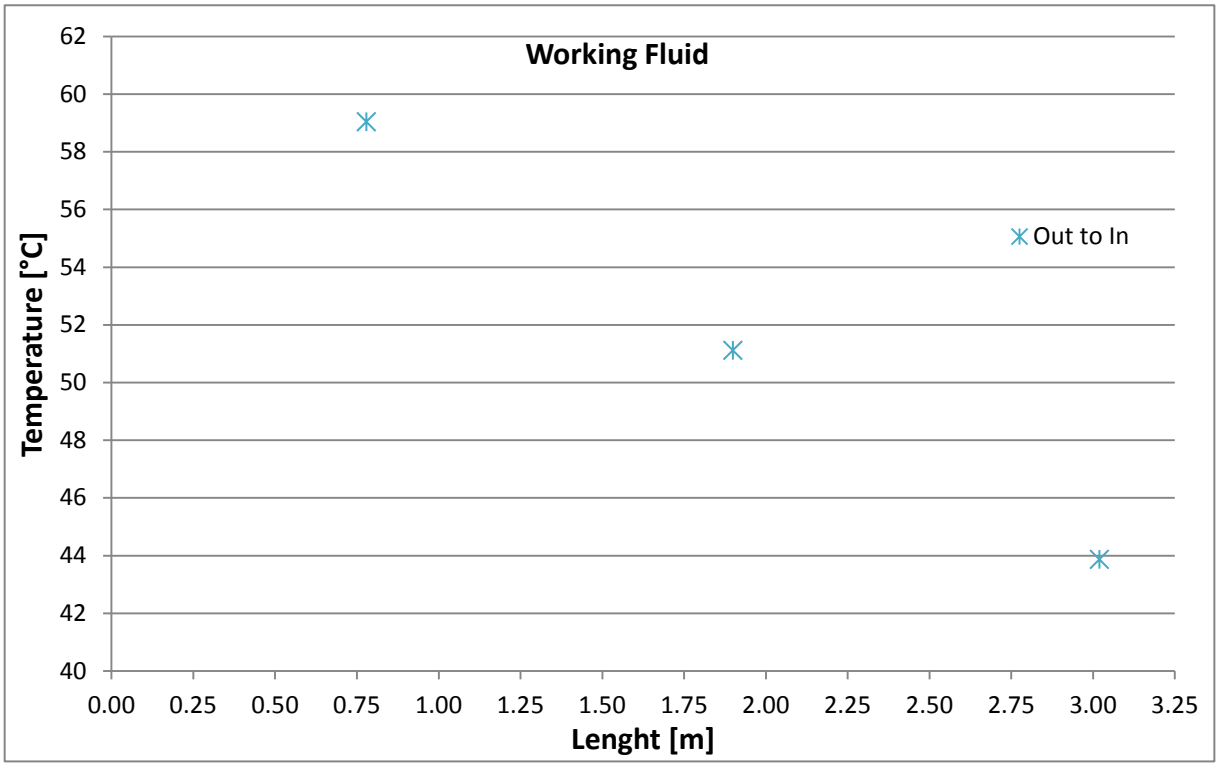

Figure 11: Example of Propane out-in for gas cooling

3.2 Heat transfer coefficient: literature review

In literature there are a lot of correlations about the calculation of the mean heat transfer coefficient during liquid or gas flow inside the tube. The aim in this part is to resort these correlations is to compare the experimental result with the literature.

As result from literature review, the most common and accurate empirical correlations are:

- Petukhov and Popov (single phase)
- Gnielinski (single phase)
- Hausen (single phase)
- Dittus Böelter (single phase)
- Cavallini et al., 2006 (condensation)

Basically, the alpha value is estimable with these empirical correlations which connect all the three dimensionless parameter Re, Pr, Nu.

- **Dittus-Boelter** [6]**:**

  The usual form of this correlation is the following:

$$Nu = C \cdot Re^m \cdot Pr^n \tag{3.5}$$

  Where *C*, *m* and *n* are specific parameters experimentally estimated for each heat transfer configuration.

$$Nu_{DB} = 0{,}026 \cdot Re^{0{,}8} \cdot Pr^{0{,}3} \tag{3.6}$$

  Valid for $2500 \leq Re < 125000$, $07 \leq Pr < 120$ and $L/D_h > 60$

- **Gnielinski (turbulent flow)** [6]**:**

$$Nu_{Gn} = \frac{f/8 \cdot (Re - 1000) \cdot Pr}{1 + 12{,}7 \cdot (f/8)^{\frac{1}{2}} \left(Pr^{\frac{2}{3}} - 1\right)} \cdot \left[1 + \left(\frac{D_h}{L}\right)^{\frac{2}{3}}\right] \quad 3.7$$

With:

$$f = (1{,}82 \cdot logRe - 1{,}5)^{-2} \quad 3.8$$

And valid for $2300 \leq Re < 5 \cdot 10^6$ and $0{,}5 \leq Pr < 10^6$

- **Gnielinski (transition flow regime)** [6]**:**

$$Nu_{Gn,trans} = (1 - \gamma) \cdot Nu_{Gn,lam,2300} + \gamma \cdot Nu_{Gn,turb,10^4} \quad 3.9$$

With:

$$\gamma = \frac{Re - 2300}{10^4 - 2300} \quad 3.10$$

$$Nu_{Gn,lam,2300} = \left(Nu_{Gn,1} + Nu_{Gn,2,2300} + Nu_{Gn,2300}\right)^{\frac{1}{3}} \quad 3.11$$

Practically, the Gnielinski correlation calculated at the limit of laminar and turbulent flow, modulated by the factor γ that places the calculated flow in the right spot of the transition zone.

- **Petukhov & Popov** [6]**:**

$$Nu_{PP} = \frac{f/8 \cdot (Re - 1000) \cdot Pr}{C + 12{,}7 \cdot (f/8)^{\frac{1}{2}} \left(Pr^{\frac{2}{3}} - 1\right)} \cdot \left[1 + \left(\frac{D_h}{L}\right)^{\frac{2}{3}}\right] \quad 3.12$$

With f like Gnielinski and:

$$C = 1{,}07 + \frac{900}{Re} - \frac{0{,}63}{1 + 10 \cdot Pr} \quad 3.13$$

Valid for $4000 \leq Re < 5 \cdot 10^6$ and $0{,}5 \leq Pr < 10^6$.

- **Hausen (for gas only)** [6]**:**

$$Nu_{Ha,1} = 0{,}0214 \cdot (Re^{0{,}8} - 100) \cdot Pr^{0{,}4} \cdot \left[1 + \left(\frac{D_h}{L}\right)^{\frac{2}{3}}\right] \quad 3.14$$

for $0{,}5 \leq Pr < 1{,}5$

$$Nu_{Ha,2} = 0{,}012 \cdot (Re^{0{,}87} - 280) \cdot Pr^{0{,}4} \cdot \left[1 + \left(\frac{D_h}{L}\right)^{\frac{2}{3}}\right] \quad 3.15$$

For $1{,}5 \leq Pr < 500$.

- **Cavallini et al., 2006 (condensation)** [7]**:**

If ($J_G > J_G^T$):

$$\alpha_A = \alpha_{LO}[1 + 1{,}128 \cdot x^{0{,}8170}\left(\frac{\rho_L}{\rho_G}\right)^{0{,}3865} \cdot \left(\frac{\mu_L}{\mu_G}\right)^{0{,}2363} \cdot (1 - \frac{\mu_L}{\mu_G})^{2{,}144} \cdot {Pr_L}^{-0{,}1} \quad 3.16$$

If ($J_G \leq J_G^T$):

$$\alpha_D = [\alpha_A \cdot \left(\frac{J_G^T}{J_G}\right)^{0{,}8} - \alpha_{STRAT}] \cdot \left(\frac{J_G}{J_G^T}\right) + \alpha_{STRAT} \quad 3.17$$

With:

$$\alpha_{LO} = 0{,}023 \cdot {Re_L}^{0{,}8} \cdot {Pr_L}^{0{,}4} \cdot \frac{\lambda_L}{D} \quad 3.18$$

$$\alpha_{STRAT} = 0{,}725\left\{1 + 0{,}741\left[\frac{1-x}{x}\right]^{0{,}3321}\right\}^{-1} [\frac{{\lambda_L}^3 \rho_L(\rho_L - \rho_G)g \cdot h_{LG}}{\mu_L\, D\, \Delta T}]^{0{,}25} + (1 - x^{0{,}087}) \cdot \alpha_{LO} \quad 3.19$$

$$J_G^T = \{\left[\frac{7{,}5}{4{,}3 \cdot {X_{tt}}^{1{,}111} + 1}\right]^{-3} + {C_T}^{-3}\}^{-\frac{1}{3}} \quad 3.20$$

$$C_T = 1{,}6 \quad hydrocarbons \quad 3.21$$

$$C_T = 1{,}6 \quad other\ refrigerant \quad 3.22$$

$$J_G = \left[\frac{x \cdot G}{g \cdot D \cdot \rho_G(\rho_L - \rho_G)}\right]^{0{,}5} \quad 3.23$$

$$X_{tt} = \left(\frac{\mu_L}{\mu_G}\right)^{0{,}1} \left(\frac{\rho_G}{\rho_L}\right)^{0{,}5} \left[\frac{1-x}{x}\right]^{0{,}9} \quad 3.24$$

3.3 Heat transfer coefficient: data reduction

This chapter shows how the data are collected and elaborated in order to calculate the heat transfer coefficient α.

The alpha coefficient is calculated in 3 different ways:

1) mean heat transfer coefficient of the whole pipe
2) mean heat transfer coefficient with small boundary conditions between the first and third measurement section
3) mean heat transfer coefficient referred to every measurement section

3.3.1 Mean/integral heat transfer coefficient

First of all is important to define the boundaries of the problem in order to understand which kind of evaluation about the alpha coefficient is possible to obtain.

For the calculation it's possible to analyze the problem in two different ways: one solution is to consider the entire test section from inlet to outlet (case 1) and the second considering the heat exchange that happens between two of the measurement sections (case2).
The energy balance of the heat exchanger results as

$$\dot{Q}_{WF,i-o} = \dot{Q}_{th,i-o} \tag{3.25}$$

with heat balance in the therminol side

$$\dot{Q}_{th,i-o} = \dot{m}_{th} \cdot c_{p,th} \cdot \left(T_{th,out} - T_{th,in}\right) \tag{3.26}$$

In this case the losses can be neglected due to their little influence.

A way to validate this balance is to directly calculate the heat in the working fluid side:

$$\dot{Q}_{WF,i-o} = \dot{m}_{WF} \cdot c_{p,WF} \cdot \left(T_{WF,out} - T_{WF,in}\right) \tag{3.27}$$

About the proprieties of the therminol and working fluids, these are calculated at the mean temperature.
Since the heat is balanced, the total heat exchanged can be calculated with the heat exchanger correlation:

$$\dot{Q}_{i-o} = K_{int,i-o} \cdot A_{int} \cdot \Delta T_{ln,i-o} \tag{3.28}$$

With the heat transferring surface:

$$A_{int} = \pi \cdot L_{i-o} \cdot D_{int} \tag{3.29}$$

And the logarithmic temperature difference:

$$\Delta T_{ln,i-o} = \frac{\left(T_{WF,in} - T_{th,out}\right) - \left(T_{WF,out} - T_{th,in}\right)}{ln\frac{\left(T_{WF,in} - T_{th,out}\right)}{\left(T_{WF,out} - T_{th,in}\right)}} \tag{3.30}$$

From the global heat transfer coefficient:

$$K_{int,i-o} = \frac{1}{R_{int} + R_{wall} + R_{ext}} = \frac{1}{\frac{1}{\bar{\alpha}_{int,i-o}} + R_{wall} + \frac{D_{int}}{\alpha_{ext} \cdot D_{ext}}} \quad 3.31$$

1) The value of the htc referred at the internal pipe:

$$\boldsymbol{\bar{\alpha}_{int,i-o} = \left(\frac{A_{int} \cdot \Delta T_{ln,i-o}}{\dot{Q}_{i-o}} - R_{wall} - \frac{D_{int}}{\alpha_{ext} \cdot D_{ext}} \right)^{-1}} \quad 3.32$$

is finally calculated.

As visible in the overall heat transfer coefficient formula, two unknowns are present: α_{int} and α_{ext}; α_{int} is the aim of this calculation and α_{ext} is the unknown of the problem; there are two possible methods to get this value:

- The first option is using the correlation of Gnielinski [8]
- Second option is to use the Wilson plot method

Due to the possibility to work directly with the measured wall temperature, rather than using htc external is possible to change the boundaries conditions of the problem, considering the heat exchange that happens between two of the measurement sections. The heat balance of this range of the working fluid side results:

$$\dot{Q}_{WF,1-3} = \dot{m}_{WF} \cdot c_{p,WF} \cdot \left(T_{WF,1} - T_{WF,3} \right) \quad 3.33$$

Considering the whole heat exchange:

$$\dot{Q}_{1-3} = K_{int,1-3} \cdot A_{1-3} \cdot \Delta T_{ln,1-3} \quad 3.34$$

With the area involved in the process of heat exchange:

$$A_{1-3} = \pi \cdot L_{1-3} \cdot D_{int} \quad 3.35$$

And the logarithmic temperature difference:

$$\Delta T_{ln,1-3} = \frac{\left(T_{WF,3} - T_{TC,3}\right) - \left(T_{WF,1} - T_{TC,1}\right)}{ln\frac{\left(T_{WF,3} - T_{TC,3}\right)}{\left(T_{WF,1} - T_{TC,1}\right)}} \quad 3.36$$

From the global heat transfer coefficient:

$$K_{int,1-3} = \frac{1}{R_{int} + R_{corr,int}} = \frac{1}{\frac{1}{\alpha_{int}} + R_{corr,int}} \quad 3.37$$

2) The heat transfer coefficient of this case is calculated as:

$$\boldsymbol{\alpha_{int,1-3}} = \left(\frac{\boldsymbol{A_{1-3} \cdot \Delta T_{ln,1-3}}}{\boldsymbol{\dot{Q}_{1-3}}} - \boldsymbol{R_{corr,int}}\right)^{\boldsymbol{-1}} \quad 3.38$$

Is important to do an explanation about the Corrective Resistance R_{corr} :

To understand the analytical approach of the problem, the actual heat flow situation in the test section is shown in Figure 12:

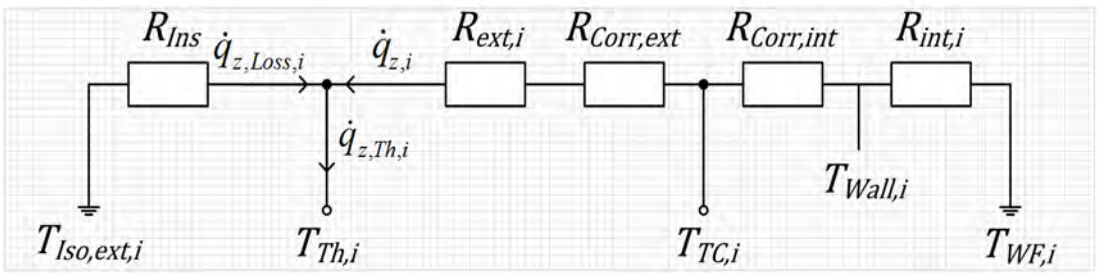

Figure 12: Thermal resistances involved in the data reduction [3]

- R_{ins}: Insulation Resistance is the resistance composed by the layer of insulating matter and the wall of the outer pipe. About the insulating layer, is used a micro-cell structured insulant named Armaflex AF developed by Armacell. This thermal resistance consider the temperature difference between the outer temperature of the isolation layer and the temperature of the cooling fluid. This temperature difference originates a heat flux towards the secondary working fluid considered like a loss in the energy balance. The considered sub-resistances are shown in Table 3.

Table 3: Layers of the isolation resistance

$\boldsymbol{Pos.}$	$\boldsymbol{Material}$	$\boldsymbol{D_n}$	$\boldsymbol{\lambda}$
		$[mm]$	$[W/m \cdot K]$
1	Outer Pipe Internal D.	48,000	
2	Outer Pipe External D.	52,000	57
3	Isolation Layer	152,000	0,033

- R_{ext}: External Resistance, it is represented by the heat transfer coefficient α_{ext} and is the thermal resistance of the shell side of the test pipe. This thermal resistance consider the temperature difference between the temperature measured by the thermocouples on the outer wall of the test pipe and the temperature measured by the thermoresistance on the cooling fluid. This value could be estimated by one of the correlation presented before but since there are components like flanges needed for the construction, RTDs and supports of the TCs the flow of the cooling fluid is disturbed and thus the actual flow behavior is not easily predictable. So this alpha value is supposed to be calculated from the energy balance or with other experimental methods.

- $R_{Corr,ext}$, $R_{Corr,int}$: Corrective Resistance; these resistances takes into account the layers that composing the thermocouple. The effects of these layers are calculated building a cylindrical thermal resistance, which dimensions are shown in Table 4 and composed like in equation 3.39 and 3.40

Table 4: Layers of the Test Pipe [3]

Pos.	***Material***	D_n	λ
		$[mm]$	$[W/m \cdot K]$
1	Pipe	14,650	57
2	Glue	18,400	1
3	TC Inconel – Inc, Internal	18,500	15
4	TC Magnesium oxide - MgO, Internal	18,680	50
5	TC	18,750	50
6	TC Magnesium oxide - MgO, external	18,820	15
7	TC Inconel – Inc, external	19,000	

$$R_{Corr,in} = \sum_{n=1}^{4} \frac{\ln \frac{D_{n+1}}{D_n} \cdot D_{int}}{2 \cdot \lambda_n} = 7{,}43 \cdot 10^{-5} \frac{m^2 \cdot K}{W} \qquad 3.39$$

$$R_{Corr,out} = \sum_{n=5}^{6} \frac{\ln \frac{D_{n+1}}{D_n} \cdot D_{int}}{2 \cdot \lambda_n} = 6{,}74 \cdot 10^{-6} \frac{m^2 \cdot K}{W} \qquad 3.40$$

In case that the TC sensor are not used for the calculation, these two resistance will be replaced by a unique resistance consisting of the entire thickness of the pipe made by only one layer of steel alloy:

$$R_{Wall} = \frac{\ln \frac{D_{ext}}{D_{int}} \cdot D_{int}}{2 \cdot \lambda_1} = 3{,}81 \cdot 10^{-5} \frac{m^2 \cdot K}{W} \qquad 3.41$$

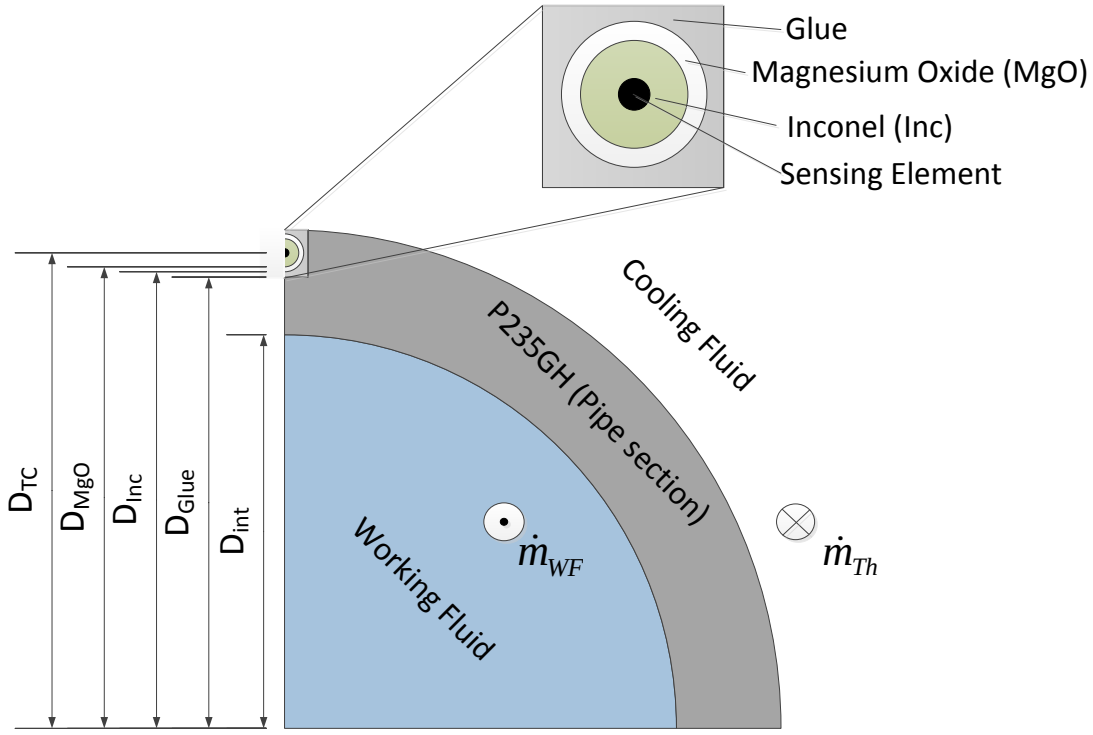

Figure 13: Composition of the layers in the wall of the test pipe [3]

- R_{int}: Internal Resistance, it is represented by the heat transfer coefficient α_{int} and is the purpose of this test rig. This thermal resistance consider the temperature difference between the inner wall temperature and the working fluid temperature. Both of them are unknown but in the first case, the problem can be overcome considering the TC´s temperature and the relative additional resistance. In the second case, it can be indirectly estimated using an energy balance that involves the heat exchanged at every measurement section. It´s possible to calculate the alpha value in both experimental and analytical way.

In the same way it is possible to calculate the internal heat transfer coefficient taking into account the outer alpha, so with restricted boundary physical boundary but enlarged thermal boundary:

$$\dot{Q}_{1-3} = K_{int,\overline{1-3}} \cdot A_{1-3} \cdot \Delta T_{ln,\overline{1-3}} \qquad 3.42$$

With logarithmic mean temperature difference:

$$\Delta T_{ln,1-3} = \frac{\left(T_{WF,3} - T_{th,3}\right) - \left(T_{WF,1} - T_{th,1}\right)}{ln\frac{\left(T_{WF,3} - T_{th,3}\right)}{\left(T_{WF,1} - T_{th,1}\right)}} \quad 3.43$$

And global heat transfer coefficient:

$$K_{int,\overline{1-3}} = \frac{1}{\frac{1}{\bar{\alpha}_{int,1-3}} + R_{wall} + \frac{D_{int}}{\alpha_{ext} \cdot D_{ext}}} \quad 3.44$$

And so the heat transfer coefficient can be expressed as:

$$\bar{\alpha}_{int,1-3} = \left(\frac{A_{int} \cdot \Delta T_{ln,\overline{1-3}}}{\dot{Q}_{1-3}} - R_{wall} - \frac{D_{int}}{\alpha_{ext} \cdot D_{ext}}\right)^{-1} \quad 3.45$$

A way to calculate the external mean heat transfer coefficient needed in this calculation is to calculate the heat balance between cooling fluid and external surface of the pipe with the restricted boundaries like in 3.38:

$$\alpha_{ext,1-3} = \left(\frac{A_{1-3} \cdot \Delta T_{ln,1-3}}{\dot{Q}_{1-3}} - R_{corr,ext}\right)^{-1} \quad 3.46$$

With logarithmic temperature difference:

$$\Delta T_{ln,1-3} = \frac{\left(T_{TC,3} - T_{th,3}\right) - \left(T_{TC,1} - T_{th,1}\right)}{ln\frac{\left(T_{TC,3} - T_{th,3}\right)}{\left(T_{TC,1} - T_{th,1}\right)}} \quad 3.47$$

3.3.2 Local Heat Transfer Coefficient

The last method in order to obtain a local heat transfer coefficient evaluation referred to every measurement section (case 3), can be developed thanks to the configuration of the RTDs in the shell side of the heat exchanger. In fact, the therminol side is equipped with five measurement sections that allow building a more accurate polynomial curve that interpolates the trend of temperature of Therminol. The curve has been calculated with excel, as a second degree polynomial.

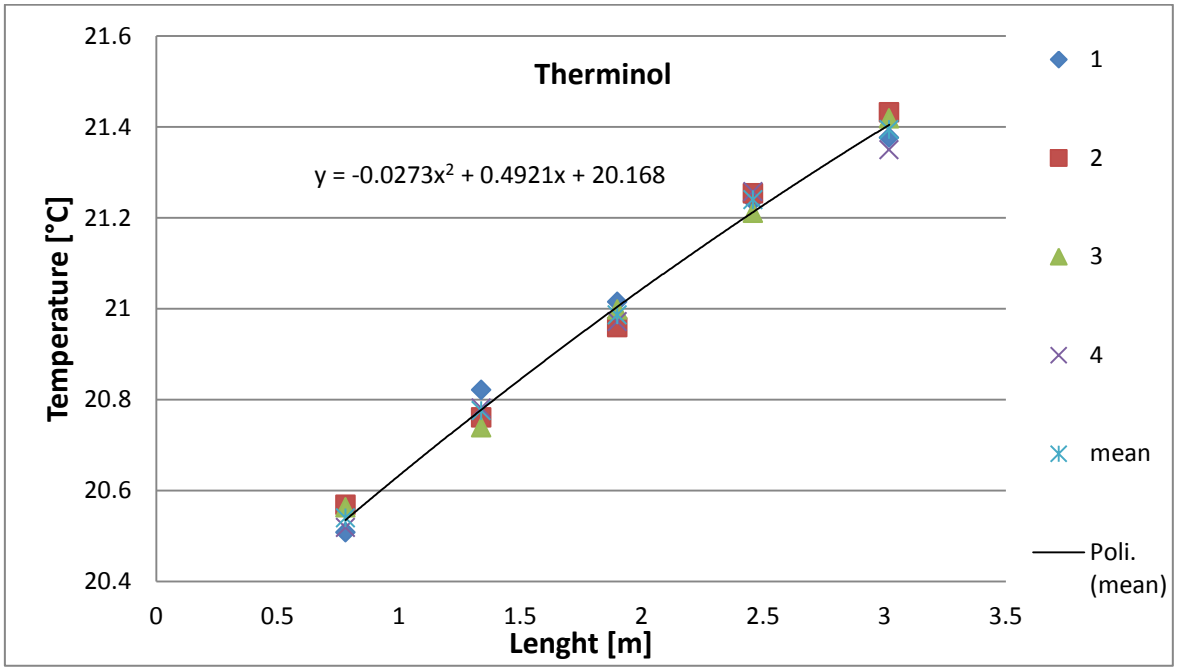

Figure 14: Temperature trend of Therminol from the five measurement sections in the oil side

This slope is involved in the calculation of the specific heat flux originated in the cooling fluid:

$$\dot{q}_{z,th,i} = \dot{q}_{z,i} + \dot{q}_{z,loss,i} \qquad 3.21$$

With specific heat loss in the i-th section:

$$\dot{q}_{z,i} = \frac{\delta \dot{Q}}{\delta \varphi \delta z} = \frac{\dot{m}_{th} \cdot c_{p,th}}{\pi \cdot D_{int}} \cdot \frac{\delta T_{th,i}}{\delta z} - \dot{q}_{loss,i} \quad 3.48$$

Defined by the temperature polynomial:

$$T_{th,i}(z) = A \cdot z^2 + B \cdot z + C \quad 3.49$$

Derived as:

$$\frac{\delta T_{th,i}(z)}{\delta z} = 2 \cdot A \cdot z + B \quad 3.50$$

And with specific heat losses:

$$\dot{q}_{loss,i} = \frac{\lambda_{Iso} \cdot 2\pi}{D_{Iso,int} \cdot ln \frac{D_{Iso,ext}}{D_{Iso,int}}} \cdot \Delta T_{Iso,i} \quad 3.51$$

Specific heat flux is now dependent on the position z along the test pipe, so it is possible to calculate it for every measurement section. This calculation is based on the hypothesis that in shell tube heat exchanger with turbulent flow the radial heat gradient of every infinitesimal section is equal to zero. The boundaries of the problem are also important here, since it is possible not to involve the external heat transfer coefficient from the shell side to tube in order to minimize calculation errors.
Considering as thermal potential the temperature difference between outer wall and bulk flow:

$$\Delta T_i = T_{WF,i} - T_{TC,i} \quad 3.52$$

The local htc is calculated in this case as:

$$\dot{q}_{z,i} = \frac{\Delta T_i}{\frac{1}{\alpha_{int,i}} + R_{corr,int}} \quad 3.53$$

3) The local heat transfer coefficient of the i-th measurement section is:

$$\boldsymbol{\alpha_{int,i} = \left(\frac{\Delta T_i}{\dot{q}_{z,i}} - R_{corr,int}\right)^{-1}} \quad 3.54$$

In the same way it is possible to calculate the external heat transfer coefficient, but in this case different thermal potential is considered:

$$\Delta T_i = T_{TC,i} - T_{th,i} \quad 3.55$$

And so the alpha value is:

$$\alpha_{ext,i} = \left(\frac{\Delta T_i}{\dot{q}_{z,i}} - R_{corr,ext}\right)^{-1} \quad 3.56$$

The local external heat transfer coefficient can be used as test for the annulus correlations, found in literature. With this value is it also possible to build a global heat transfer coefficient but referred to a single section.

3.4 Pressure drop

A calculation of pressure drop is important for these motivations:

- A comparison between the value measured by the differential pressure sensor and the value from pressure drop correlation has to be made in order to confirm the validation of the acquisition system about pressure drop.

- A reliable value of pressure drop is important because the properties of the fluid are calculate at the mean value of pressure and the htc coefficient depends from these proprieties:

$$P_{mean} = P_{AP5,6} - \frac{dp01}{2} \tag{3.57}$$

- Pressure drops during evaporation and condensation (in this case) changing the pressure change also the saturation temperature and is important to take into account of this.

3.4.1 Pressure drop single phase

The pressure drop in pipe flow is given by [9]:

$$\Delta P = \zeta \frac{l}{di} \frac{\rho \cdot {w_i}^2}{2} \tag{3.58}$$

The drag coefficient ζ depends on the Reynolds number for flow within the tube,

$$Re = \frac{w_i \rho d_i}{\mu} \tag{3.59}$$

And is calculated using the Gnielinski correlation [6]:

$$\zeta = (1{,}82 \cdot logRe - 1{,}5)^{-2} \tag{3.60}$$

and valid for $2300 \leq Re < 5 \cdot 10^6$ and $0{,}5 \leq Pr < 10^6$

The proprieties of the fluid refer to the average pressure and temperature in the tube.

3.4.2 Pressure drop two-phase: Separated flow models for flows inside plain tubes

In this chapter, methods to predict the two phase pressure drops for flows inside tubes (horizontal) will be presented [10]; this method consider different values for the speed of the liquid and gas phase.
Basically, the two phase pressure drops for flows inside tubes are the sum of three contributions:

$$\Delta p_{total} = \Delta p_{static} + \Delta p_{mom} + \Delta p_{frict} \tag{3.61}$$

The static pressure drop is given by

$$\Delta p_{static} = \rho_{hom} g H \sin\theta \tag{3.62}$$

For a horizontal tube, $\Delta p_{static} = 0$ because $H = 0$.
The momentum pressure drop reflects the change in kinetic energy of the flow and is given by:

$$\Delta p_{mom} = {G_{tot}}^2 \left\{ \left[\frac{(1-x)^2}{\rho_L (1-\varepsilon)} + \frac{x^2}{\rho_G \varepsilon} \right]_{out} - \left[\frac{(1-x)^2}{\rho_L (1-\varepsilon)} + \frac{x^2}{\rho_G \varepsilon} \right]_{in} \right\} \tag{3.63}$$

Since the this method considers the two phase to be artificially separated into two streams, each flowing in its own pipe, the area of these two pipes are proportional to the void fraction calculated with the Zivi model [11] (1964):

$$\varepsilon = \left[1 + \frac{(1-x)}{x} \left(\frac{\rho_G}{\rho_L} \right)^{0,67} \right]^{-1} \tag{3.64}$$

In order to obtain the latest frictional parameter Δp_{frict} is useful to introduce a parameter called two-phase multiplier and indicated with $\emptyset^2$.
There are different methods to predict the two-phase frictional pressure drop based on a two-phase multiplier and in this work the **Friedel correlation 1979,** [10] is used. This method is basically reccomended when (μ_L/μ_G) is less than 1000.

Through this multiplier is possible to extract Δp_{frict} as

$$\Delta p_{frict} = \Delta p_L \emptyset_{fr}{}^2 \quad 3.65$$

Where Δp_L is calculated for the liquid-phase and given by

$$\Delta p_L = 4 f_L \left(\frac{L}{d_i}\right) G^2 \left(\frac{1}{2\rho_L}\right) \quad 3.66$$

with liquid friction factor f_L,

$$f_L = \frac{0{,}079}{Re_L{}^{0{,}25}} \quad 3.67$$

His two-phase multiplier is:

$$\emptyset_{fr}{}^2 = E + \frac{3{,}24FH}{Fr_H^{0{,}045} We_L^{0{,}035}} \quad 3.68$$

With the dimensioless factors:

$$Fr_H = \frac{G^2}{gdi\rho_{HOM}{}^2} \quad 3.69$$

$$E = (1-x)^2 + x^2 \frac{\rho_L f_G}{\rho_G f_L} \quad 3.70$$

$$F = x^{0{,}78}(1-x)^{0{,}224} \quad 3.71$$

$$H = \left(\frac{\rho_L}{\rho_G}\right)^{0{,}91} \left(\frac{\mu_G}{\mu_L}\right)^{0{,}19} \left(1 - \frac{\mu_G}{\mu_L}\right)^{0{,}7} \quad 3.72$$

And the liquid Weber We_L is defined as:

$$We_L = \frac{G^2 d_i}{\sigma \rho_{HOM}} \tag{3.73}$$

Using the definition of the homogeneous density ρ_{HOM}:

$$\rho_{HOM} = \left(\frac{x}{\rho_G} + \frac{1-x}{\rho_L}\right)^{-1} \tag{3.74}$$

This method is always applicable in our case since the viscosity ratio is less than 1000 in every measurement.

4 General overview of the data reduction excel file

The target of this chapter, which is connected about the arguments with the previous one, is to show the structure and the different sections of new data reduction tool.

4.1 File typologies

There are two different typologies of data reduction files, one for the single phase analysis (liquid/gas cooling) and the second one for the double phase analysis (condensation) in order to adapt the correlation and the calculation of the fluid properties for each case.

4.2 Operating istructions

First of all is important to show how to use the program in order to get the data results.
Since is possible to extract the sampling file from the LabVIEW software for each measurement session, the first step is to calculate an average value about all the information obtained and copy this line in the first line of the data reduction excel file as input of the program.

	A	B	C	D	E	F	G	H	I	
1	Average value	→	11,79	13,00	2,42	33,74	37,66	0	0	
2		Zeit	AP1_MPP	AP2_MPP	MPP Power	RTD01	RTD02	MG<_(83A04)	MG>_(83F25)	ML<
3		13:18:20	11,79	12,99	2,411	33,72	37,65	0	0	
4		13:18:41	11,79	12,99	2,411	33,72	37,65	0	0	
5		13:19:02	11,79	12,99	2,411	33,74	37,67	0	0	

Figure 15: Example of raw data from the LabVIEW software

	A	B	C	D	E	F	G	H	I	J
1	11,62435396	16,04000704	8,198608714	33,13756836	47,18671061	0	0,063471429	3,32E-05	0	0,000
2	AP1_MPP	AP2_MPP	MPP Power	RTD01	RTD02	MG<_(83A04)	MG>_(83F25)	ML<_(2100-6)	ML>_(2100-15)	MCIRC

Figure 16: Input to put in the first line of the data reduction excel file

This is the only one manual operation that is necessary to do with the aim to introduce the input about the measurement.

4.3 Geometry information

Carrying on with the file is important to understand the meaning originate from the geometry information.
This information is fixed in each file.

Geometry information								
D_1,in (process)	D_1,out (process)	D_2,in (oil)	D_2,out (oil)	TC Magnesiumoxid/	TC	TC Magnesium	TC Inconel/ Inc	Lot
0,0147	0,019	0,048		0,01882	0,01875	0,01868	0,0185	0,0184

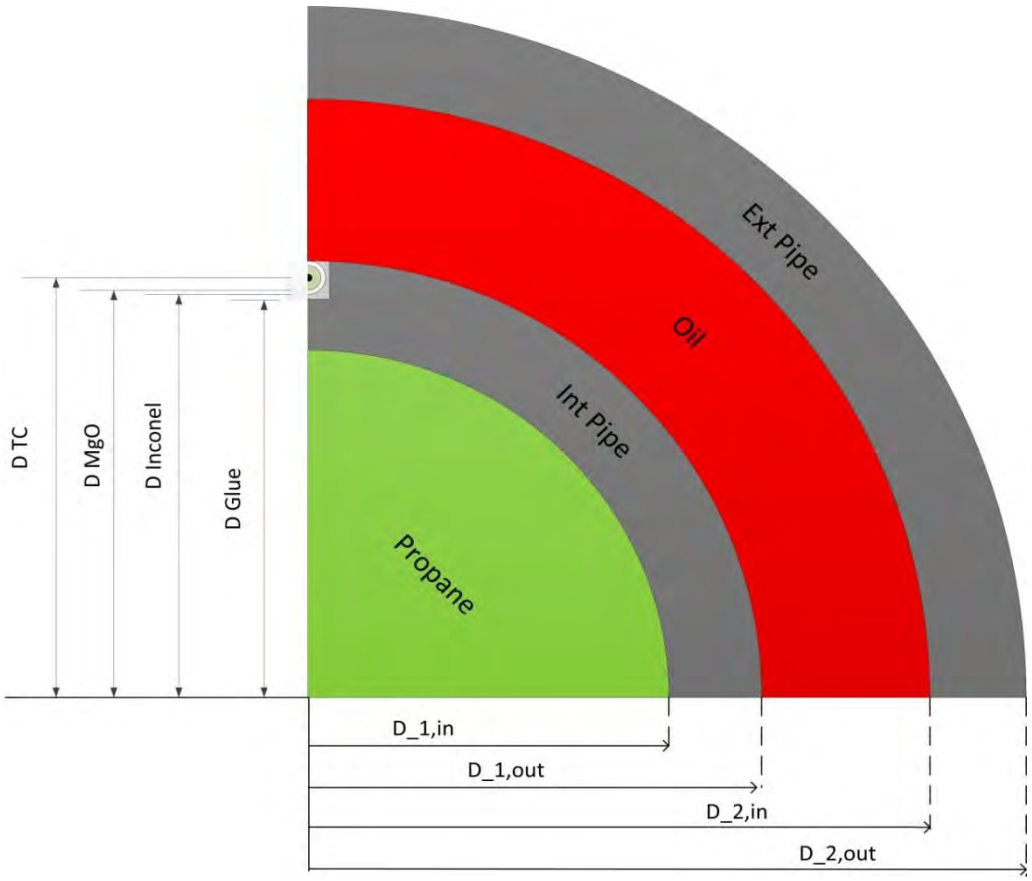

Figure 17: Diameter information

dpinlet	RTD12	Pipe In	begin of heat	Th_0 (Inlet Oil)=	Section 1 (TC_1)	RTD 1-2 (inbe	Section 2 (TC_2)	RTD 2-3 (inbet	Section 3 (TC_3	Th_4 (outlet oil)=RTD13/14	end of heat	Pipe Out	dpoutlet	RTD15
-0,219	-0,119	0	0,705	0,762	0,78	1,34	1,9	2,46	3,02	3,038	3,094	3,4	3,621	3,721

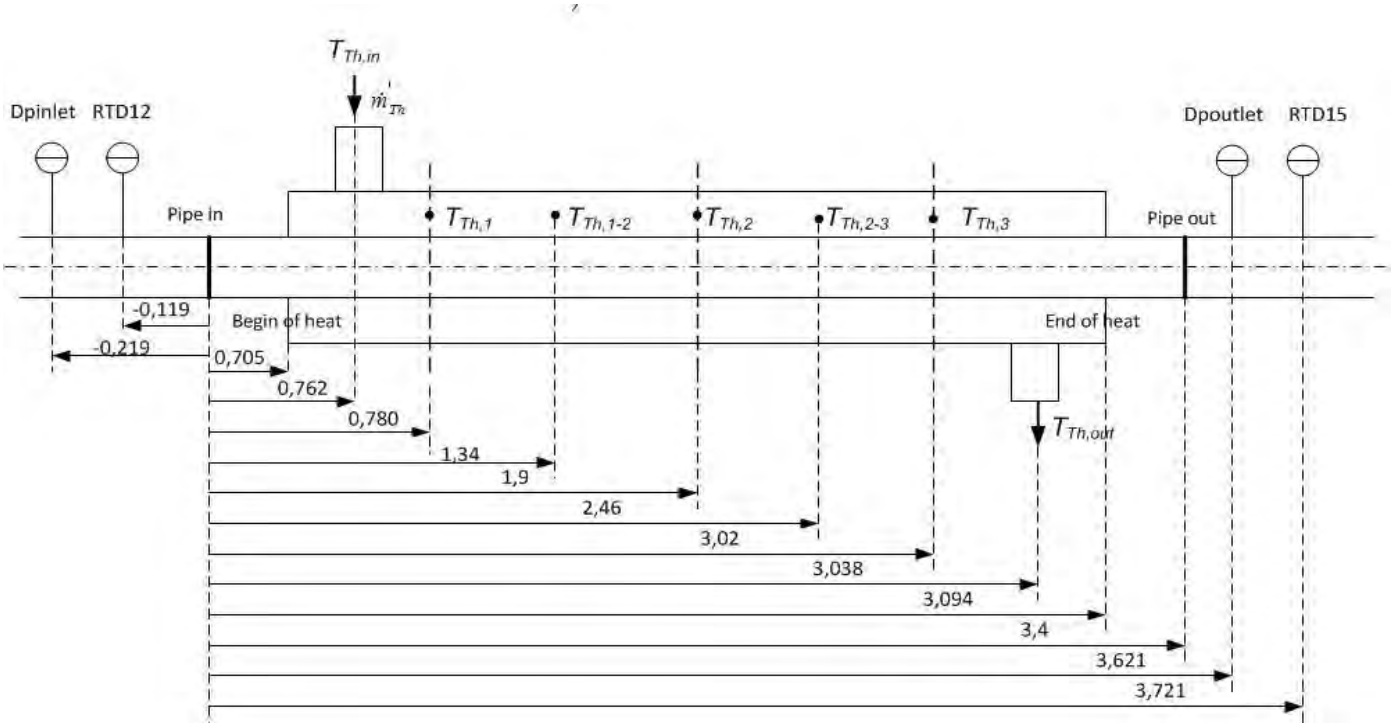

Figure 18: Length information

4.4 Fluids information

This section involves the properties and the characteristics of the working fluid (propane) and secondary fluid (therminol).

- Therminol:

Therminol		
Mass		
MSECTS	Re_th	G
kg/s	[-]	kg/m²s
0,6568	10109	430,4

Figure 19: Mass flow rate of therminol from the flow sensor

Properties				
cp_th	lambda_th	rho_th	mu_th	Pr_th
	W/m*K	kg/m^3	Pa*s	
2,098	0,110	761	0,0012	23,60

Figure 20: Proprieties of therminol based on mean temperature value

For the calculation of the proprieties of the oil the producer catalog recommends to use these equations:

- $\rho\left[\frac{kg}{m^3}\right] = A + B \cdot T(°C) + C \cdot T^2(°C) + D \cdot T^3(°C)$
- $c_p\left[\frac{kJ}{kg \cdot K}\right] = A + B \cdot T(°C) + C \cdot T^2(°C) + D \cdot T^3(°C) + E \cdot T^4(°C)$
- $\lambda\left[\frac{W}{m \cdot K}\right] = A + B \cdot T(°C) + C \cdot T^2(°C)$
- $\mu\left[\frac{mm^2}{s}\right] = e^{\left(\frac{A}{T(°C)+B}+C\right)}$

T= mean value of the oil temperature between in-out of the test section

Table 5: Constant to use for the properties determination [12]

	A	B	C	D	E
ρ	776,257	−0,696982	−0,000131384	$-2{,}09079 \cdot 10^{-6}$	
cp	2,01422	0,00386884	$2{,}05029 \cdot 10^{-6}$	$-1{,}12621 \cdot 10^{-8}$	$3{,}86282 \cdot 10^{-11}$
λ	0,112994	−0,00014781	$1{,}61429 \cdot 10^{-7}$		
μ	−3562,69	146,4	−2,68168		

- Propane:

Propane					
MG<_(83A04)	MG>_(83F25)	ML<_(2100-6)	ML>_(2100-15)	m_wf	G_wf
0,0003	0,084506657	3,29429E-05	0,000	kg/s	kg/m^2*s
0,084507	kg/s	0,000033	kg/s	0,0845	501

Figure 21: Mass flow rate of propane from the Coriolis sensors in the gas line (MG) and liquid line (ML)

AP5,6	DP01	p_mean
(bar)	(mbar)	(bar)
11,98062651	198,8872949	11,881
offset DP 01	20,18	

Figure 22: Pressure information of the propane

The pressure value at the inlet of the test section is measured by the pressure sensor with the information of the pressure drop by the differential pressure sensor.

Is important the information about the offset DP 01; this is a set value present at the launch of the software that change for each measurement session and that should be keep and put as input in this cell in order to have a right value of the pressure drop (DP01 – offset).

Propan single phase							
cp	Rho	mu	Lambda	Prantl	Re	Quality	
kW/K	kg/m^3	Pa*s	W/m*K				
2,0820	22,7746	0,00000918	0,02277756	0,8392	799946	#Superheated	vapor

Figure 23: Proprieties of the propane

The Proprieties of the propane are calculated directly through the link Refprop-excel and the implementation is different for the single phase case to the 2-phase case (in this case the proprieties are extracted separately for the liquid and vapour phase and calculated at the mean value of pressure).

4.5 Duty calculation

As the previous section, this part is built in order to calculate the heat transfer between the two fluids, respectively Oil and propane:

$$\dot{Q}_{th1,2} = \dot{m}_{th} \cdot c_{p,th} \cdot \left(T_{th,2} - T_{th,1}\right) \qquad 4.1$$

And,

$$\dot{Q}_{WF1,2} = \dot{m}_{WF} \cdot c_{p,WF} \cdot \left(T_{WF,1} - T_{WF,2}\right) \qquad 4.2$$

Duty Oil				
C_point,th	Q_th,i-o	q_th_int_heated_lenght	Q_th,1-3	q_th,1-3
kW/K	W	W/m^2	W	W/m^2
1,378	2121,4	19293	1778,20	17248

Figure 24: Example for Duty oil

Duty propane				
C_point,wf	Q_wf,i-o	q_wf,i-o	Q_wf,1-3	q_wf,1-3
	W	W/m^2	W	W/m^2
0,1759	2274,10	20683	2132,26	20683

Figure 25: Example for Duty propane (duty calculation not possible in condensation because the vapour quality x is calculated from the balance between oil and propane)

Legend:

- i-o: heat transfer between inlet and outlet
- 1-3: heat transfer between first and third measurement section

Furthermore, is useful verify the heat balance between oil and propane:

%Q_wf-oil,i-o	%Q_wf-oil,1-3
7,20%	19,91%

Figure 26: Heat balance

4.6 Temperature and vapour quality section

The file is equipped with a general overview relating to the temperature involved in the test section and the vapour quality trend (only in 2-phase conditions).
Basically, this section is subdivided in order to highlights the different trend of the temperature starting from the oil until the working fluid.

Temperature - Propan and oil									
object	T_in	1st section	1 - 2 section	2nd section	2 - 3 section	3rd section	T_out	Delta T	T_mean
Oil temperature									
external wall temperature									
internal wall temperature									
propane linear temperature									
propane in-out temperature									
propane out-in temperature									

Figure 27: Summary relating to the temperature involved in the heat exchanger

Object:

- Oil temperature: this line is represented by the temperature measured from the RTD (resistance temperature detector) installed in the oil side
- External wall temperature: temperature measured from the TC (thermocouple) installed in the external wall of the internal pipe
- Internal wall temperature: temperature of the internal wall pipe of the internal tube extract from the TC values and taking into account also of the different layer of the sensor and the thickness of the pipe
- Propane linear/in-out/out-in temperature: these methods are already descripted in the **chapter 3.1;** only in the case of condensation is possible to obtain another method for the propane linear temperature based on the saturation pressure measured with the AP5,6 sensor instead of the value of the temperature from the RTD12

After this overview is suitable to present the temperature graphs included in the data reduction file that transduce these numerical information.

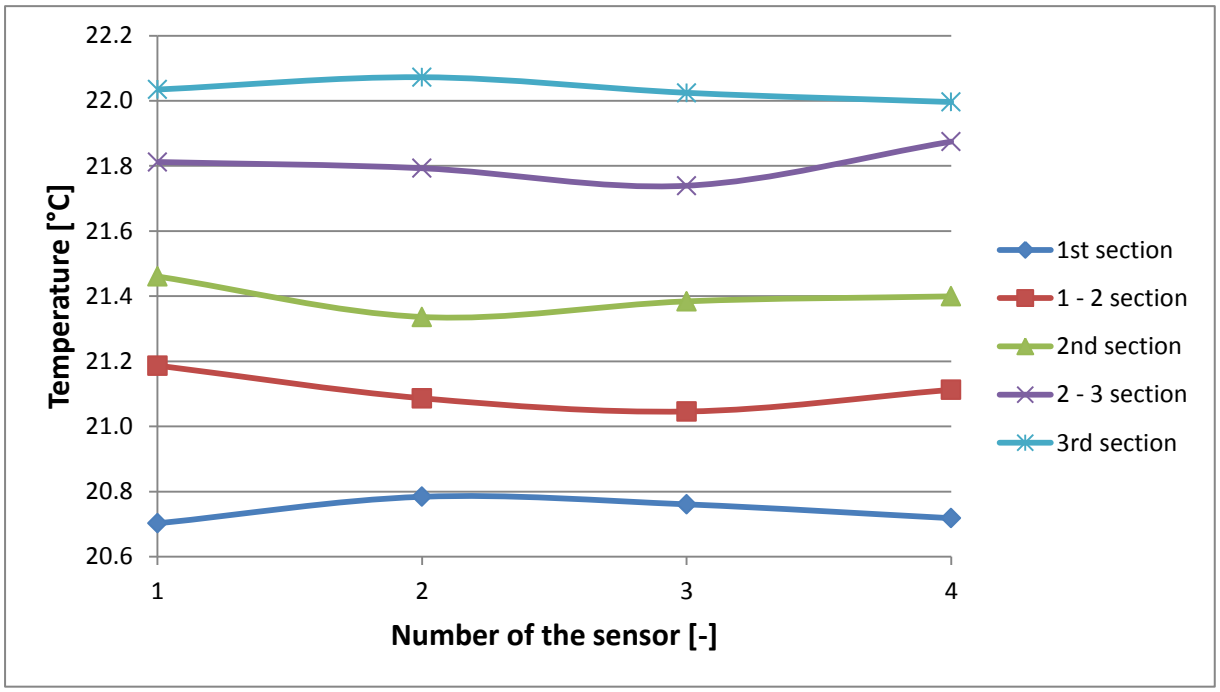

Figure 28: Trend of the temperature of the oil in each section

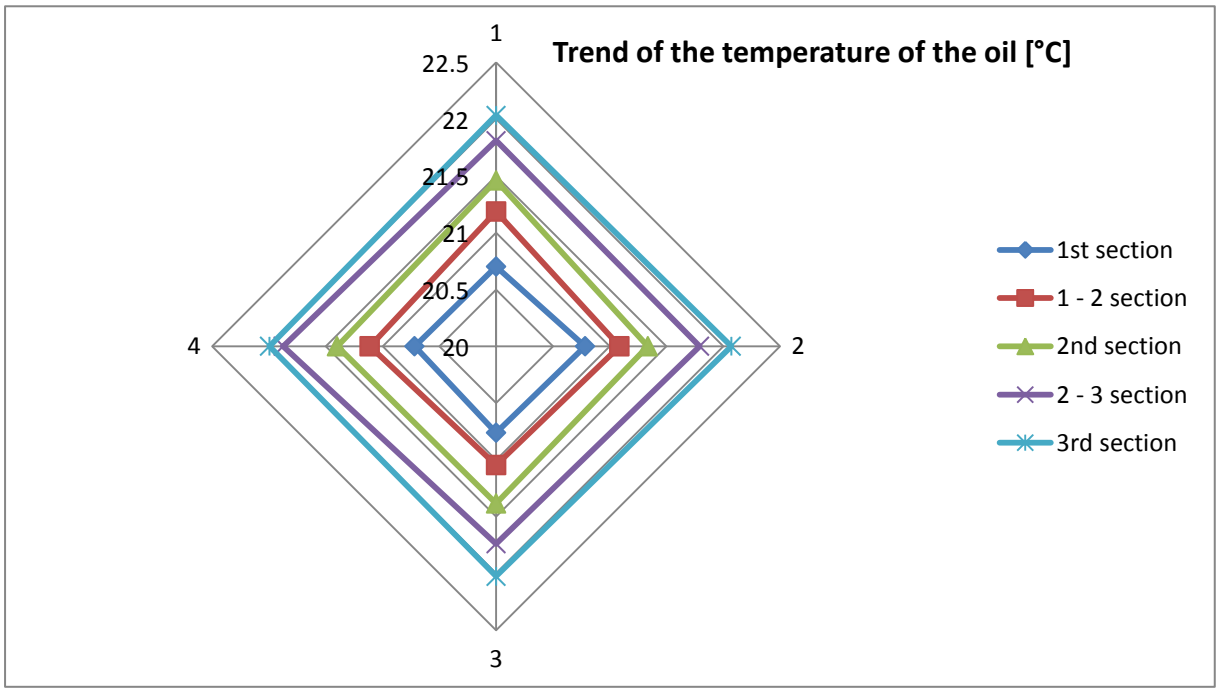

Figure 29: Trend of the temperature of the oil along the cross section

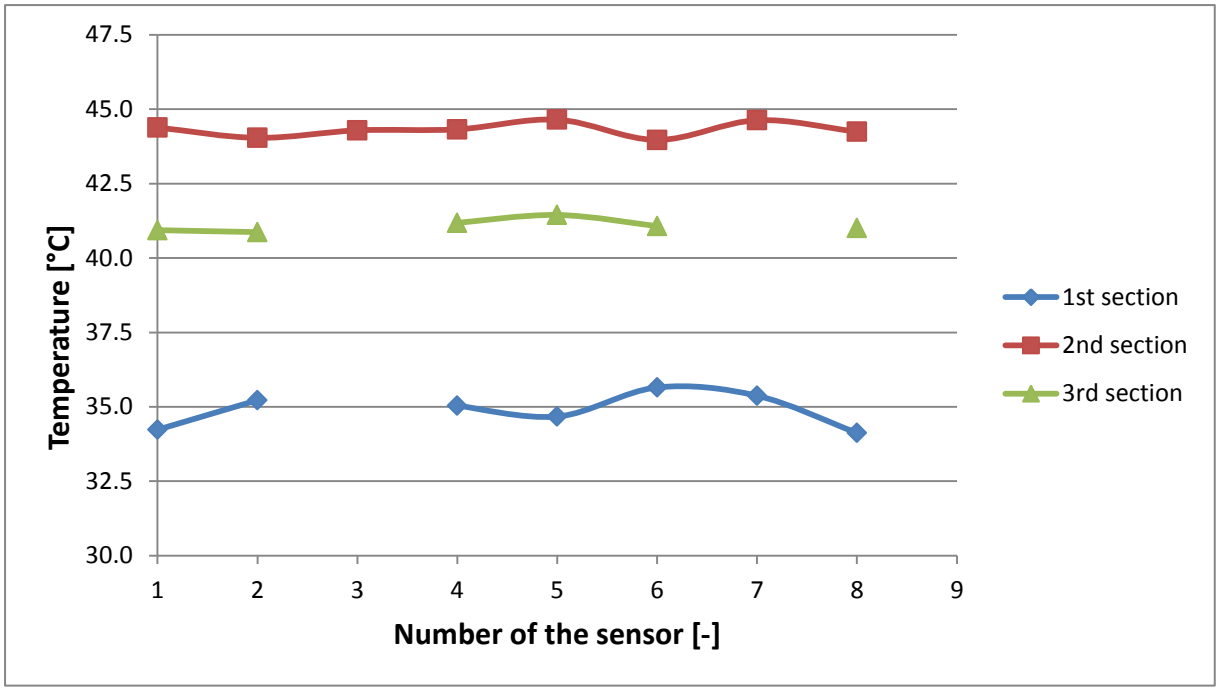

Figure 30: Trend of the temperature of the external wall in each section (the white space means that some TC are unreliable and are out of the measurement)

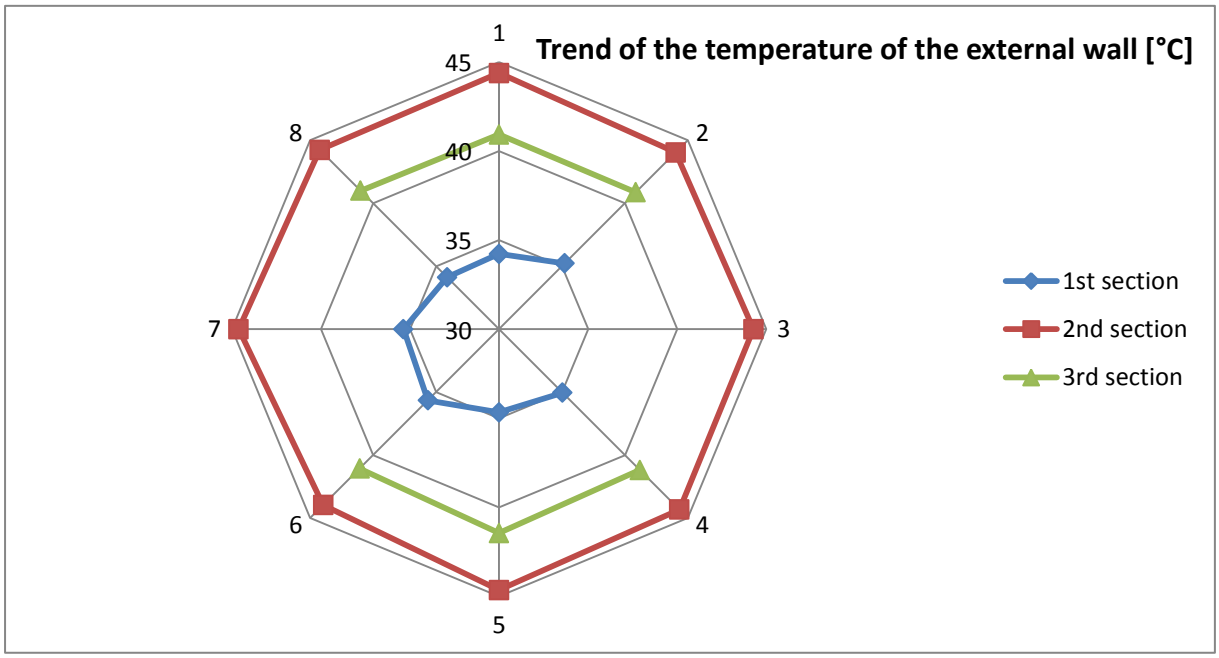

Figure 31: Trend of the temperature of the external wall along the cross section in the internal pipe

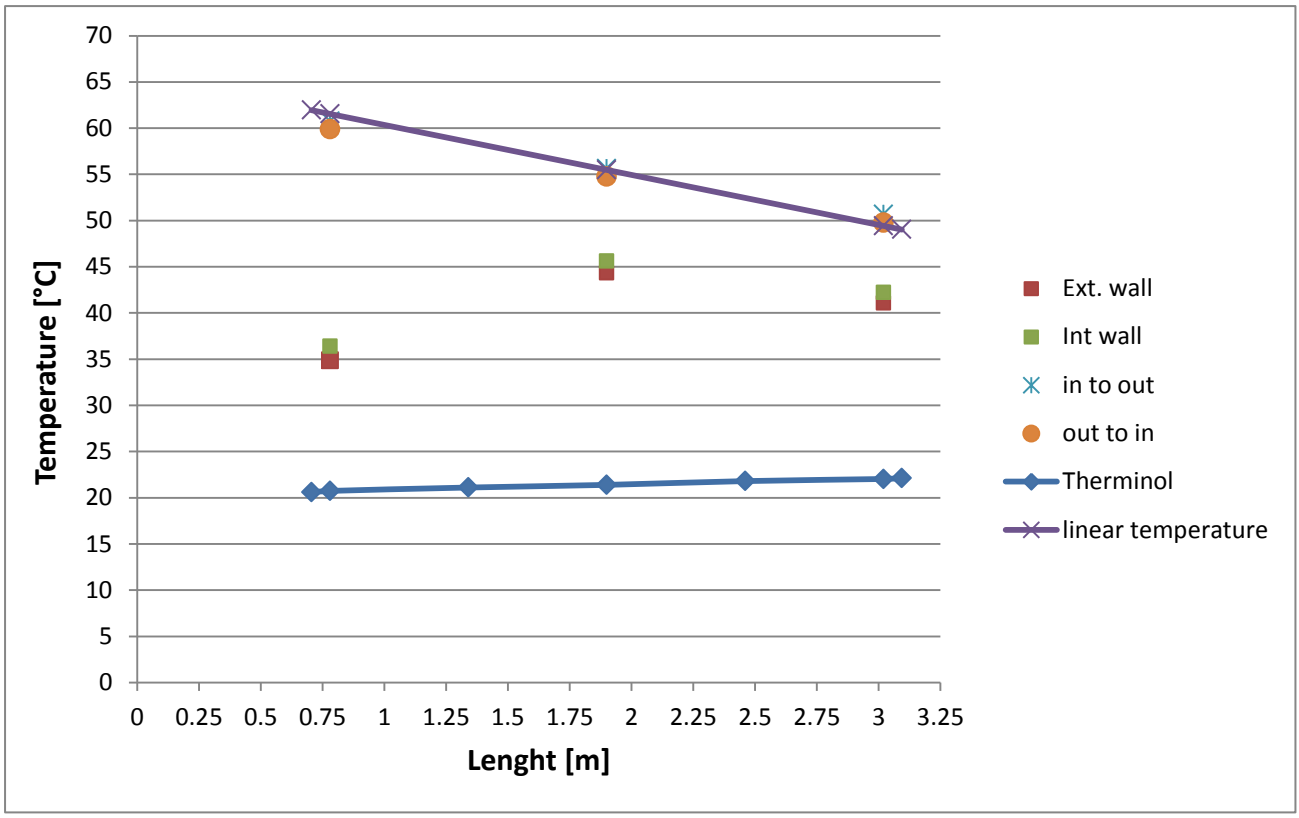

Figure 32: Final overview (in this case from gas cooling data reduction)

Vapour quality - Propan								
object	x_in	1st section	1 - 2 section	2nd section	2 - 3 section	3rd section	x_out	Delta x
2-ph propane quality x mass	Quality (Coriolis)	Quality	Quality	Quality	Quality	Quality	Quality	delta Q out-in
	[-]	[-]	[-]	[-]	[-]	[-]	[-]	
	0,494122373	0,47	0,435009717	0,41	0,357435345	0,33	0,317990469	-0,176131904
2-ph propane LV-->RP	Quality	Quality	Quality	Quality	Quality	Quality	Quality	delta Q out-in
	[-]	[-]	[-]	[-]	[-]	[-]	[-]	
	0,509592794	0,49	0,450480138	0,42	0,372905765	0,35	0,334099382	-0,175493412

Figure 33: Summary relating to the trend of the vapour quality along the tube

Object:

- 2-ph propane quality x mass: start value is from the mass flow sensors in the liquid and gas line
- 2-ph propane: the start value is calculated from the REFPROP tool

- In both cases the quality along the tube is calculated from the balance between working fluid and oil.

4.7 Heat transfer coefficient section

This is one of the most important sections and represents the final result of the measurement and gives the comparison between the literature and the experimental result; as described in the chapter 3.3, the alpha coefficient is calculated in 3 different ways:

1) mean heat transfer coefficient referred to every measurement section

It is possible to extract 3 different values of the heat transfer coefficient in single-phase due to 3 different methods to calculate the propane temperature along the test section.

Propane HTC Calculation per Measurement Section									
WF Temp.	Delta1 (1-3)	Alpha_in,1	%Alpha Petu	Delta2 (1-3)	Alpha_in,2	%Alpha Petu	Delta3 (1-3)	Alpha_in,3	%Alpha Pet
	°C	W/m^2*K		°C	W/m^2*K		°C	W/m^2*K	
In-Out	29,30	630	-52,75%	12,79	1332	-0,08%	10,38	1423	6,74%
Out-In	28,55	647	-51,45%	12,04	1424	6,76%	9,64	1546	15,95%
Linear	30,15	612	-54,13%	12,72	1340	0,50%	9,11	1647	23,51%

Figure 34: Htc coefficient calculated for each measurement section (1, 2, and 3) in single phase condition of the working fluid

It is possible to extract 2 different values of the heat transfer coefficient in condensation due to 2 different methods to calculate the propane temperature along the test section.

Propane HTC Calculation per Measurement Section									
WF Temp.	Delta1 (1-3)	Alpha_in,1	%Alpha Cav	Delta2 (1-3)	Alpha_in,2	%Alpha Cav	Delta3 (1-3)	Alpha_in,3	%Alpha Cav
	°C	W/m^2*K		°C	W/m^2*K		°C	W/m^2*K	
Linear based on temperature	19,18	1183	-66,41%	8,17	3260	0,23%	8,14	3382	15,93%
Linear based on pressure	19,45	1165	-66,92%	8,48	3110	-4,39%	8,50	3203	9,78%

Figure 35: Htc coefficient calculated for each measurement section (1, 2, and 3) in condensation

2) mean heat transfer coefficient with small boundary conditions between the first and third measurement section

	LMTD Propane HTC Calculation (integral)					
	Alpha(1-3) W/m^2*K	%Alpha Petu	Alpha(1-2) W/m^2*K	%Alpha Petu	Alpha(2-3) W/m^2*K	%Alpha Petu
In-Out	893	-33,07%	916	-31,30%	1426	6,95%
Out-In	937	-29,70%	962	-27,83%	1536	15,22%
Linear	928	-30,39%	953	-28,54%	1533	14,99%

Figure 36: mean heat transfer coefficient in single-phase condition

Legend:

- (1-3): mean alpha coefficient between the first and the third section
- (1-2): mean alpha coefficient between the first and the second section
- (2-3): mean alpha coefficient between the second and the third section

	LMTD Propane HTC Calculation (integral)					
	Alpha(1-3) W/m^2*K	%Alpha Cav	Alpha(1-2) W/m^2*K	%Alpha Cav	Alpha(2-3) W/m^2*K	%Alpha Cav
Linear based on temperature	1863	-42,15%	1673	-50,60%	3566	15,60%
Linear based on pressure	1807	-43,89%	1624	-52,07%	3387	9,79%

Figure 37: mean heat transfer coefficient in condensation case

3) mean heat transfer coefficient of the whole pipe

Through the calculation of the external alpha coefficient for each measurement section is possible extract the internal alpha coefficient; the problem is that this value is not reliable because $\boldsymbol{\alpha\_oil} \ll \boldsymbol{\alpha\_propane}$ and a little error in the calculation of the alpha external correspond to a bigger error in the internal alpha.

Oil HTC Calculation per Measurement Section		
Alpha_out,1	Alpha_out,2	Alpha_out,3
W/m^2*K	W/m^2*K	W/m^2*K
1296	588	629

Figure 38: Htc coefficient of the oil calculated for each measurement section (1, 2, and 3)

	DT_ml(th-wf)	KA (1-3)	K_i (1-3)	Alpha(1-3)	%Alpha Petu
	°C	W/m^2*K	W/K	W/m^2*K	
In-Out	32,93	47,79	463,51	1930	44,75%
Out-In	32,17	48,91	474,40	2134	60,06%
Linear	32,56	48,33	468,80	2026	51,90%

Figure 39: example of the mean heat transfer coefficient of the whole pipe in single-phase condition

On other side there are the results from the correlations:

Propane HTC Correlat	Liquid cooling / Gas cooling							Gas cooling	
Nu Dittus	Alpha Dittus	Friction f.	Nu Gnielin.	Alpha Gn.	C Petukhov	Nu Petukhov	Alpha Pet.	Nu Hausen	Alpha Ha
	W/m^2*K			W/m^2*K			W/m^2*K	gas only	W/m^2*K
918,3	1420	0,013	866,6	1340	1,00	862,4	1333	860,1	1330

Figure 40: Htc correlation for the liquid/gas cooling of Dittus Böelter, Gnielinski, Petukhov and Popov

Condensation 2° section							
Xtt (Lochkhart-Marti	Jg Increasing Ratio of Sh	Jg^T	Alpha Cavallini et a	alphaLiq	alphaStrati	Ct (hydrc	Tsat
[-]	[-]		W/m^2*K				[°C]
0,500	2,58594581	1,48125	3252,380542	1255,42	1204,039	1,6	44,2351

Figure 41: Htc correlation for Condensation of Cavallini et al., 2006 [9]; this alpha is calculated for each measurement section in function of the vapour quality x

In order to check the flow pattern inside the tube the tool is equipped with the map of Breber:

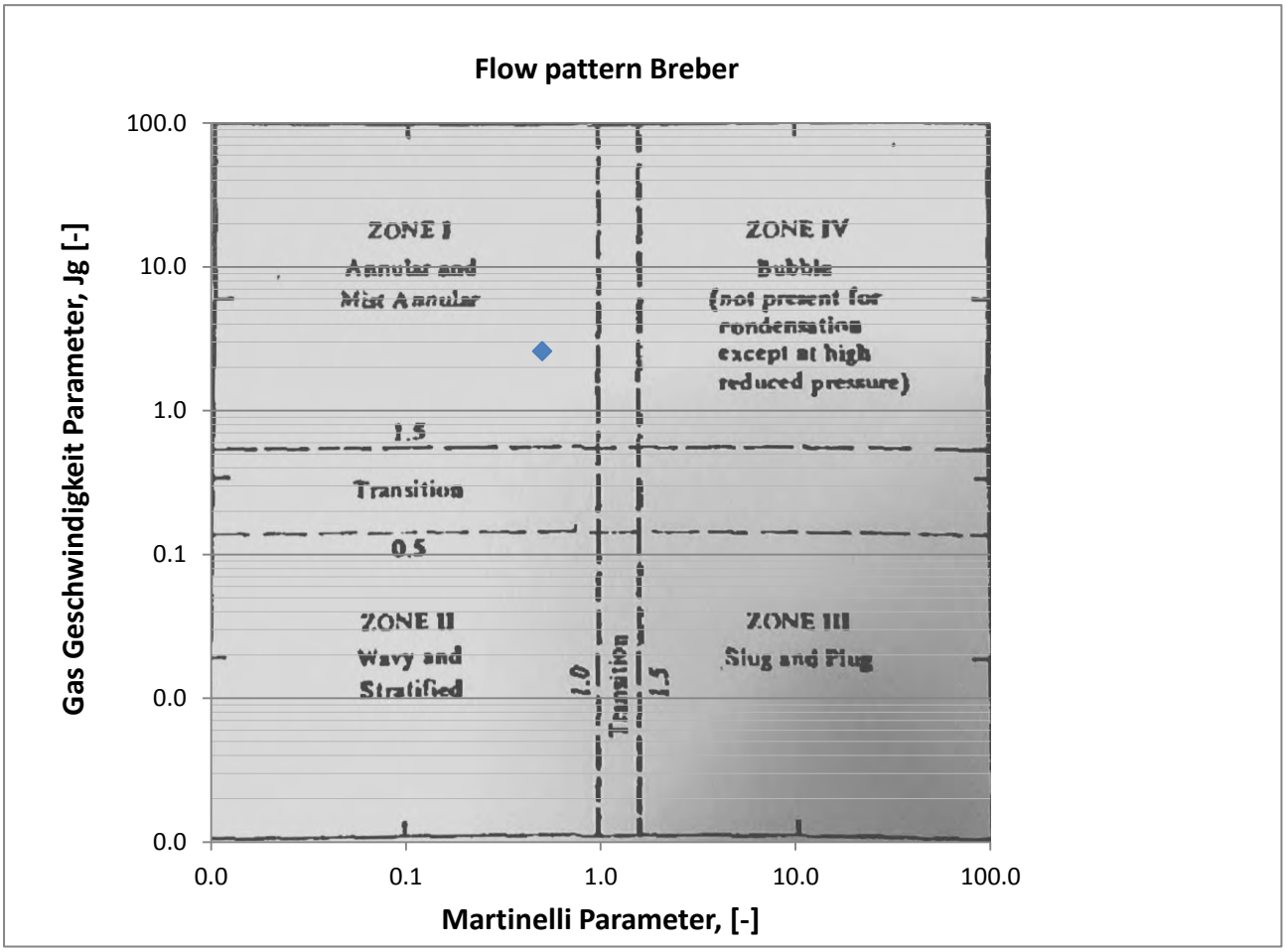

Figure 42: Map of Breber [2]

All the correlations are descripted in the chapter 3.2.

4.8 Pressure drop

The final section is dedicated to the pressure drop in single and double phase; the correlations used are descripted in the chapter 3.4.

	deltaP correlation	velocity wf
Pa	10144,50144	16,31593684
bar	0,101445014	
mbar	101,4450144	
%	9,9%	

Figure 43: Pressure drop for single phase

pressure drop-Friedel	in	out		
liquid density	460	460	Φfr^2	7,431408355
vapour density	33,54203739	33,49318666	E	1,83821002
Δpmom	-267,0795077		FrH	105,512815
void fraction Zivi	0,787360355		F	0,429747287
Δpfrict	3925,005358		H	6,599337621
ΔpL	528,1644031		WeL	3618,749117
Δptot [Pa]	3658		sigma	0,004730663
Δptot [bar]	0,036579259			
Δptot [mbar]	36,5792585			

Figure 44: Pressure drop in 2-phase condition

4.9 Final summary

In this line are reported the principal result with the aim to have a fast method to compare the different measurements

measureament	Re_wf	velocity wf	Prandtl wf	T_in,wf	T_out,wf	Delta T_wf	T_in,
G03	601784	16,31593684	0,8426	61,83959416	46,88142339	14,96	2

Figure 45: Summary for each measurement

5 Commissioning with propane

The commissioning of the test facility with propane has the aim to create, check and improve the procedure for the early approach with the entire facility in order to have a right way to fill the working fluid inside the cycle and to be secure about the safety of this operation.

5.1 Filling procedure

For safety and technical reasons the filling amount should be as little as possible but as much as needed.

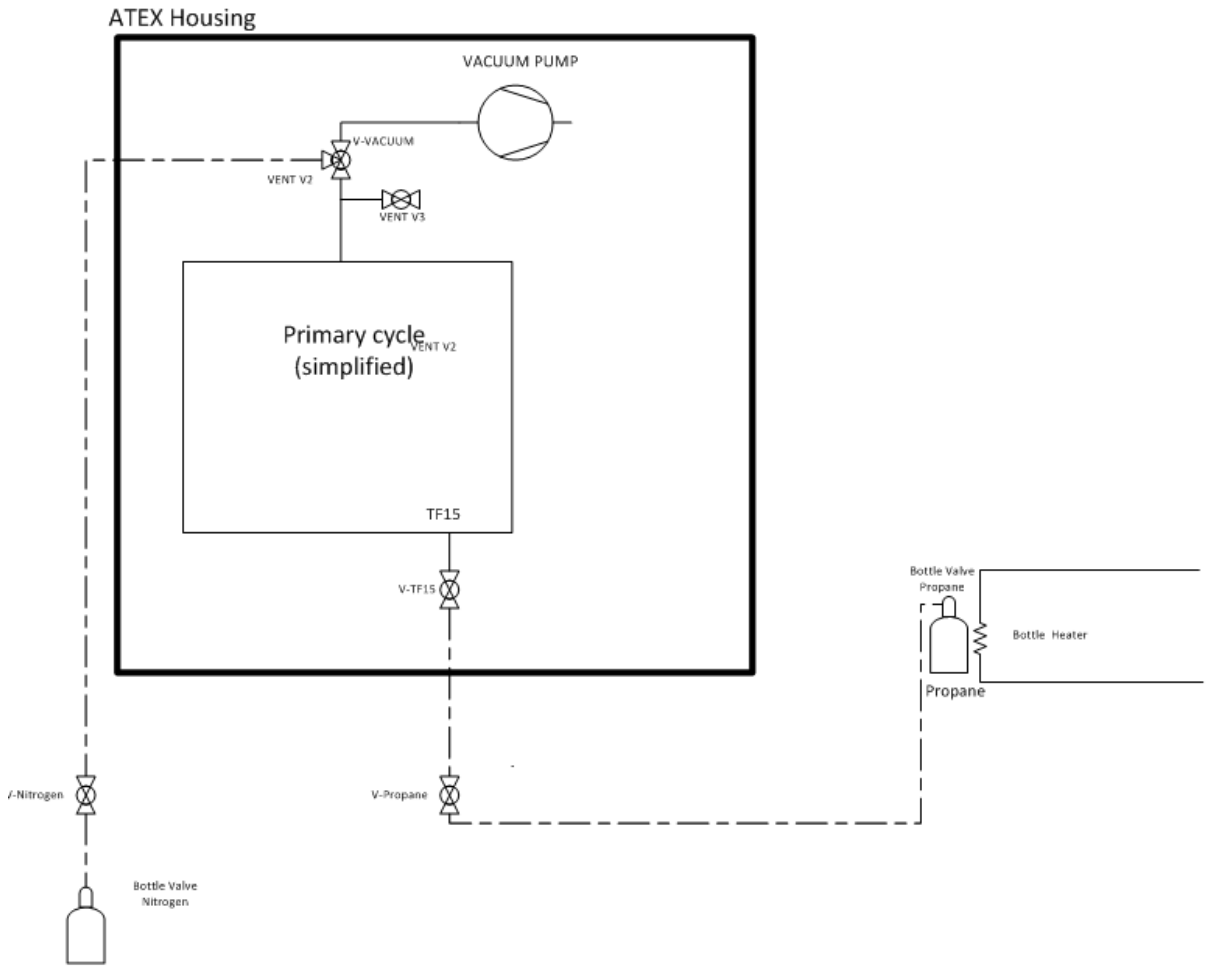

Figure 46: Layout for the filling process

Steps for the filling process:

- Preparation for the filling:

1. First of all a pressure test of the test rig with opened valves [VENT-V2] and [V-TF-15] has to be conducted successfully
2. Gas alarm system of the test rig and the lab-view software have to be activated
3. Close all outgoing ball valves (including [V-Nitrogen] and [V-P-Flush], [V-Vacuum]
4. Open all internal ball valves ([SDV 1], [SDV 2], … , [SDV 7] including [VENT-V2] and [VTF-15])
5. Connect Vacuum Pump to the flange "connection vacuum"
6. Transport nitrogen and propane bottles from the bottle store to the laboratory and label and weigh all propane bottles

- Filling procedure:

1. Connect capillary tubes [N2] from nitrogen bottle to the valve [V-Nitrogen] and [P2] from propane bottle to [V-Propane]
2. Open nitrogen bottle and pressurize [N2]; after this step is advisable to check with the leak detector spray the sealing in the connection between nitrogen bottle and [V-Nitrogen]
3. Vacuum process: in order to avoid the o2 presence in the test rig a vacuum pump is installed; so, the aim is to vacuumize the test rig to 0.1 bar. Afterwards (stop vacuum pump), nitrogen from valve [V-Nitrogen] is introduce in the test rig with a pressure of 2.5 bar and meanwhile open valve [VENT-V3] carefully to release the pressure and close it when the pressure in the test rig reaches the pressure between 1.05 ÷ 1.1 bar.
   Close the valve [V-Nitrogen] and [VENT V2] and seal the valve [VENT-V3] with a blind flange; afterwards dismount the tube [N2], close the connection of [V-nitrogen] with a cap and start again the vacuum pump with the aim to vacuumize test rig to 0.1 bar.
   Cool down test rig as much as possible using the loop cooling A, cooling B and cooling C. In this process the Multi phase Pump remains off.

Close valve [V-Vacuum] and stop the vacuum pump; Dismount the vacuum pump and seal the vacuum-valve-flange with a blind flange.
Remove the vacuum pump from the Atex-zone

4. Now is time to introduce the propane in the test rig; first of all the, connection between heater and propane bottle is done and we can open the bottle valve propane; after this step is advisable to check with the leak detector spray the sealing in the connection between propane bottle and [V-Propane]
5. Open Valve [V-P-Flush] for 15 seconds and close the valve
6. Use Valve [V-Propane] to connect tube [p2] and tube [p1]
7. Turn on bottle heater, wait until the bottle is empty and turn off.
8. Close [bottle valve propane]
9. Use [v-propane] to connect tube [p2] and tube [p flush 1]
10. Dismount [p2] and propane bottle; [p2] is filled with propane, this propane will exhaust in the lab
11. Weigh propane bottle and remove it from the lab; repeat this procedure until the test rig is filled and then close [V-TF15].
    Dismount tube [p2], close former connection of [p2] of [V-Propane] with a cap and close tube [P flush 2] with a cap.
12. Calculate and document the total filling amount
13. Check the propane concentration in the housing
14. Stop the fan for 15 minutes and check the propane concentration again
15. Start the fan
16. Document the propane concentration with and without fan and use leak detector spray to check the connection of the blind flanges "vent" and "vacuum" and the valves [VENT V2] and [V-TF15]
17. Test rig is filled

- <u>Emptying process:</u>

    1. Weigh all propane bottles in the bottle store and calculate the desired filling amount for each bottle in order to have an idea about the capacity of each bottle
    2. Bring at least two full nitrogen bottles in the lab
    3. Open valve [V-boem] and [V-Nitrogen] and [V-p-flush] remain closed
    4. Use Valve [V-Propane] to connect tube [p1] and tube [p-flush-1] and remove the caps of [tube P flush 2] and [V-Propane]
    5. Connect tube [p2] with [V-Propane]

6. Bring empty propane bottle in the lab and put the propane bottle in a vessel on a scale
7. Connect capillary tube [p2] and the bottle
8. Put ice in the vessel and document the weight
9. Open the [bottle valve propane] and use [V-Propane] to connect [p1] and [p2]; wait until the bottle's desired filling amount is reached and document the weight of filled bottle, water/ice and the vessel
10. Close the [bottle valve propane] and use [V-Propane] to connect [p1] and [p-flush-1]; afterwards dismount tube [p2] from the bottle valve and remove the vessel and the bottle from the scale
11. Bring filled propane bottle out of the lab in the gas bottle store
12. Advice: Applying this method the pressure in the test rig can be decreased up to 6 bar (presuming a bottle temperature of 10°C).
    If the emptying process stagnates, the test rig should be slightly heated to 40°C, using Cooling A, B or C.
    Otherwise, if the filling process stagnates and the heating of the test rig and cooling of the bottles doesn't help any more:
    calculate the remaining propane mass (estimated 9kg for a volume of 300 l and a Temperature of 40°C if only gas phase in the test rig)

13. Remove the cap of [V-Nitrogen], connect [n1] to both [VENT V2] and [V-Nitrogen]; open the [nitrogen bottle valve] and the valve [valve-nitrogen]
14. Flush the test rig and open Valve [V-boem] periodically; flush at least with 2 bottles of Nitrogen (79l)
15. Check propane concentration in the housing
16. Remove the blind flange of the bleed valve
    open Valve [VENT V3]
    check propane concentration
    close valve [V-boem]
    check propane concentration
    close [valve-nitrogen]
    close [bottle valve nitrogen]
    dismount [n2]
    bring propane bottle in the gas store
17. Stop fan for 15 minutes, meanwhile check and document the propane concentration
18. Emptying process finished

5.2 Leakage test

In order to avoid fire risks, by means of a first start of the facility with the propane, leakage test with nitrogen are the first step. The second step is to run the test rig with propane and perform the same test carried out before.
For this purpose, in order to check possible leakages in the test rig, the pressure time dependency is analysed as shown in Figure 47; pressure and temperature are measured by an absolute pressure and a temperature sensors involved in the cycle. With this method is possible to obtain a rough idea about leakages in the test rig and to ensure this fact, is advisable to check with the leak detector spray the sealing in the connection.
About the graph in order to reduce the complexity, a small number of sensors were chosen with the purpose to represent the whole cycle:

1. Pressure sensors: AP4 and AP5,6
2. Temperature sensors: RTD02, RTD03, RTD04, RTD05

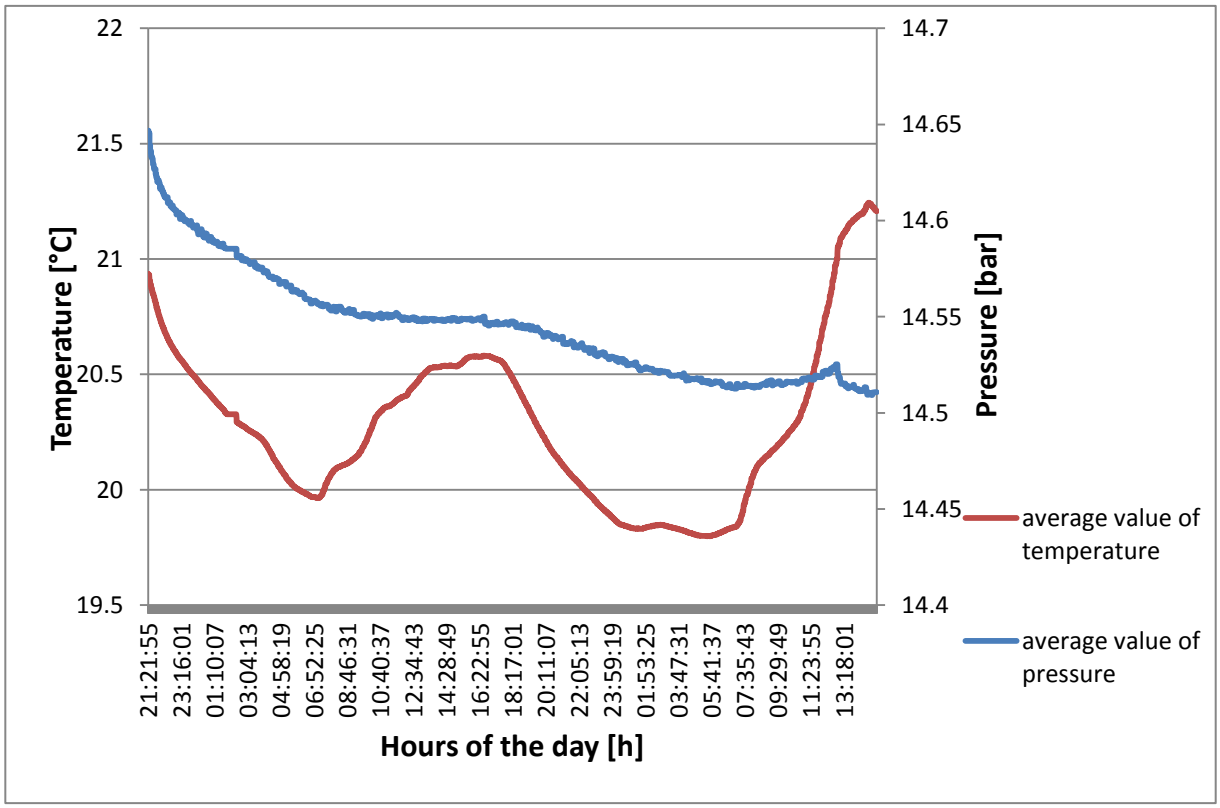

Figure 47: nitrogen pressure and temperature (vs. time) trend analysis of the test facility

Evaluation criteria:

1) The trend analysis in the first part shows a strange tendency compared to the rest of the graph, probably due to facility´s start up, in other words this can be maybe justified from small leakages and cavities in the sealing that have to be pressurized in the first stage.
   For this reason the calculation of the Leakage rate is done not considering the first part of the chart.

2) About the evaluation of the leakage rate, a temperature T= 20,5 °C is chosen and for this value , 2 pressure points are extract in correspondence to the rising trend of the temperature:

   Pressure sampled at the temperature T= 20.5 °C:

   Initial pressure = 14,549047 bar
   Final pressure = 14,517206 bar
   ΔP = 0,031841 bar
   Time between the 2 points Δt = 80451 s
   Facility volume V = 280 l

$$\text{Leakage rate} = \frac{\Delta P \cdot V}{\Delta t} \qquad 5.1$$

Results:

$$\text{Leakage rate} = 0{,}11082 \ \frac{\text{mbar l}}{\text{s}}$$

$$Leakage\ rate = \ 110{,}82 \ \frac{\text{mbar m}^3}{\text{s}}$$

$$\text{Leakage rate} = \ 11{,}082 \ \frac{\text{Pa l}}{\text{s}}$$

The results reveal a low leakage rate presence in the test rig.
Therefore, second step is to launch the test rig with propane and perform the same test.
About the graph in order to reduce the complexity, a small number of sensors were chosen with the purpose to represent the whole cycle:

1. Pressure sensors: AP4 and AP5,6
2. Temperature sensors: RTD02, RTD03, RTD04, RTD05

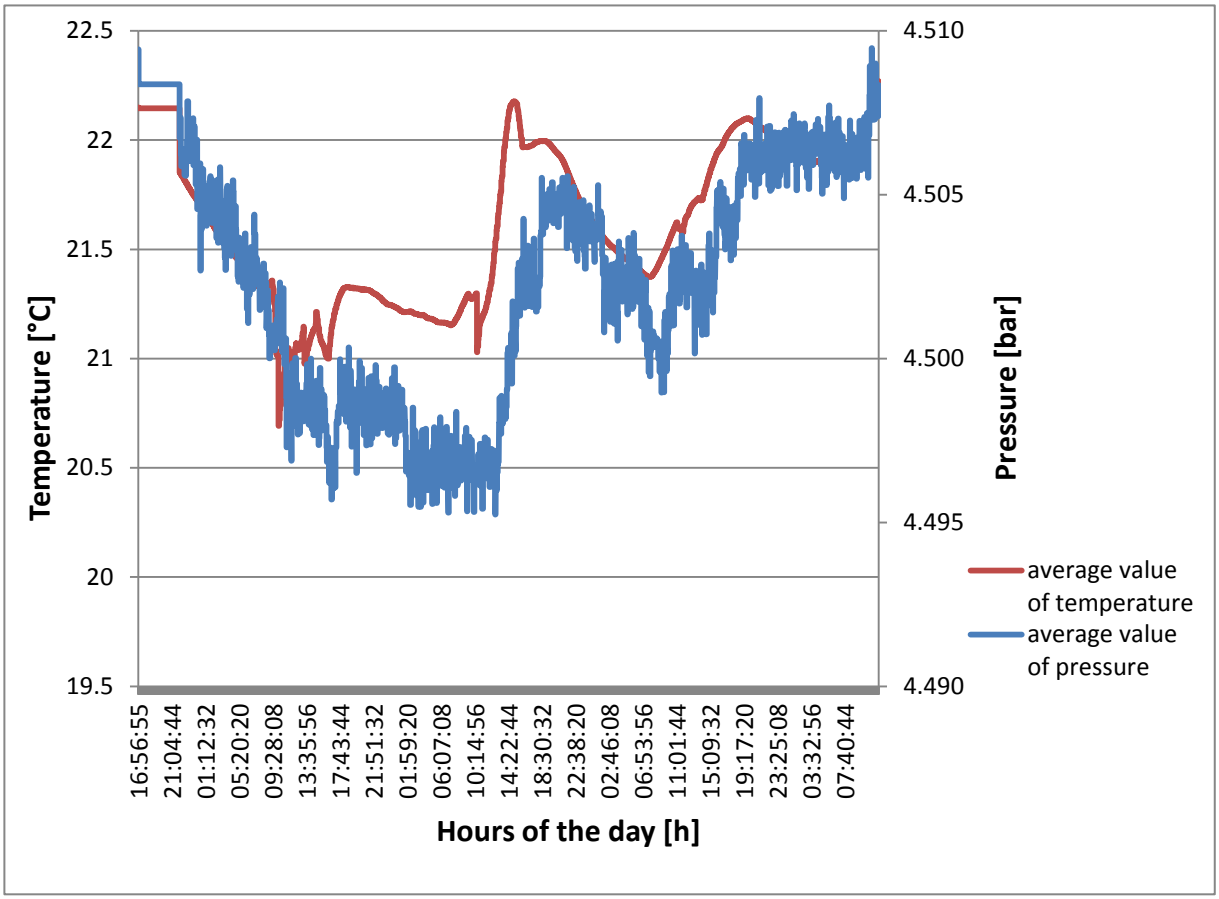

Figure 48: propane pressure and temperature (vs. time) trend analysis of the test facility

Evaluation criteria:

1) About the evaluation of the leakage rate, a temperature T= 20,7 °C is chosen and for this value , 2 pressure points are extract in correspondence to the value of the temperature:

   Pressure sampled at the temperature T= 20.7 °C:

   Initial pressure = 4,5059565 bar
   Final pressure = 4,5020145 bar
   ΔP = 0,003942 bar
   Time between the 2 points Δt = 217203 s
   Facility volume V = 280 l

$$\text{Leakage rate} = \frac{\Delta P \cdot V}{\Delta t} \qquad 5.2$$

Results:

$$\text{Leakage rate} = 0{,}005081698 \ \frac{\text{mbar l}}{\text{s}}$$

$$\text{Leakage rate} = \ 5{,}081697767 \ \frac{\text{mbar m}^3}{\text{s}}$$

$$\text{Leakage rate} = 0{,}508169777 \ \frac{\text{Pa l}}{\text{s}}$$

Results reveal a very low leakages presence in the test rig.

6 Experimental results

In this chapter the results of the measurements are shown in order to understand the functionality of the cycle in use with saturated propane.
It is interesting in general to check if the entire facility is able and how to reach specific desired points and to verify if the results are reliable or not in order to validate the experimental outputs.

The conducted measurements are reported in this sequence:

1) Liquid cooling
2) Gas cooling
3) Condensation

Scheduling:

LIQ COOLING	FIX CONDITIONS	
	Pin=12 bar	Tin= 33,8 °C
Reynolds number [-]		
Program	option	facoltative option
		1000
		2000
		5000
	10000	
		15000
	25000	
50000		
	75000	
100000		
	125000	
150000		
	175000	
200000		
	225000	
250000		
300000		

Figure 49: Liquid cooling plan

GAS COOLING	FIX CONDITIONS	
	Pin=12 bar	Tin= 62 -78 °C
Reynolds number		
Program	option	
	50000	
	100000	
150000		
200000		
250000		
300000		
350000		
400000		
500000		
600000		
700000		
800000		

Figure 50: Gas cooling plan

Condensation	Fix conditions	
	Pin=12 bar - 15 bar	
	G=300 kg/m^s	
vapor quality x [-]		
Program	option	
0		
0.1		
	0.2	
0.3		
	0.4	
0.5		
	0.6	
0.7		
	0.8	
0.9		
1		

Figure 51: Condensation plan

6.1 Measuring with the KIIR Test Facility

The components of the facility that have to be activated before starting the measurements are: the LabVIEW software that is used to control the rig and to save the measured values collected from it, the multiphase pump that allow the movement of the process fluid in the primary cycle and all the necessary secondary cycles that permit to set the temperatures of the working fluid.
The inlet secondary cycle heats the working fluid in order to set the inlet temperature of the test rig. When the LabVIEW software is booting and the pump is on, all the valves are set to 100% open and the rotational speed of the pump is set to 400 rpm, the minimum value that allows the pump to run. This is the starting configuration of every measurement session and during this time it is important to pay attention to the flow condition in the pump and the fact that all the valve, gas and liquid side, are fully open. Afterwards, the *SECTS* and *SECTSI* are turned on with a specific temperature set in the thermostat; if change is necessary it, temperature should be changed carefully.
Once the wanted mass flow of the working fluid is set, it is important to wait for the inlet temperature of the working fluid to become stable.
The mass flow can be regulated by the needle valve situated in the primary cycle, by RV6 installed in the bypass or by the rotational speed of the pump or by a combination of the valve of liquid side (RV4 and RV5) and gas side (RV1, RV2 and RV3); with these valve collocates in the liquid and gas side, it's also possible to set the vapour quality. These possibilities, contribute to vary the pressure lost in the rig, and so it is always important to check the working condition of the pump, with the aim to work inside the available range of pressure for it. In this way is it possible to set the desired fluid characteristic before the recording.
After a measuring session, the facility has to be stopped. The right way to do this is to shut down the heater of the SECTSI and let run the whole plant for five minutes, in order to cool the fluids in it. Afterward it is possible to shut off the entire components and at last to close the LabVIEW software.

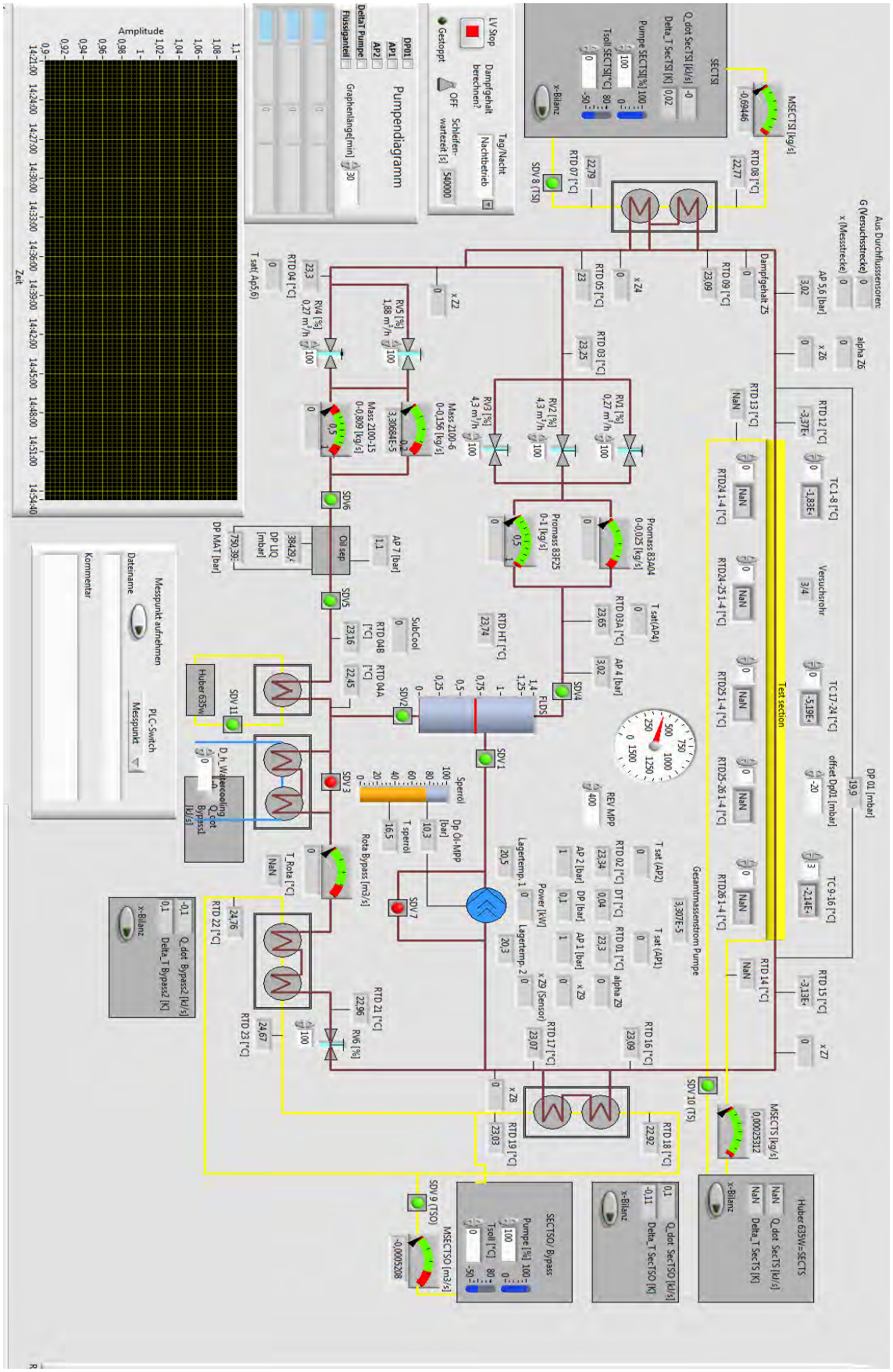

Figure 52: LabVIEW screen

6.2 Liquid Cooling

First of all it is important that the measurements are carried out in steady state conditions, because it doesn't make sense to start with the data acquisition meanwhile the values measured by the sensors are not stable. Furthermore is also important to verify the reproducibility relative the same test in order to check any strange behaviour and to confirm the validation of the data acquisition. This information is done with the aim to get reliable data acquisition.
The liquid cooling test is lead with a constant pressure P_{in}=12 bar and with different values of Reynolds number.
The parameters that are important to control and to verify, about steady state conditions are:

1. Mass flow rate G [kg/(m^2*s)]
2. Pressure upstream the test rig measured by AP5,6 sensor
3. Temperature upstream test rig measured by RTD12

As explained before, to manage these parameters, mass flow (so, the Reynolds number) is regulated by the needle valve situated in the primary cycle, pressure is regulated by the heat exchanger in the bypass line and finally, temperature at the inlet of test rig is controlled by the Huber 825 W upstream the oil separator.

6.2.1 Steady state conditions

In order to compare the steady state conditions of these 3 parameters it's useful to take a look to the Figure 53 to get an idea about the fluctuation.
G and pressure upstream the test rig measured by AP5,6 sensor are in each measurements quite constant but instead of this good results the temperature upstream test rig measured by RTD12 is a difficult parameter to handle.
This fact could be due to the reason that these points were recorded before the system was stable.

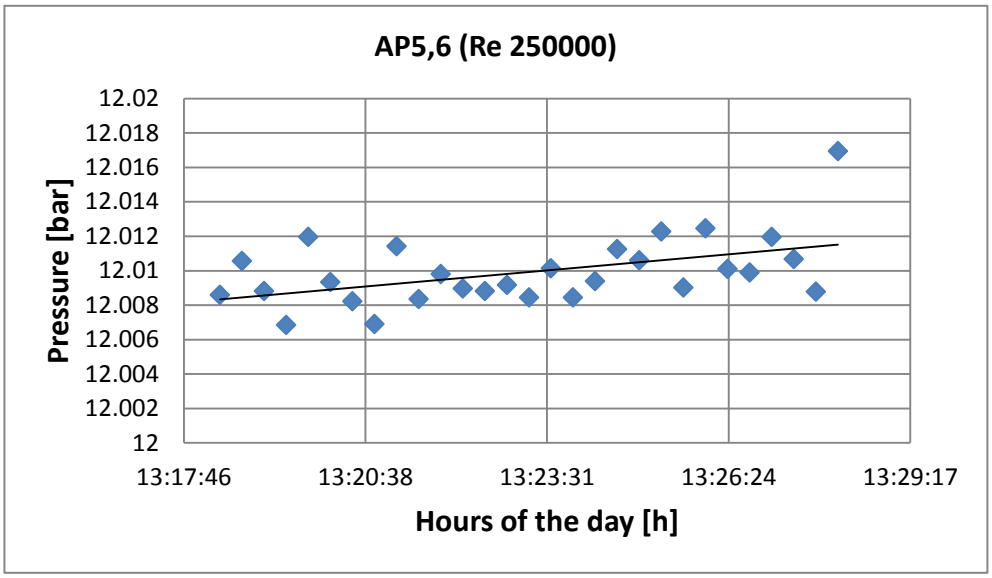

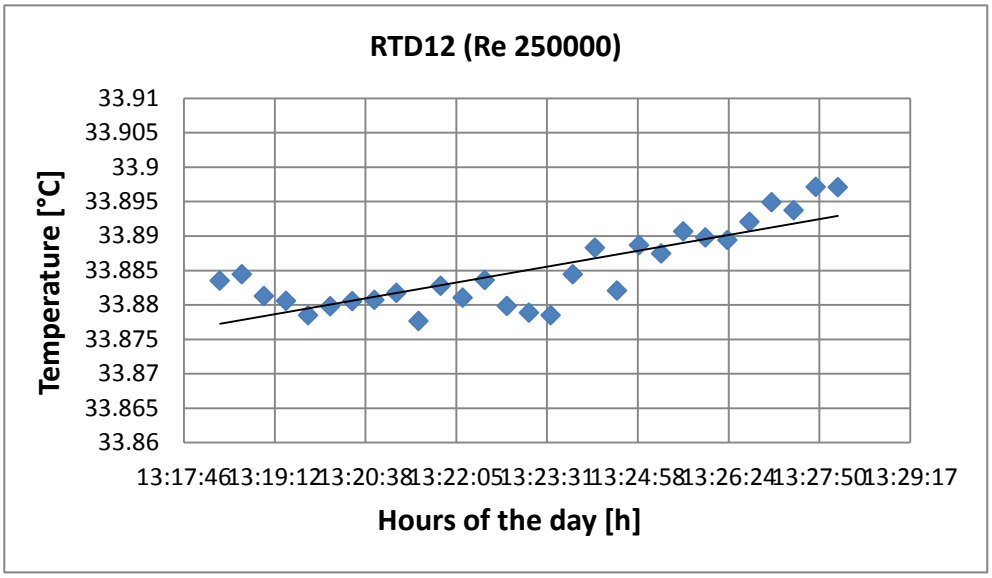

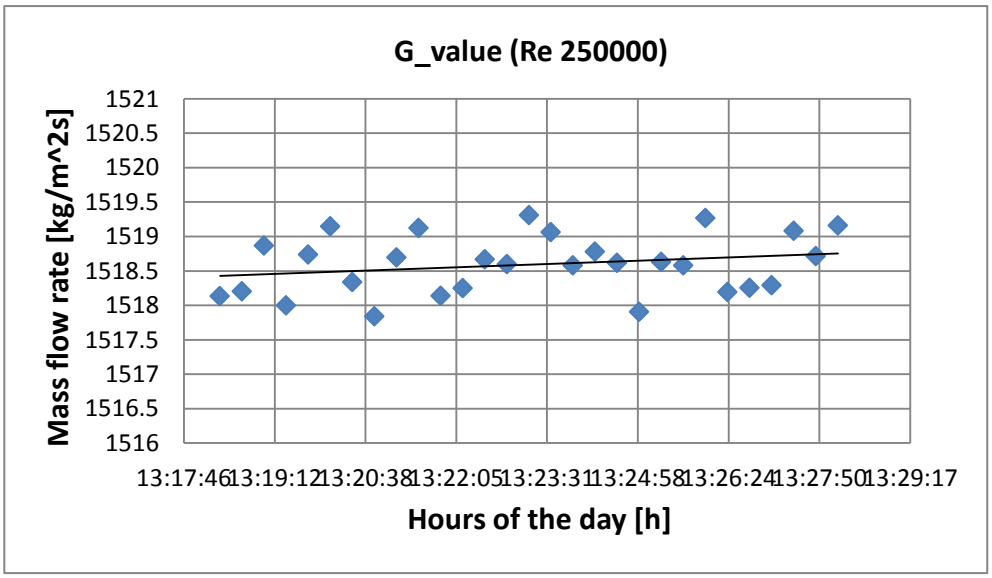

Figure 53: G, Pressure by AP5,6 ,Temperature by RTD12 with Re250·10^3

Table 6: maximum deviation ΔT in some measurements

Re [-]	Maximum deviation ΔT [°C]
250·10^3	0,019468
200·10^3	0,02128
150·10^3	0,060837
125·10^3	0,295892
100·10^3	0,2952
75·10^3	0,263747
50·10^3	0,075717

In conclusion it´s possible to assert that the facility works with in a stable conditions, with the advice that the control of temperature sometimes requires more time to reach the stable condition.

6.2.2 Reproducibilty

Reproducibility is the concordance rate between the results of the same sample when the measurements are conducted with different conditions like: measurement method, observant, place, time, conditions of use. In order that an affirmation about the reproducibility is considerable it is necessary to specify the conditions that change.

The purpose of this chapter is to verify how the test rig is able to set a particular and predefined condition, the parameters that change are the time that measurements are registered (different days) and the observant.

The desire points (in order to reach Re250·10^3 and Re200·10^3) are listed in Table 7:

Table 7: Reproducibility tests:

	G_wf [kg/(m^2*s)]	P (AP 5,6) [bar]	nr.test [-]
1	1512	12	2
2	1210	12	2

The reproducibility of the results is observed and compared using the coefficient of variation, also known as relative standard deviation, defined as:

$$COV = \frac{Standard\ Deviation}{Mean\ Value} \tag{6.3}$$

The specific mass flow G of the working fluid shows very good reproducibility (0,55% for Re250·10^3 and 0,43% for Re200·10^3). The working fluid flow is connected to the Reynolds number that means that also this number shows a good reproducibility. The inlet temperature of the working fluid has a small deviation (0,03% for Re 250·10^3 and 0,26% for Re200·10^3). Considering the calculated inside heat transfer coefficient the test nr.1 shows good results with a deviation of 1,96% , and the test nr.2 shows higher deviation of 2,69%.
In light of the above, it is possible to state that the facility works with a good reproducibility.

6.2.3 Heat transfer coefficient

Since this is the purpose of the test facility, the results about the heat transfer coefficient are shown in this chapter.
First of all it is important to introduce a problem about the first measurement section; In fact, the pipe of secondary cycle that supplies the coolant in the shell side is mounted in the proximity of the first measurement section and the fluid flows direct on the sensor, influencing especially the wall temperature and so on the results of the heat transfer coefficient.
Therefore, the main focus on this stage is between the second and third measureament section; In order to avoid these problems a different configuration of the shell side is in design phase.
For the comparison between experimental and predicted results, the single phase correlations available are Dittus Boelter, Gnielinski, and Petukhov.
From these possibilities, comparisons with the different correlations and with the different methods to extract the temperature of propane are done.

As explain in the third chapter, the heat transfer coefficient value is extracted with different methods; one, with the aim to obtain a specific value for each section (eq.3.41) and the second one to obtain a mean value of alpha coefficient measured using smaller boundary conditions (eq. 3.25).
Recapitulating, the experimental alpha coefficients considered in the evaluation are:

- Htc 2: local heat transfer coefficient in the second section
- Htc 3: local heat transfer coefficient in the third section
- Htc 2-3: integral heat transfer coefficient between second and third sections

Before to start with the discussion of the results is important to introduce the energy balance problem.

6.2.4 Problem with the early measurement with the heat balance

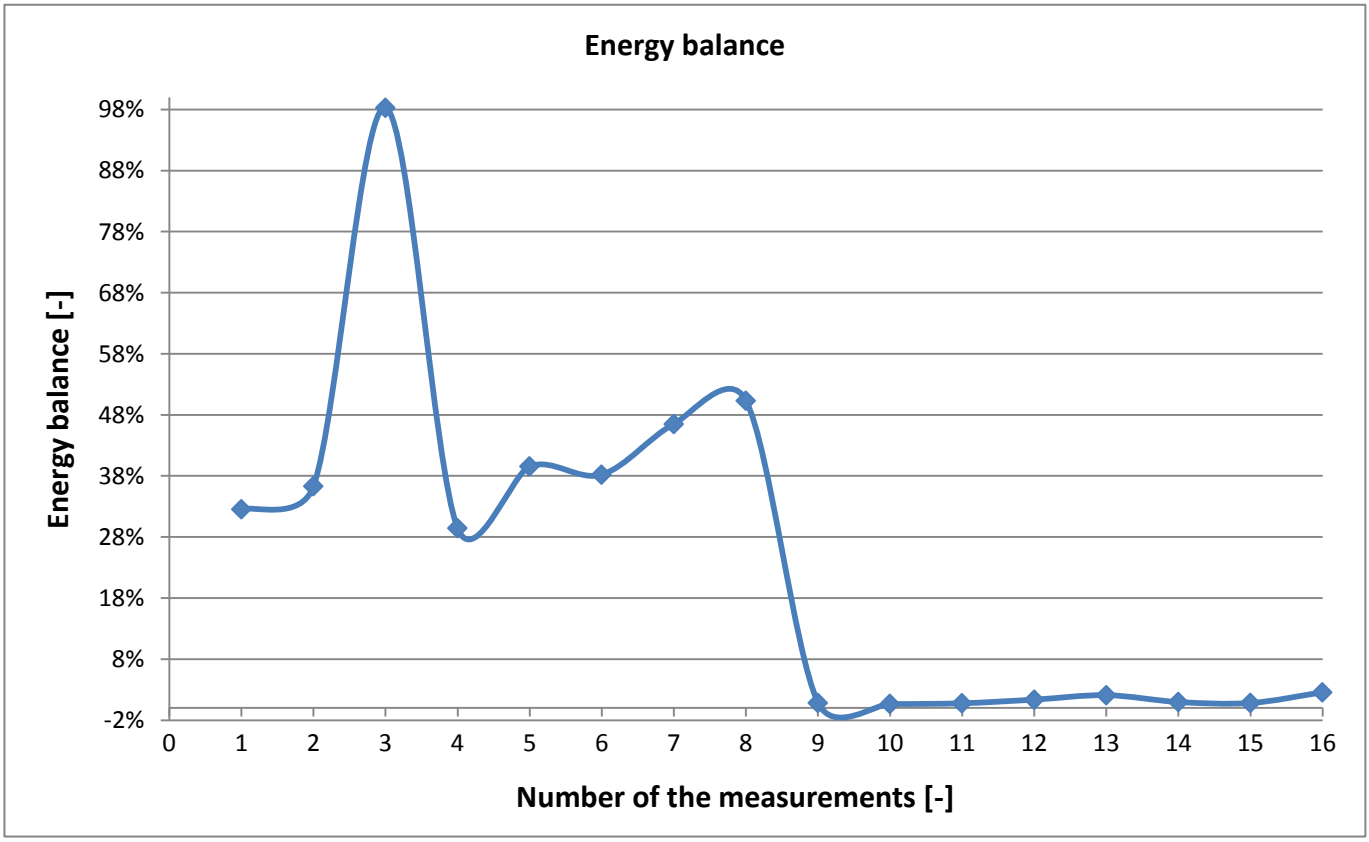

Figure 54: Energy balance from inlet to outlet of the heat exchanger

As reported in the Figure 54, the first 8 measurements give higher disagreement about the energy balance greater than 30%, due to the inadequate thermic insulation of the test section.

In fact, analysing the trend of the oil temperature between in and out of the heat exchanger like shown in Figure 58 is feasible to note the influencing of the heat loss between secondary fluid (oil) and the environment.

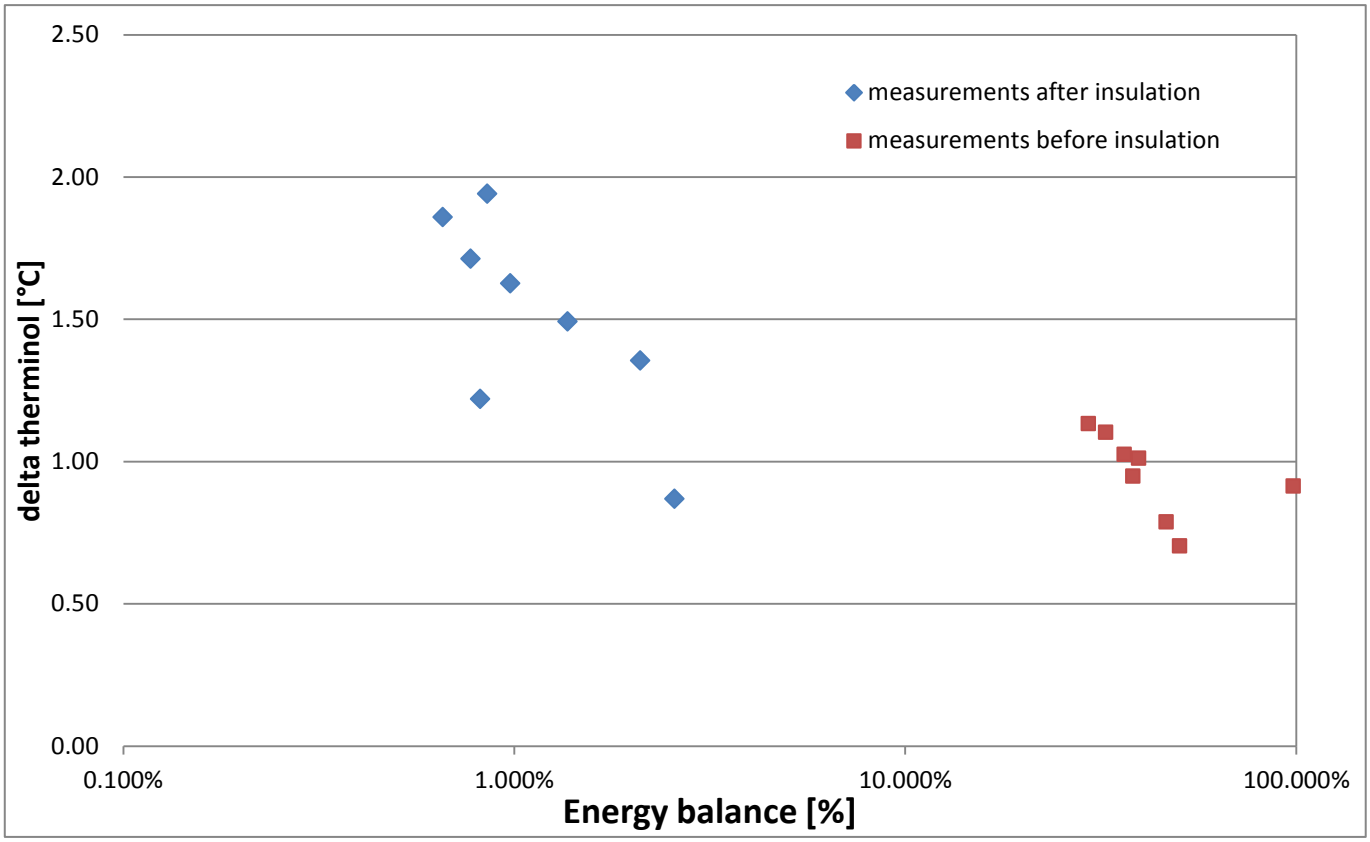

Figure 55: trend of the oil temperature

The results that give high discordance for the energy balance are the early points before the improvement of the thermic insulation of the test section.

The fact to have three different methods with the aim to calculate the propane temperature throughout the pipe is valuable to check some problems about the energy balance between oil and propane in the achievement of the results.
In effect, with the propane linear temperature method is not evident the influencing of the heat loss between secondary fluid (oil) and the environment between the measurements section on the alpha coefficient like shown in Figure 56.

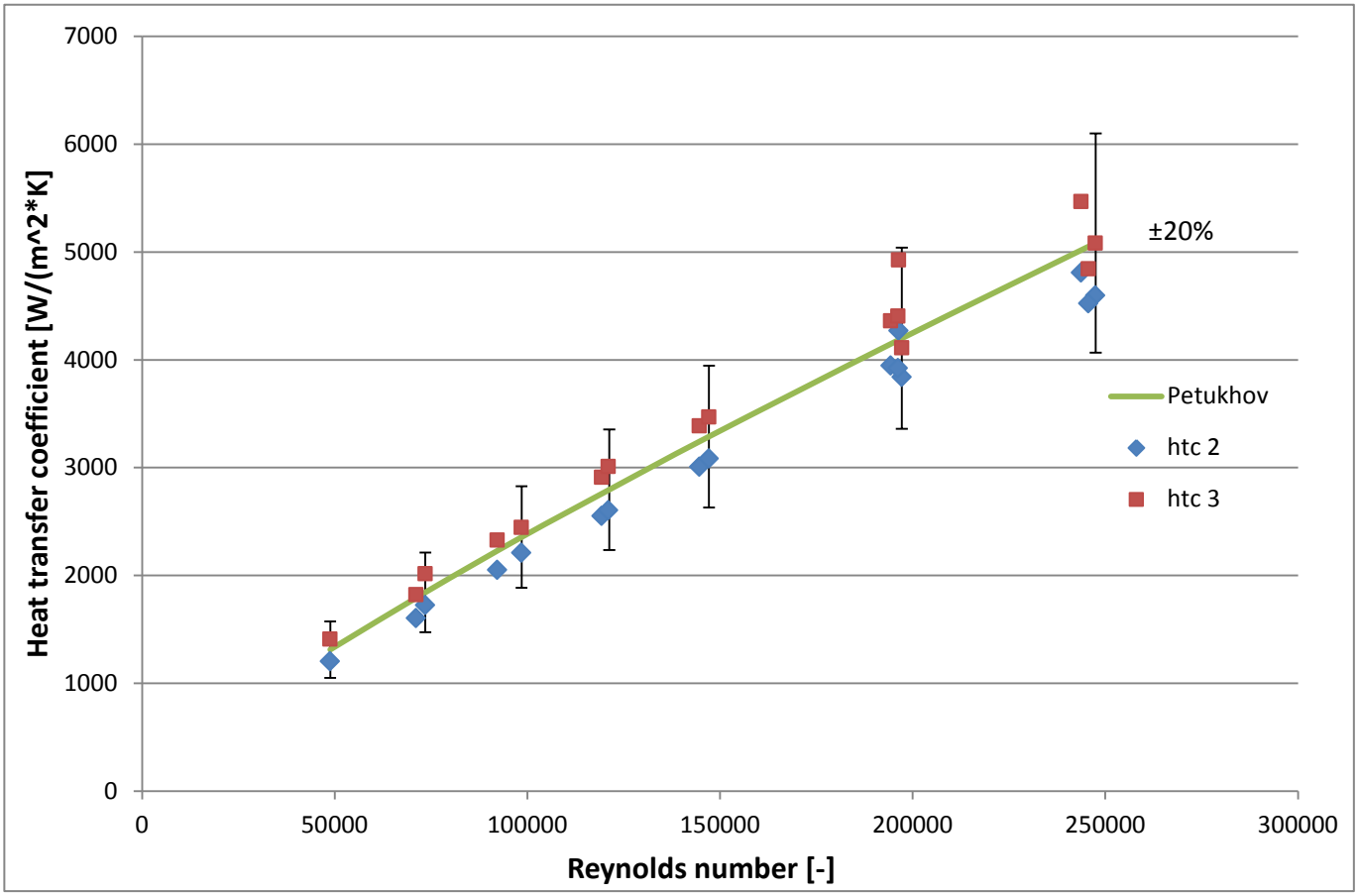

Figure 56: Comparison between calculated internal htc and measured htc using the slope of the oil side

The other two methods based on the heat balance show a higher discrepancy about the comparison between the predicted and experimental alpha coefficient.

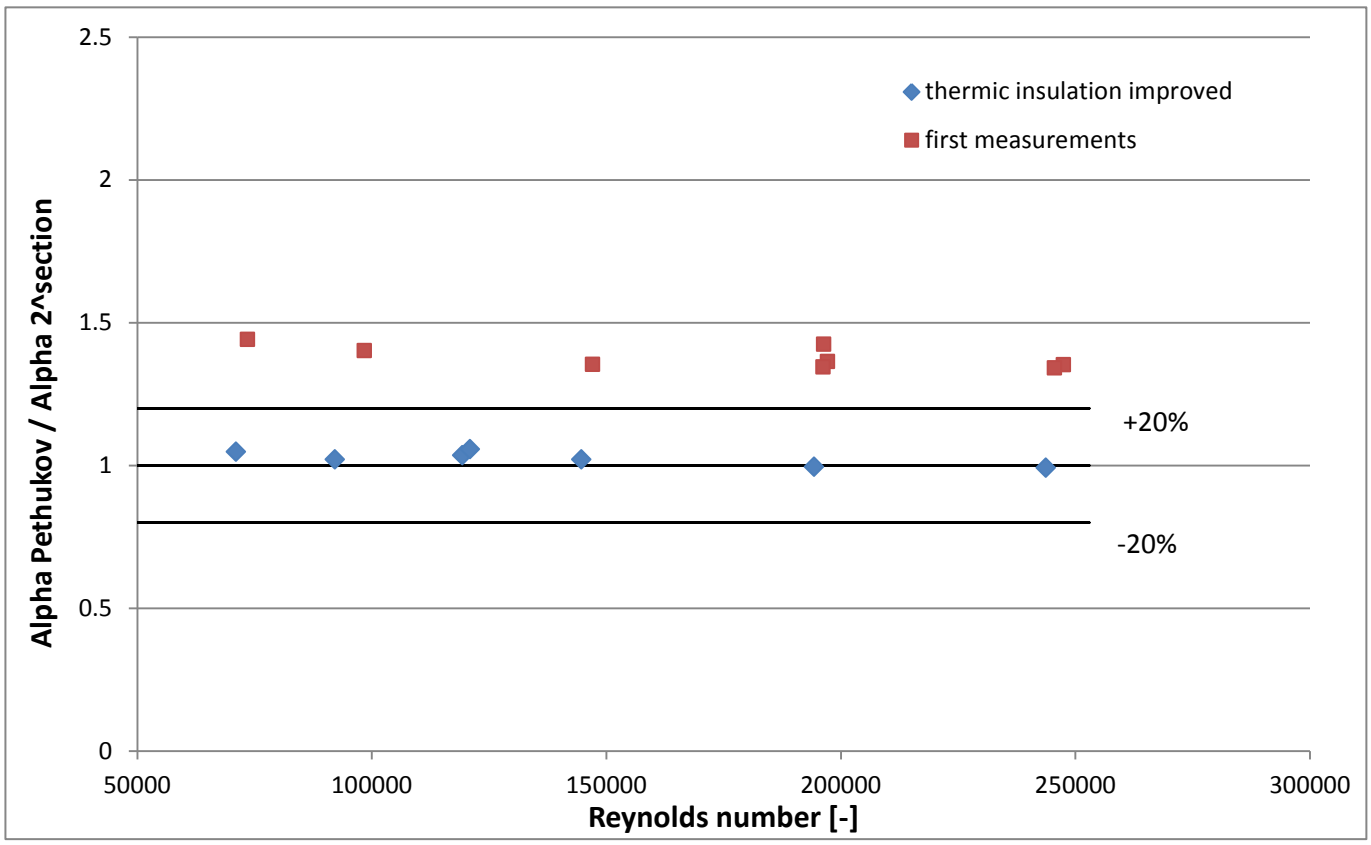

Figure 57: Comparison between the ratio between the predicted internal htc and measured htc in the second section using the propane in-out method for the temperature

6.2.5 Results

As a consequence, to avoid unreliable results it is better focusing with the data that belong to the right energy balance.
First of all it is important to compare the different correlations with the aim to have an idea about the variation of the results.

Table 8: Comparison between experimental internal htc and predicted Dittus-Boelter correlation [6] in function of the temperature determination of the propane inside the tube

n.measurement=8	Temperature determination of the working fluid								
	linear			in-out			out-in		
discrepancy % Dittus-B	mean %	peak %	min %	mean %	peak %	min %	mean %	peak %	min %
htc 2	18,4%	27,9%	8,5%	20,0%	28,4%	13,3%	21,5%	29,4%	16,4%
htc 3	34,7%	45,5%	27,3%	29,70%	39,1%	22,30%	31,6%	40,3%	25,4%
htc_2-3	34,6%	48,0%	23,6%	33,1%	45,0%	24,9%	34,9%	46,2%	27,9%

Table 9: Comparison between experimental internal htc and predicted Gnielinski correlation [6] in function of the temperature determination of the propane inside the tube

n.measurement=8	Temperature determination of the working fluid								
	linear			in-out			out-in		
discrepancy % Gnielinski	mean %	peak %	min %	mean %	peak %	min %	mean %	peak %	min %
htc 2	7,3%	-12,1%	-2,8%	5,9%	-8,6%	-2,5%	4,7%	-7,9%	-1,7%
htc 3	5,5%	10,5%	2,3%	2,19%	5,7%	0,67%	3,2%	6,6%	0,3%
htc_2-3	5,4%	12,4%	0,2%	4,3%	10,2%	0,0%	5,7%	11,1%	2,3%

Table 10: Comparison between experimental internal htc and predicted Petukhov correlation [6] in function of the temperature determination of the propane inside the tube

n.measurement=8	Temperature determination of the working fluid								
	linear			in-out			out-in		
discrepancy % Petukhov	mean %	peak %	min %	mean %	peak %	min %	mean %	peak %	min %
htc 2	4.1%	-8.5%	-0.2%	2.9%	-5.4%	0.6%	2.0%	-4.6%	-0.7%
htc 3	9.3%	14.3%	6.2%	5.32%	9.3%	1.55%	6.9%	10.3%	4.1%
htc_2-3	9.2%	16.2%	4.3%	8.0%	13.9%	3.7%	9.5%	14.9%	6.2%

A first overview reveals huge discrepancy with the Dittus-Boelter correlation due to the roughness of the formula; otherwise the others two give not huge differences between the correlations; in fact analysing the standard deviation of the results shown in Table 11:

Table 11: Standard deviation between the results of the correlations involved in the calculation

	Standard deviation								
	%(Petukhov - Gnielinski)								
	linear			in-out			out-in		
discrepancy %	mean %			mean %			mean %		
htc 2	2.3%			2.1%			1.9%		
htc 3	2.7%			2.2%			2.6%		
htc_2-3	2.7%			2.6%			2.7%		

The conclusion of this first part is that the Gnielinski and Petukhov correlation give more or less the same comparison, with few percentage points of difference.
Keep going with the data analyzing is possible to choose one correlation in order to focus the attention in other topics; in this case Petukhov correlation is the choice.
The second step is to verify which method to extract the temperature of the working fluid through the pipe is more reliable.
With the in-out and out-in methods available, is better focusing on them because based on the energy balance between primary and secondary, feasible due the heat transfer that is extract thanks to the 5 measurement sections in the shell side and not just a linear connection between RTD12 and RTD15 with the propane linear temperature.
Considering the Table 10, the in-out methods seems probably to give the most reliable results with a mean discrepancy of 2,9% for the alpha coefficient in the second section, 5,32% for the third section and 8% for the integral alpha coefficient showing a good reliability.
For this motivation the next graphs are plotted taking into account of this method.
In this way it is possible to have a fast overview and comparison about the results obtained.

The internal alpha coefficient in the second and third section gives good results like visible in Figure 58 that means that the results from these two sections are very reliable.
Finally, the mean value of alpha coefficient 2-3 calculated using the integral method (chapter 3.3.1) is reported in Figure 59; it is possible to extract the dimensionless number of Nusselt and confirm that also with this method, second and third section gives reliable results.

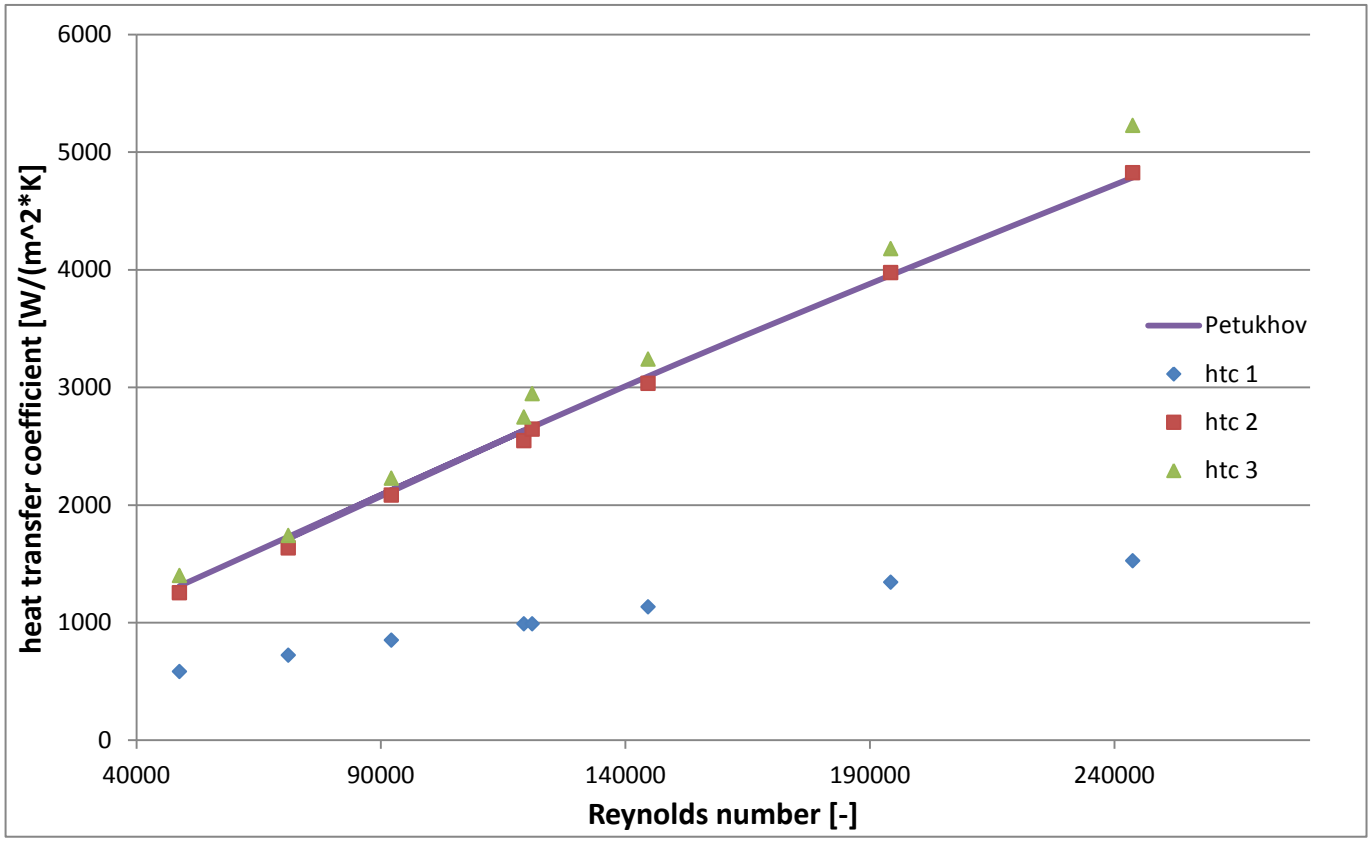

Figure 58: Comparison between local experimental internal htc and Petukhov correlation [6] using the slope of the oil side

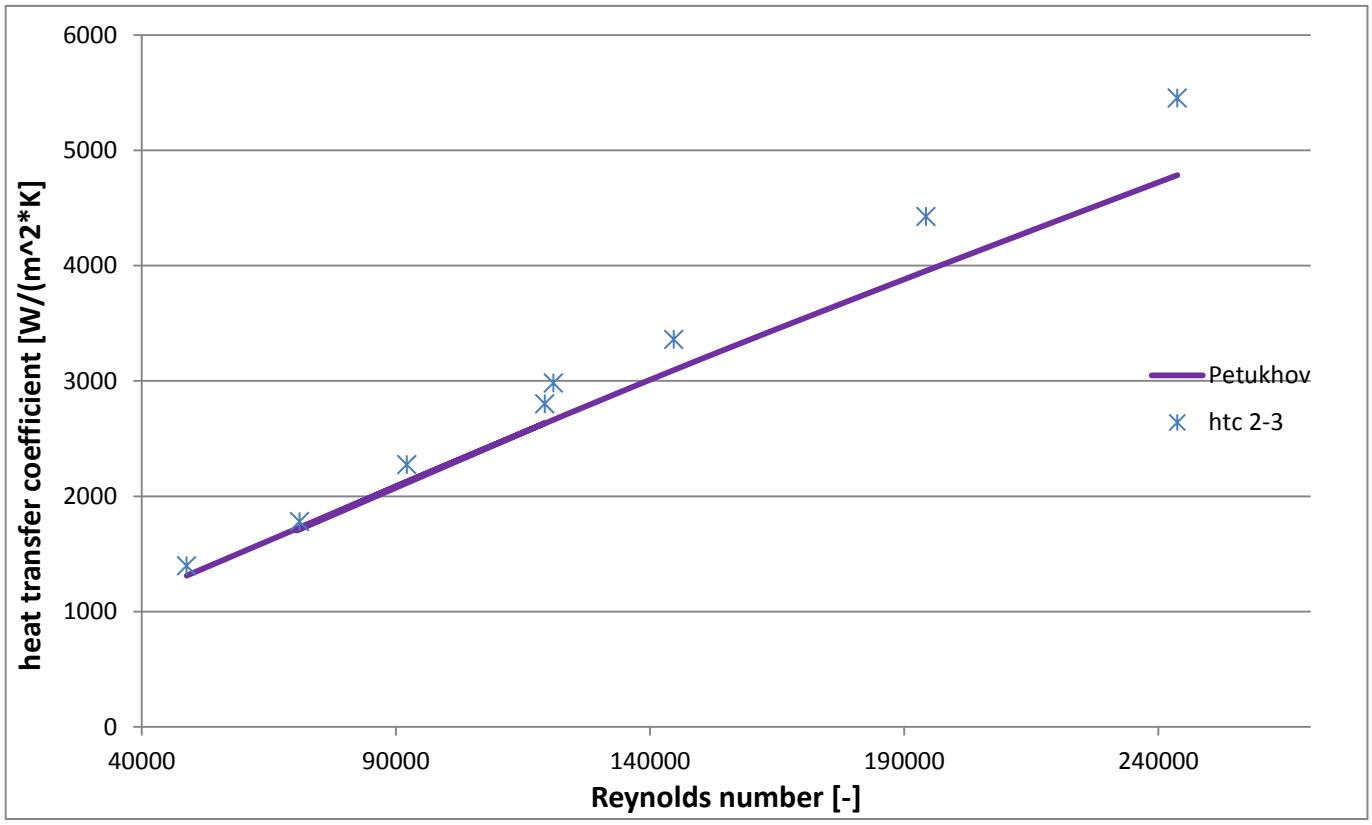

Figure 59: Comparison between integral value of htc and Petukhov correlation [6]

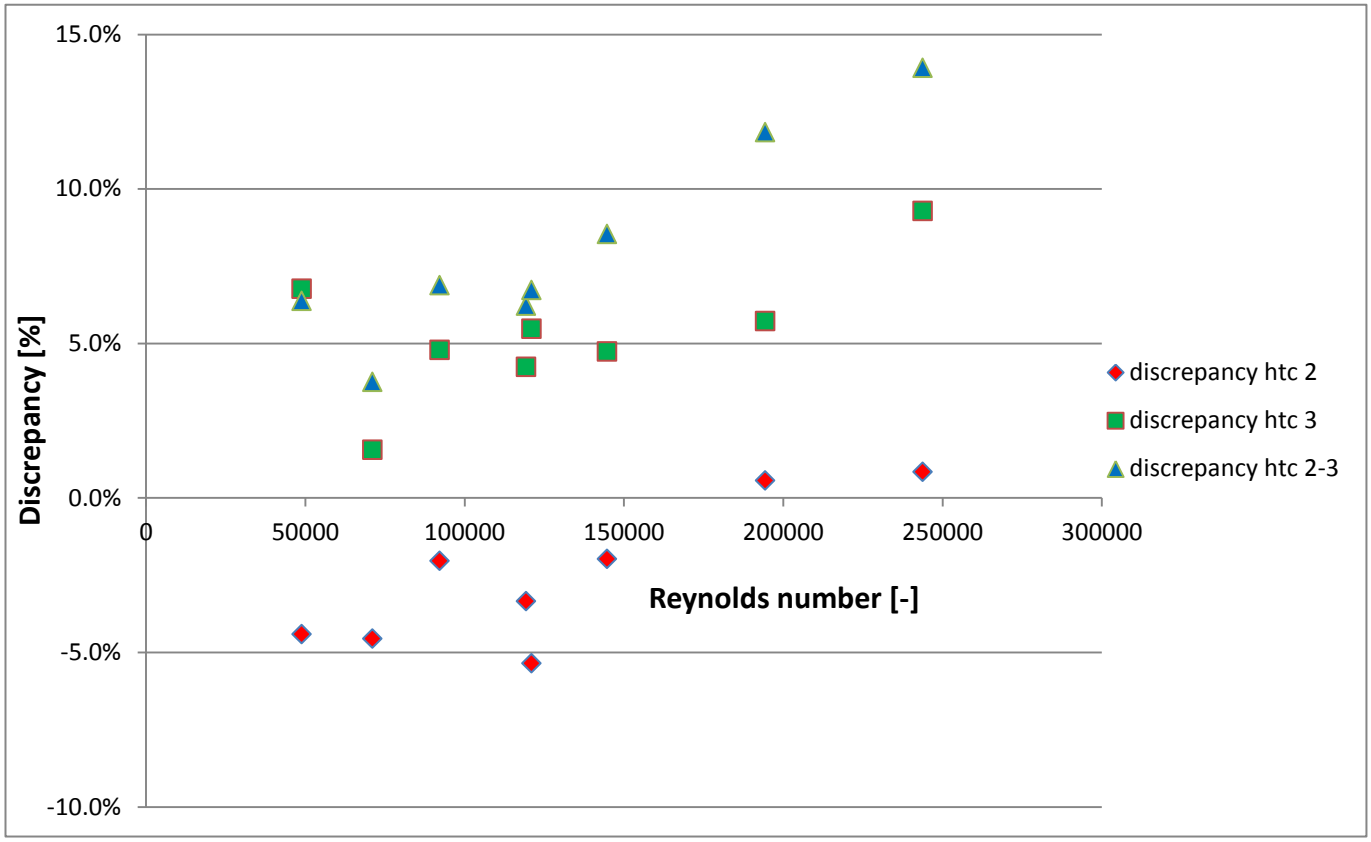

Figure 60: Relative discrepancy between experimental htc and Petukhov correlation [6]

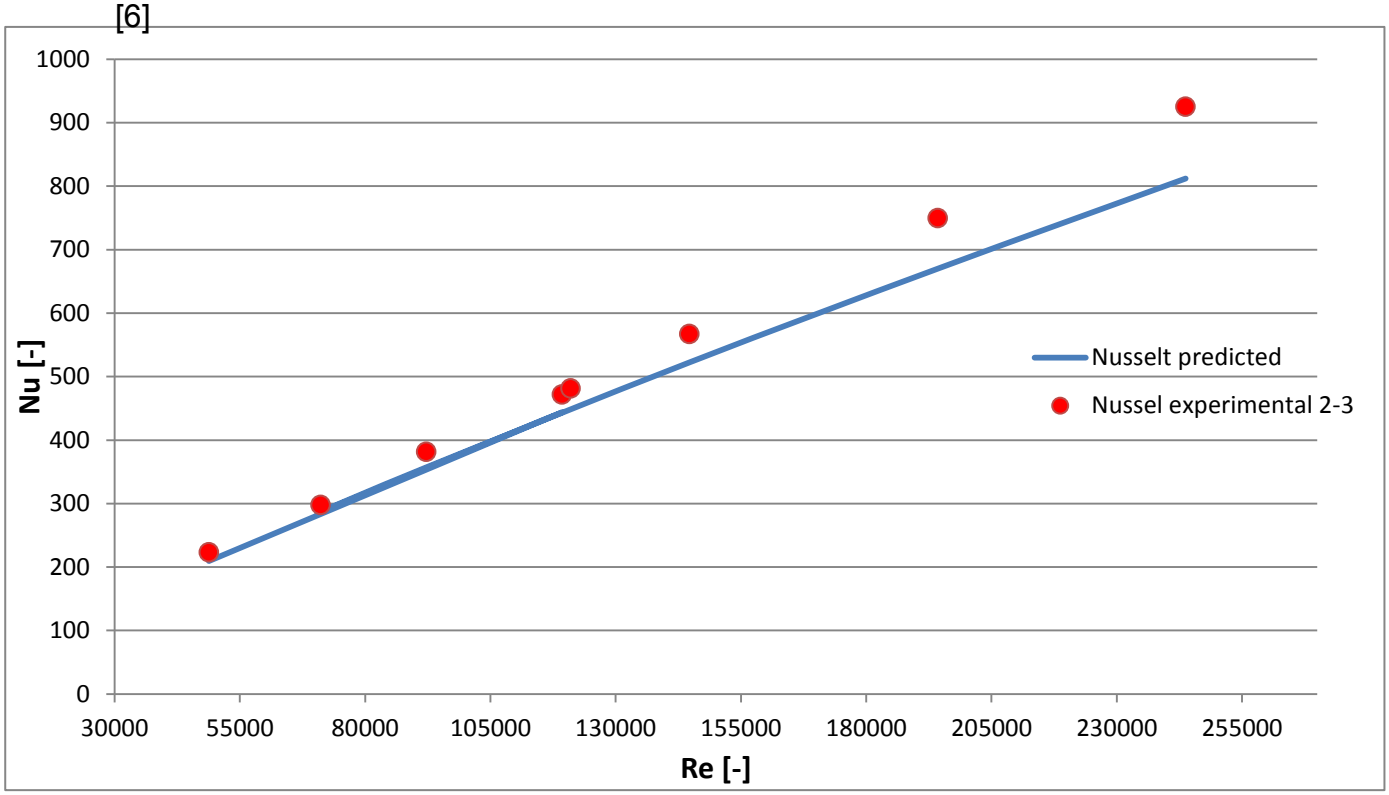

Figure 61: Comparison between calculated Nusselt (using Petukhov correlation [6]) and measured Nusselt using smaller boundary conditions between sections 2-3

6.2.6 Pressure drop

The aim of this part is to compare the pressure drop data between the experimental value and the literature (chapter 3.4.1) [9].

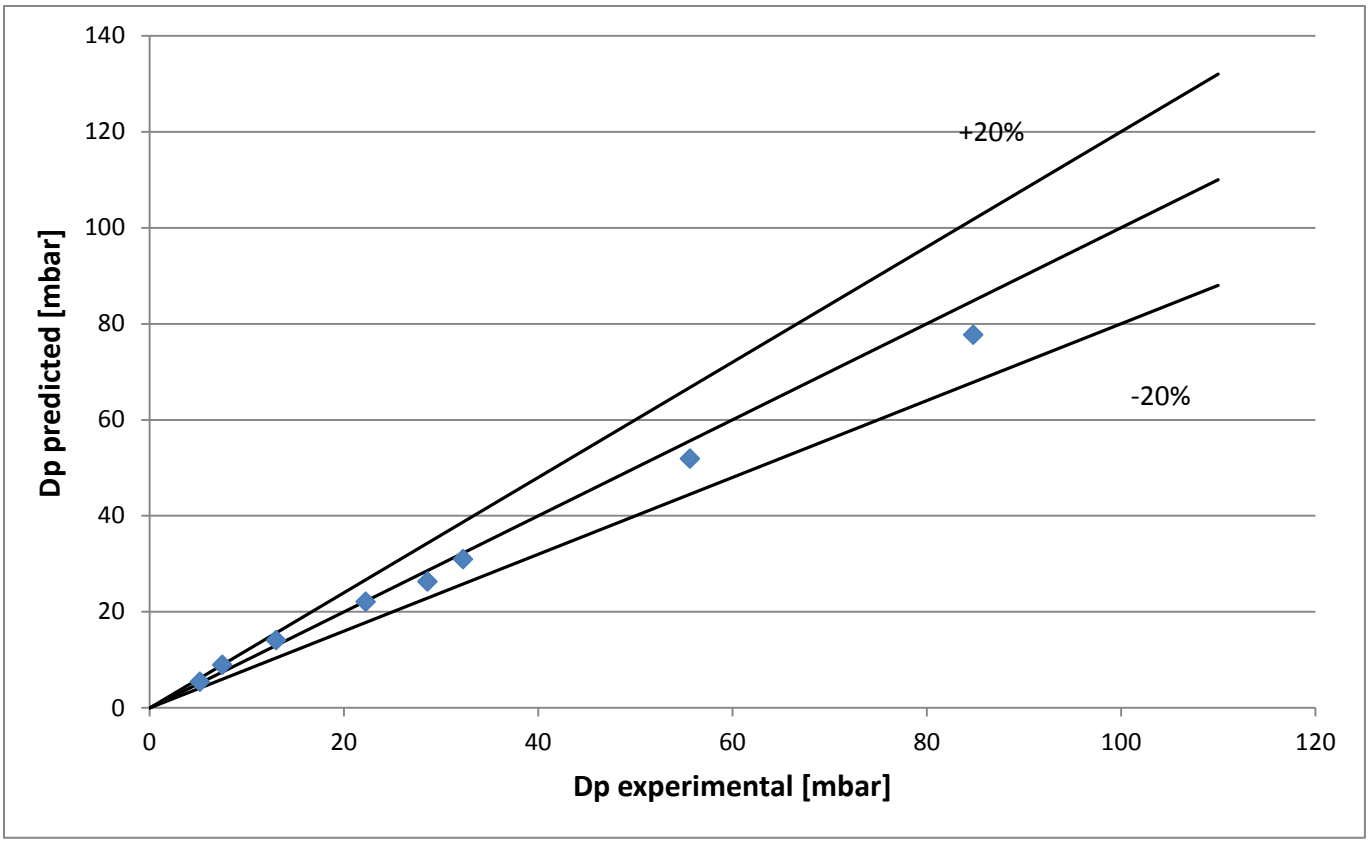

Figure 62: Comparison between experimental and predicted pressure drop [9]

The figure show as all the experimental pressure drop points in the liquid cooling measurements are in agreement with the predicted value within a range of $\pm 20\%$

The comparison give a mean discrepancy for the all 8 measurements about liquid cooling of 7,3%, a peak of -16% and a minimum discrepancy of 1%.
These results permit to validate the experimental data acquisition about the pressure drop.

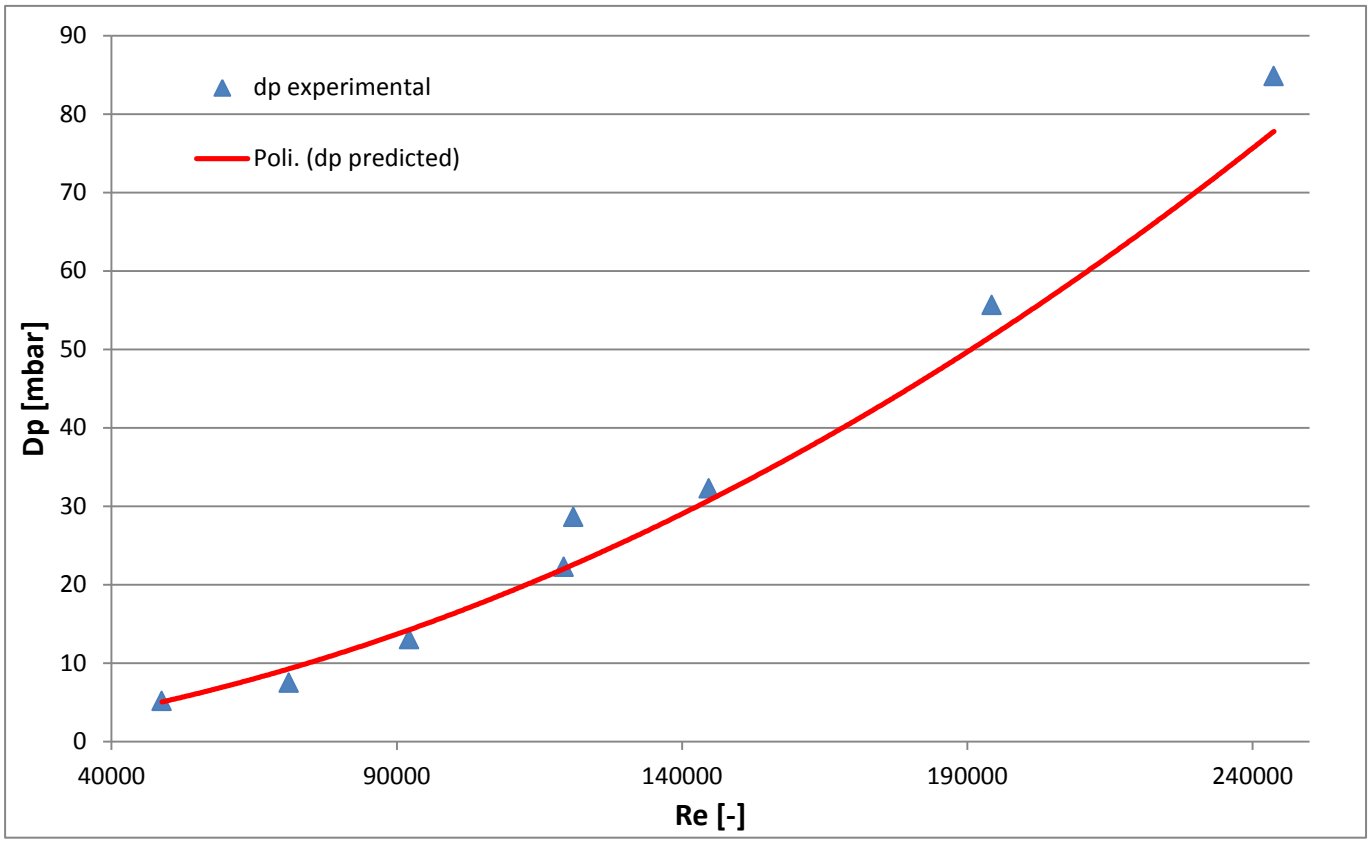

Figure 63: Comparison between experimental and predicted pressure drop [9] in function of the Reynolds number in the liquid cooling measurement

6.3 Gas Cooling

As explained before in order to get reliable data it is important that the measurements are carried out in steady state conditions.
Furthermore it is also important to verify the reproducibility relative the same test in order to check any strange behaviour and to confirm the validation of the data acquisition
The gas cooling test is lead with a costant pressure P_{in}=12 bar in the test section, a set temperature t=20°C for the inlet of therminol and with different values working fluid mass flow rate in order to reach different Reynolds numbers.
The parameters that are important to control and to verify, about steady state conditions are:

1. Mass flow rate G [kg/(m^2*s)]
2. Pressure upstream the test rig measured by AP5,6 sensor
3. Temperature upstream test rig measured by RTD12

For the management of these parameters, is possible to follow the same advices of the liquid cooling chapter.

6.3.1 Steady state conditions

With the purpose to verify these conditions one random representative measurement is chosen and analysed. In this case test with Re=600· 10^3 is the choice like shown Table 12.

Table 12: maximum deviation

Maximum deviation AP	Maximum deviation ΔT	Maximum deviation G
[bar]	[°C]	G [kg/m^2*s]
0,015238	1,75973	3,657372

The mass flow rate G and the pressure upstream the test rig measured by AP5,6 sensor are in this measurement quite constant but the temperature upstream test rig measured by RTD12 show an higher fluctuation and an unstable working condition, especially in the last 3 minutes of the sampling; this fact means that the control of temperature sometimes requires more time to reach the stable condition or that even after long periods it doesn't become stable because the controller should be optimized.

6.3.2 Reproducibilty

The purpose of this chapter is to verify how the test rig is able to set a particular and predefined condition, the parameters that change are the time that measurements are registered (different days) and the observant.
The desired points (in order to reach Re400· 10^3 and Re800· 10^3) are listed in Table 7:

Table 13: Reproducibility tests:

	G_wf [kg/(m^2*s)]	P (AP 5,6) [bar]	nr.test [-]
1	250	12	2
2	501	12	2

The reproducibility of the results is observed and compared using the coefficient of variation, also known as relative standard deviation, defined as:

$$COV = \frac{Standard\ Deviation}{Mean\ Value} \tag{6.3}$$

The specific mass flow G of the working fluid shows very good reproducibility (1,46% for Re800· 10^3 and 1,43% for Re400· 10^3). The working fluid flow is connected to the Reynolds number that means that also this number shows a good reproducibility. The inlet temperature of the working fluid has a small deviation (0,05% for Re 800·

10^3 and 0,26% for Re400· 10^3). Considering the calculated inside heat transfer coefficient the test nr.1 shows good result with deviation of 1,56% and the test nr.2 shows higher deviation of 2,51%.
In light of the above, it is possible to state that the facility works with a good reproducibility.

6.3.3 Heat transfer coefficient

The problems about the first measurement section are explained in the previous chapter and the same considerations are valid also in this case.
For the comparison between experimental and predicted results, the single phase correlations available are Dittus Boelter, Gnielinski, Hausen and Petukhov. From these possibilities, comparisons with the different correlations and with the different methods to extract the temperature of propane are done.
First of all is important to compare the different correlations with the aim to have an idea about the variation of the results; the experimental alpha coefficient considered in the evaluation are:

- Htc 2: local heat transfer coefficient in the second section
- Htc 3: local heat transfer coefficient in the third section
- Htc 2-3: integral heat transfer coefficient between second and third sections

Table 14: Comparison between experimental internal htc and predicted Petukhov correlation [6] in function of the temperature determination of the propane inside the tube

n.measurement=21	Temperature determination of the working fluid								
	linear			in-out			out-in		
discrepancy % Petukhov	mean %	peak %	min %	mean %	peak %	min %	mean %	peak %	min %
htc 2	5.2%	-11.2%	-0.5%	5.1%	-11.7%	0.8%	5.4%	13.2%	-0.3%
htc 3	18.1%	24.0%	8.4%	3.61%	9.5%	0.01%	11.7%	22.6%	4.5%
htc_2-3	10.6%	19.5%	2.1%	4.3%	9.9%	-0.2%	12.4%	21.5%	-0.1%

Table 15: Comparison between experimental internal htc and predicted Gnielinski correlation [6] in function of the temperature determination of the propane inside the tube

n.measurement=21	Temperature determination of the working fluid								
	linear			in-out			out-in		
discrepancy % Gnielinski	mean %	peak %	min %	mean %	peak %	min %	mean %	peak %	min %
htc 2	5,39%	-11,69%	0,01%	5,46%	-12,25%	0,50%	5,14%	12,69%	-0,72%
htc 3	17,48%	23,51%	8,02%	3,69%	8,78%	-0,18%	11,17%	21,74%	4,05%
htc_2-3	10,07%	19,02%	1,54%	4,21%	9,46%	0,03%	11,92%	20,96%	-0,72%

Table 16: Comparison between experimental internal htc and predicted Hausen correlation [6] in function of the temperature determination of the propane inside the tube

n.measurement=21	Temperature determination of the working fluid								
	linear			in-out			out-in		
discrepancy % Hausen	mean %	peak %	min %	mean %	peak %	min %	mean %	peak %	min %
htc 2	5,65%	-12,19%	-0,12%	5,16%	-12,11%	0,19%	5,68%	14,11%	-0,63%
htc 3	18,04%	25,22%	7,51%	4,05%	8,94%	0,19%	11,70%	21,82%	3,56%
htc_2-3	10,60%	20,51%	0,96%	4,82%	10,84%	0,30%	12,45%	22,48%	-0,57%

A first overview reveals not huge differences between each correlation; in fact analysing the standard deviation of the results shown in Table 13, is possible to confirm this first impression.

Table 17: Standard deviation between the results of the all correlations involved in the calculation

	Standard deviation %(Petukhov - Gnielinski - Hausen)		
	linear	in-out	out-in
discrepancy %	mean %	mean %	mean %
htc 2	0.2%	0.2%	0.3%
htc 3	0.3%	0.2%	0.3%
htc_2-3	0.3%	0.3%	0.3%

The conclusion of this first part is that the different correlations give more or less the same comparison instrument, with few percentage points of difference.
Carry on with the data analysing is so possible to choose one correlation in order to focus the attention in other topics; in this case Petukhov correlation is the choice like in the liquid cooling case.
The second step is to verify which method to extract the working fluid of the propane through the pipe is more reliable.
Since the in-out and out-in methods are based on the energy balance between primary and secondary fluid, to start the investigation is essential that it is adequate for these measurements obtained.

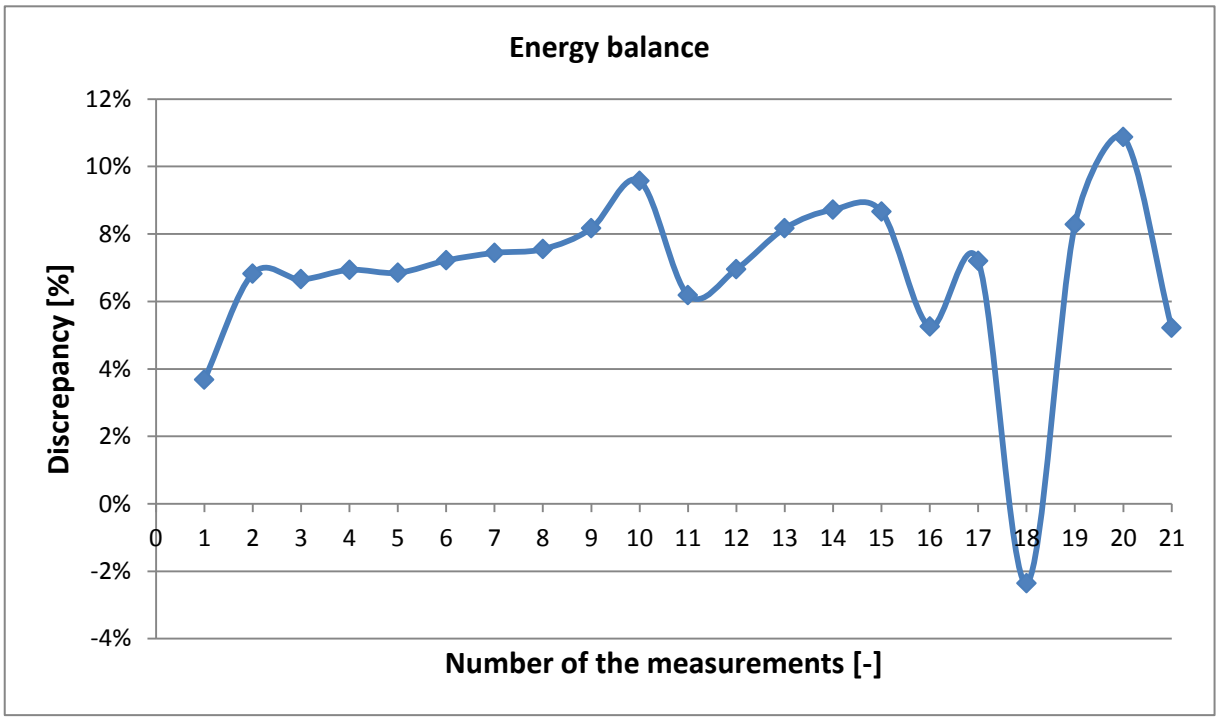

Figure 64: Energy balance from inlet to outlet of the heat exchanger

Based on experience, less than 15% is possible to consider the energy balance appropriate and since the propane linear temperature is just a temperature line connection between the two RTD12 and RTD15, is better to consider the in-out and out-in methods because are founded on the heat transfer that is extract in the oil side thanks to the 5 measurement sections in the shell side.
Considering the Table 14, the in-out methods seems probably to give the most reliable results with a mean discrepancy of 5,1% for the alpha coefficient in the

second section, 3,61% for the third section and 4,3% for the integral alpha coefficient showing a good .

For this motivation the next graphs are plotted taking into account of this method.

In this way is possible to have a fast overview and comparison about the results obtained.

The internal alpha coefficient in the second and third section gives good results like visible in Figure 61 that means that the results from these two sections are very reliable.

Finally, the mean value of alpha coefficient 2-3 calculated using the integral method is reported in Figure 62; it is possible to extract the dimensionless number of Nusselt and confirm that also with this method, second and third section of measurement works gives reliable results.

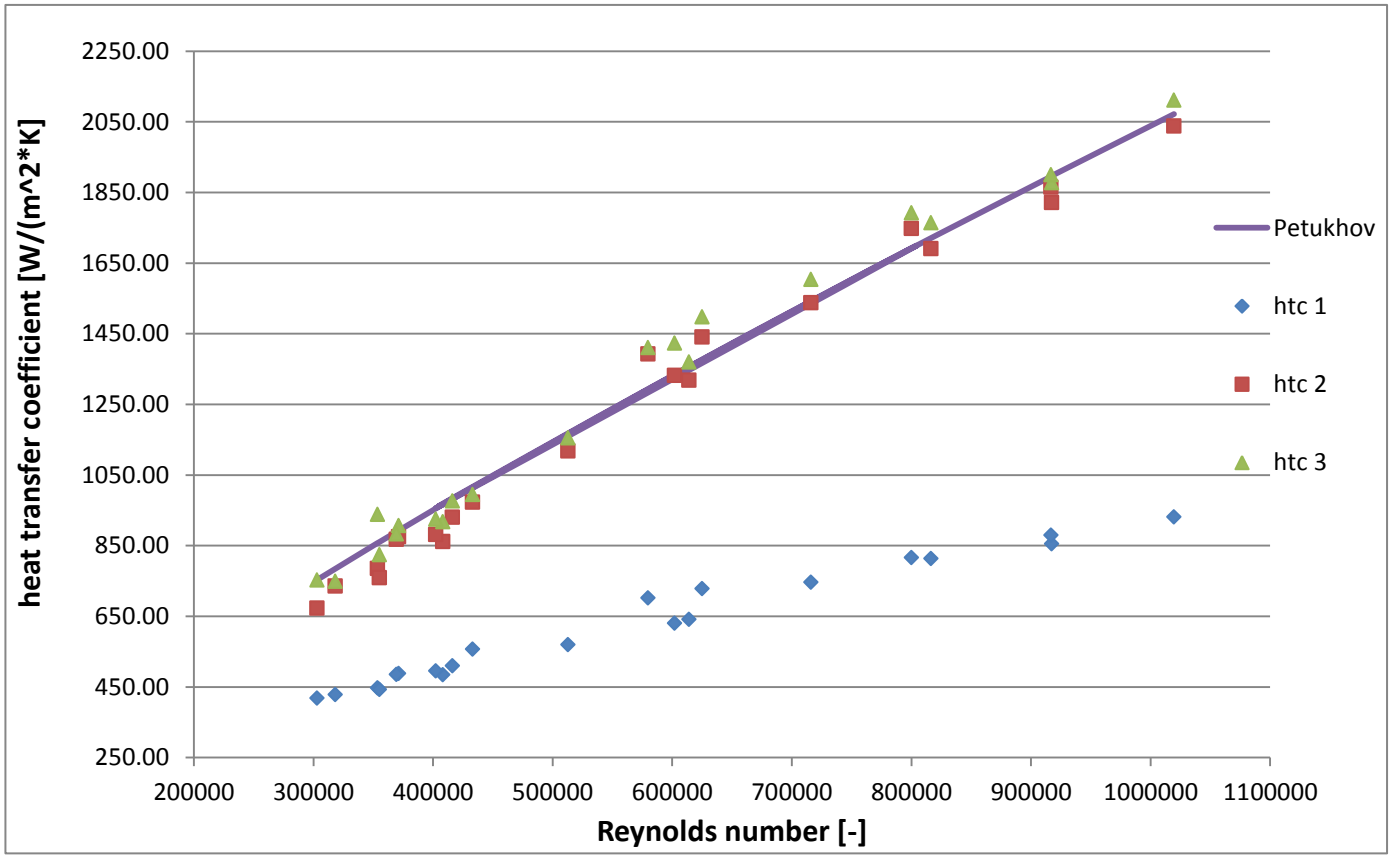

Figure 65: Comparison between experimental internal htc and Petukhov correlation [6] using the slope of the oil side

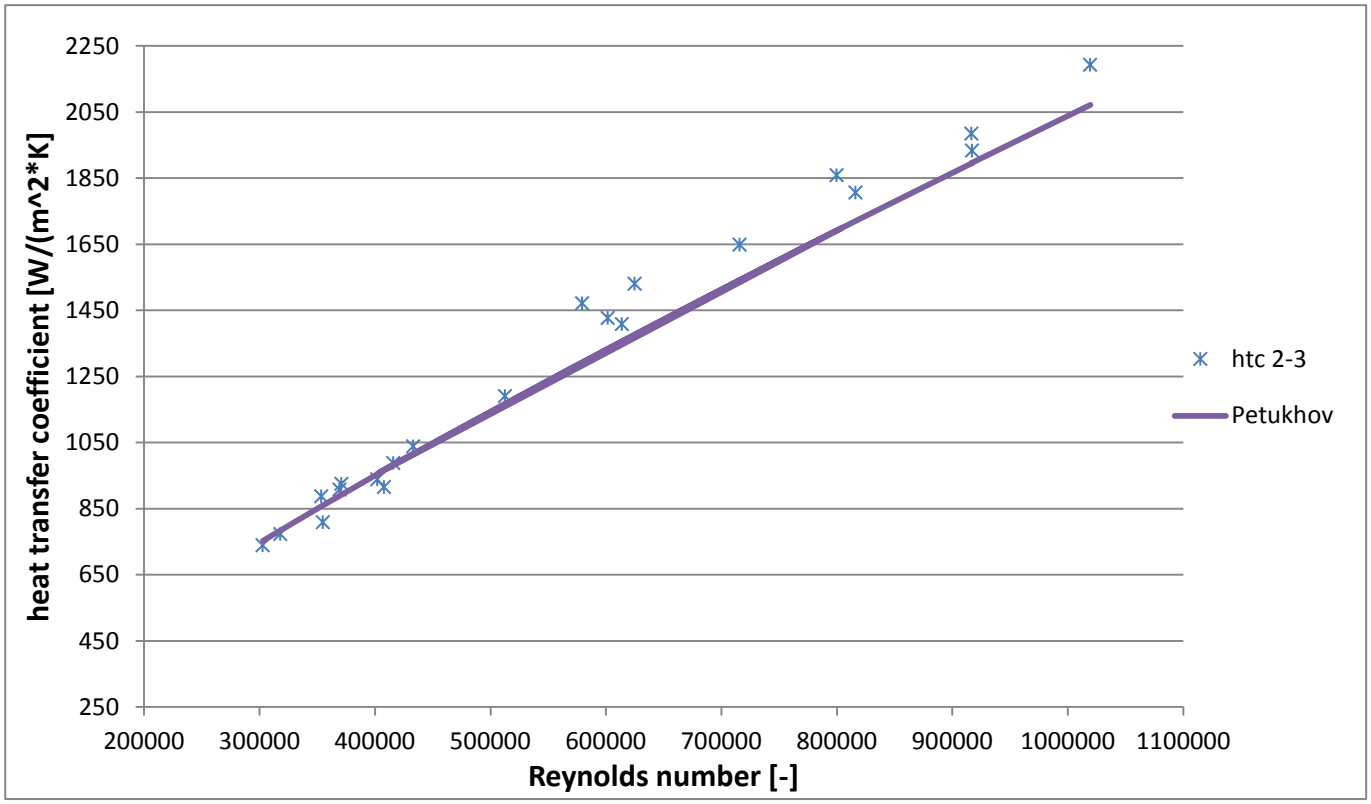

Figure 66: Comparison between integral value and Petukhov correlation [6]

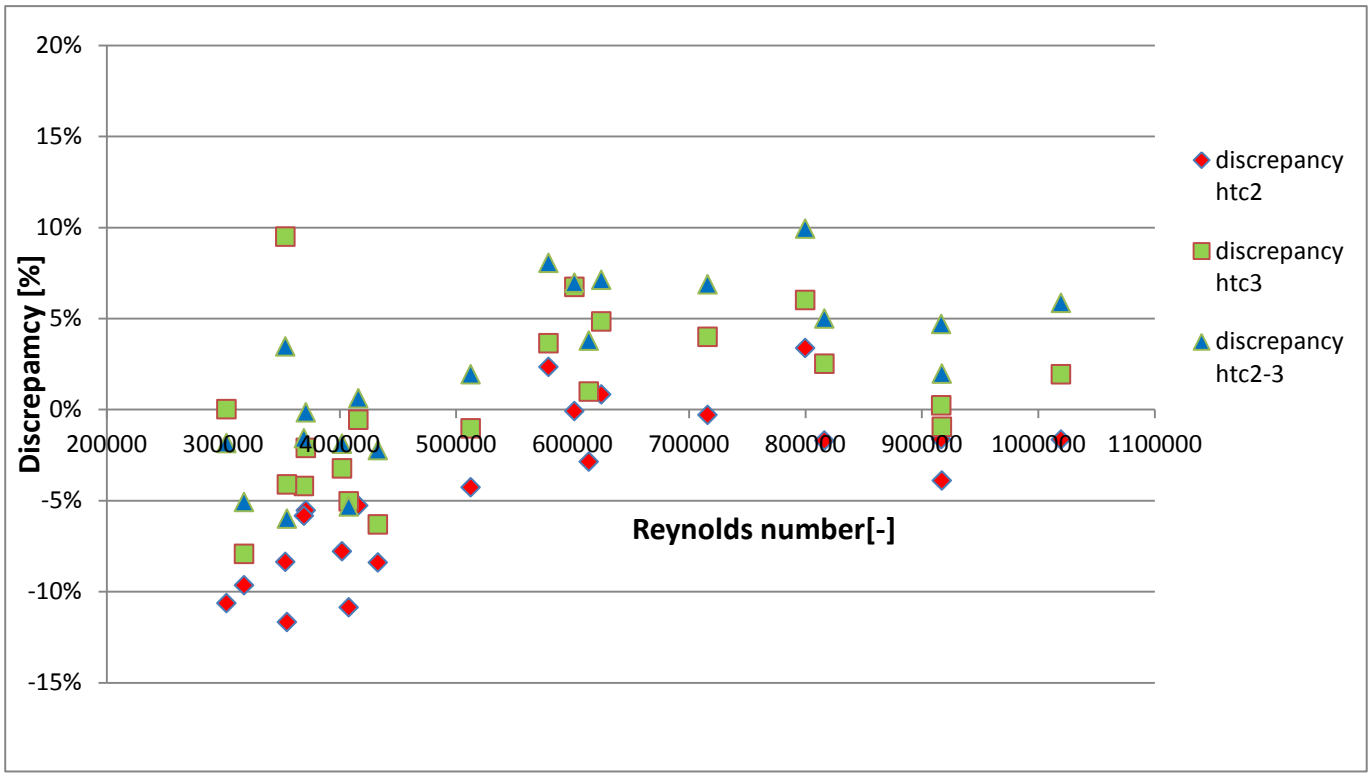

Figure 67: Relative discrepancy between experimental htc and Petukhov correlation [6]

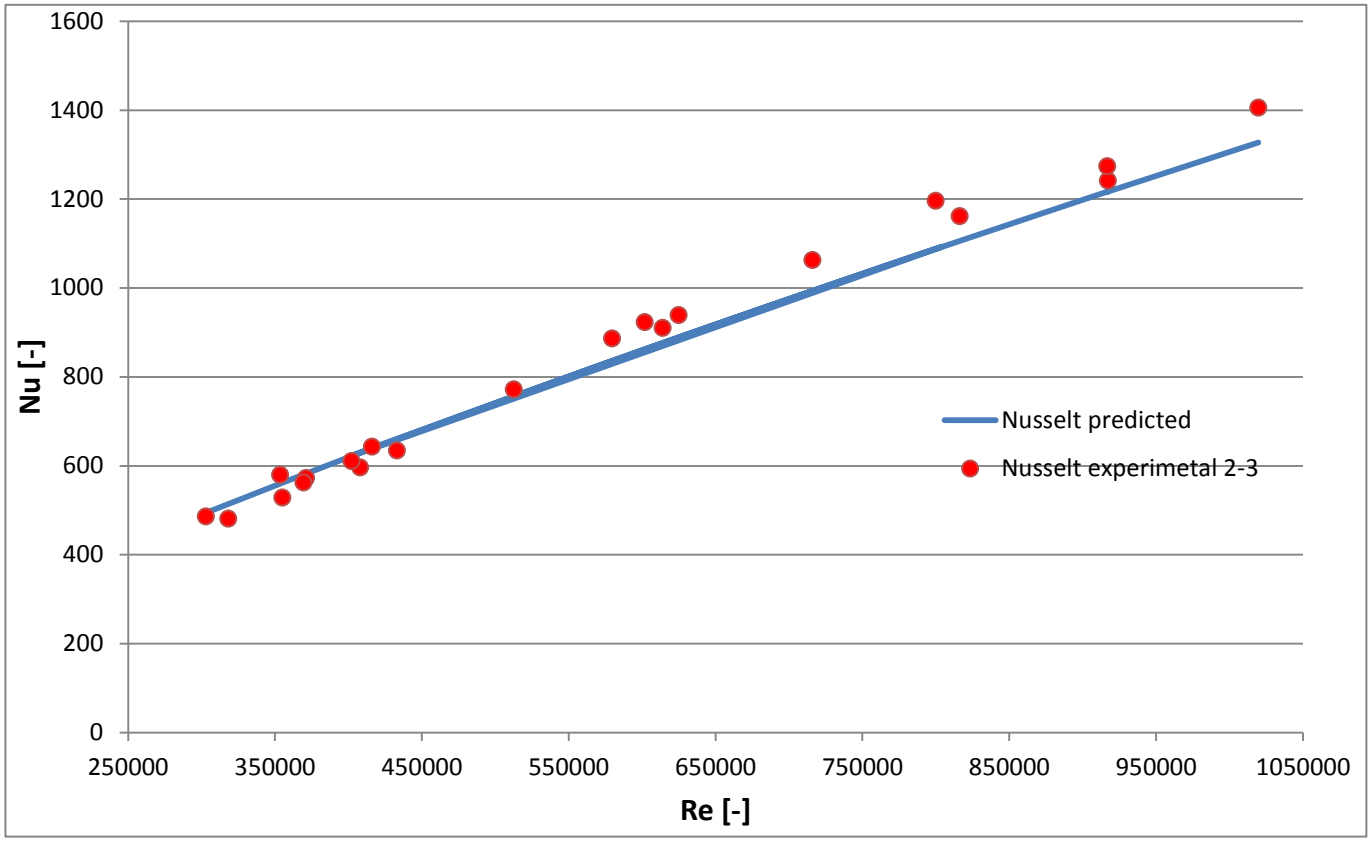

Figure 68: Comparison between calculated Nusselt (using Petukhov correlation [6]) and measured Nusselt using smaller boundary conditions between sections 2-3

6.3.4 Pressure drop

The aim of this part is to validate and to compare the pressure drop data between the experimental value and the literature (chapter 3.4.1) [9].

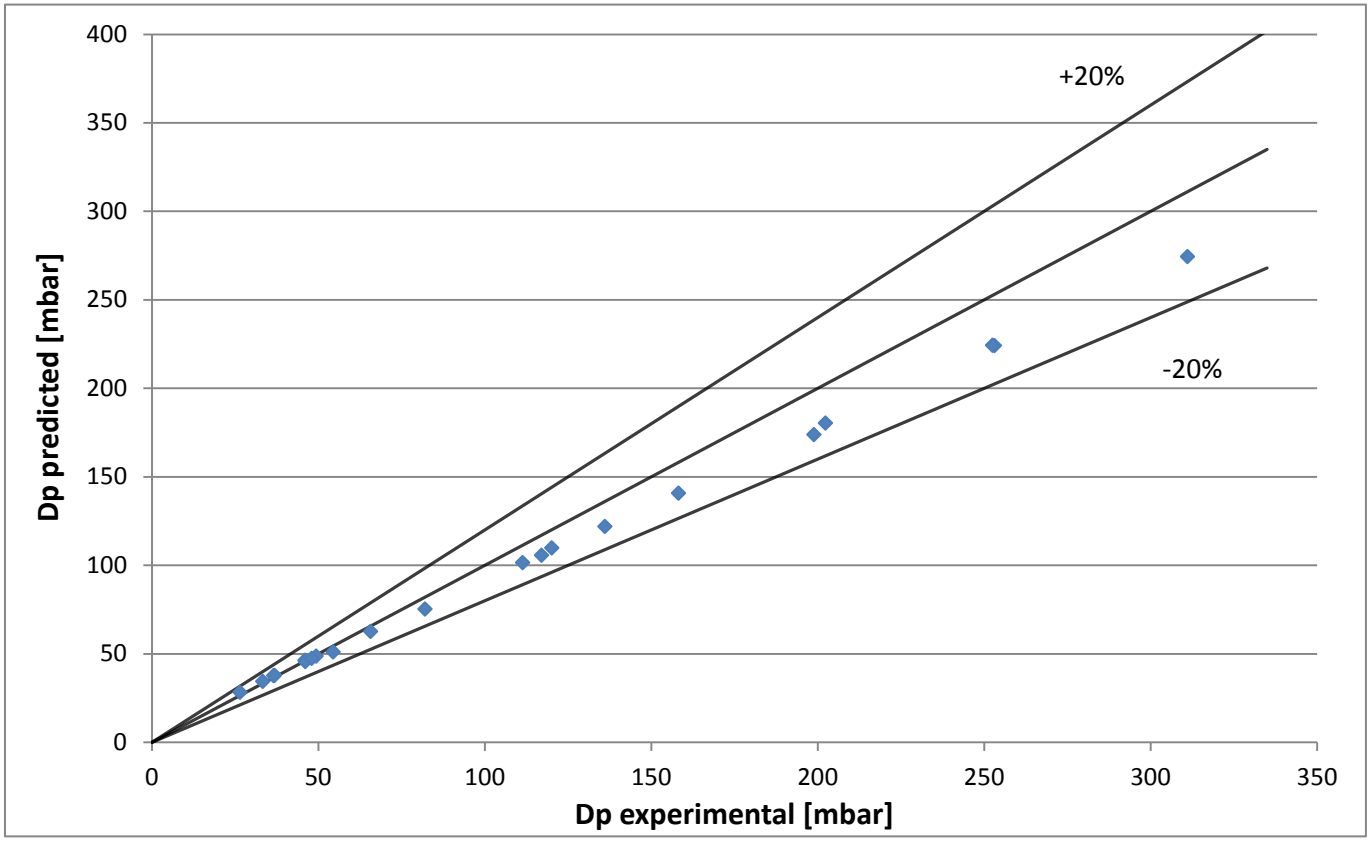

Figure 69: Comparison between experimental and predicted pressure drop [9]

The comparison give a mean discrepancy for the all 21 measurements about gas cooling of 8%, a peak of 14,5% and a minimum discrepancy of -0,3%.
These results permit to validate the experimental data acquisition about the pressure drop.

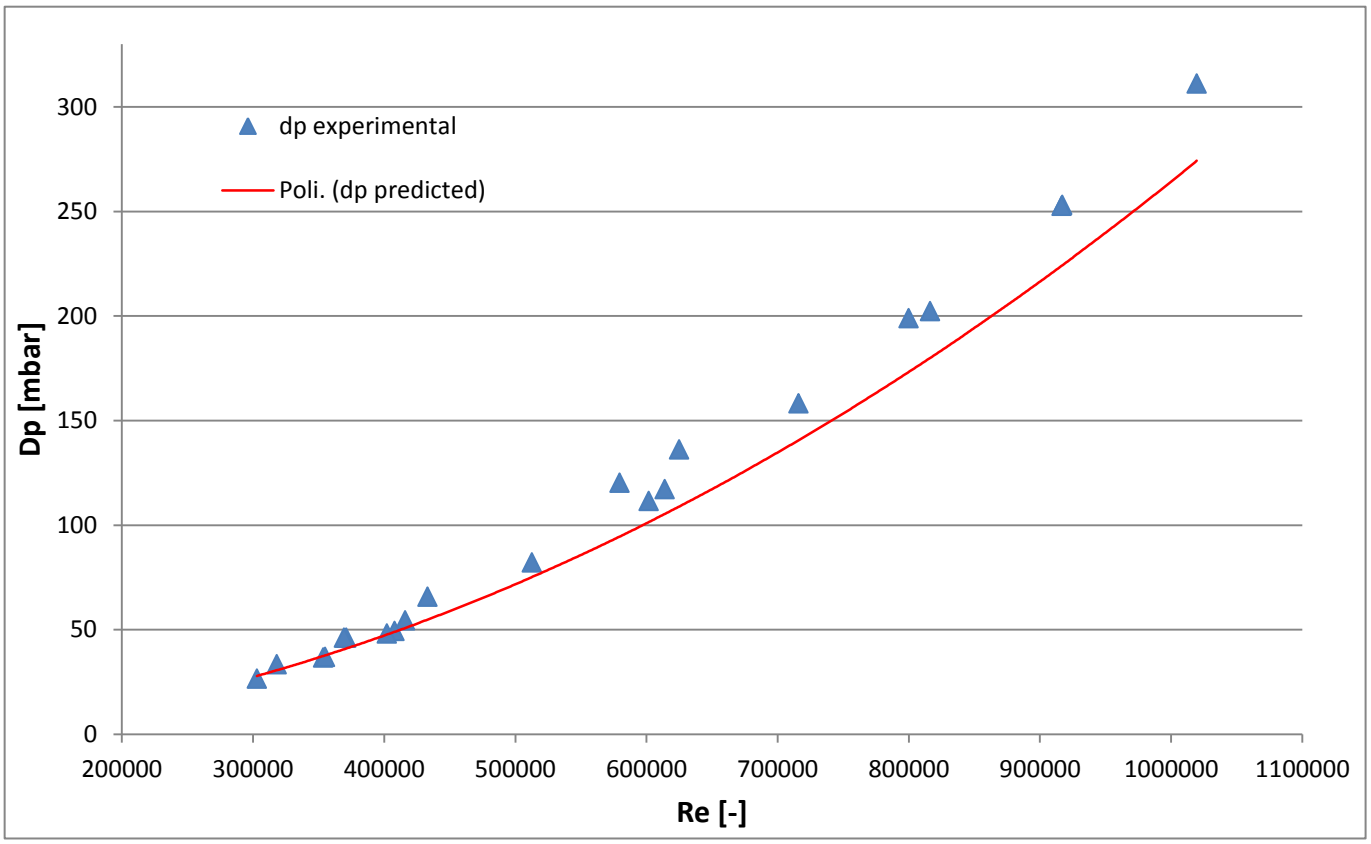

Figure 70: Comparison between experimental and predicted pressure drop [9] in function of the Reynolds number in the gas cooling measurements

6.4 Condensation

The condensation test is led with a costant pressure P_{in}=12 ÷15 bar in the test section, a set temperature t=5°C as inlet of therminol and with different values of working fluid mass flow rate in gas and liquid line, with the aim to obtain different values of the vapour quality at the inlet of the test section.

The parameters that are important to control and to verify, about steady state conditions are:

1. Mass flow rate G [kg/(m^2*s)]
2. Pressure upstream the test rig measured by AP5,6 sensor

For the management of these parameters, the procedure is the same of the previous.

6.4.3 Steady state conditions

With the purpose to verify these conditions one random representative measurement is chosen and analysed.
In this case test with vapour quality x=0,5 is the choice like shown in Figure 60.

Table 18: maximum deviation

Maximum deviation AP	Maximum deviation G
[bar]	G [kg/m^2*s]
0,06	6.49

G and pressure upstream the test rig measured by AP5,6 sensor are in this measurement quite constant.

6.4.4 Reproducibilty

The desire points (in order to reach vapour quality x=0,5 and x= 0,7) are listed in Table 19:

Table 19: Reproducibility tests:

	x [-]	G_wf [kg/(m^2*s)]	P (AP 5,6) [bar]	nr.test [-]
1	0.5	300	15	2
2	0.7	300	12	2

The reproducibility of the results is observed and compared using the coefficient of variation, also known as relative standard deviation, defined as:

$$COV = \frac{Standard\ Deviation}{Mean\ Value} \tag{6.3}$$

The vapour quality of the working fluid shows very good reproducibility (2.657% % for the test nr.1 and 3.365% for the test nr.2) and also the specific mass flow G of the working fluid shows 0.29% for the test nr.1 and 0.04% for the test nr.2. The inlet pressure (and so the temperature because in saturation conditions) of the working fluid has a small deviation (0.278% for the test nr.1 and 0,295% for the test nr.2). Considering the calculated inside heat transfer coefficient with the integral method, the test nr.1 shows an high deviation of 7.532% and the test nr.2 shows a lower deviation of 0.746%.

In light of the above, it is possible to state that the facility do not give strange and very different results between the same desire point and it is possible to state that the facility works with a good reproducibility in condensation.

6.4.5 Heat transfer coefficient

For the comparison between experimental and predicted results, the correlation available is Cavallini et al., 2006 correlation [7].
Since it is the only correlation, a comparisons with the different methods to extract the temperature of propane are done.
In 2-phase conditions, is not possible to calculate the propane duty and the methods are a little bit different compared to the 1-phase cases.

The experimental alpha coefficient considered in the evaluation are:

- Htc 2: local heat transfer coefficient in the second section
- Htc 3: local heat transfer coefficient in the third section
- Htc 2-3: integral heat transfer coefficient between second and third sections

In addition to the propane linear temperature based on the temperature sensor RTD12, there is also another possibility to extract this value of temperature based on the pressure sensor AP5,6 (in saturation, pressure and temperature are represented with the same curve).

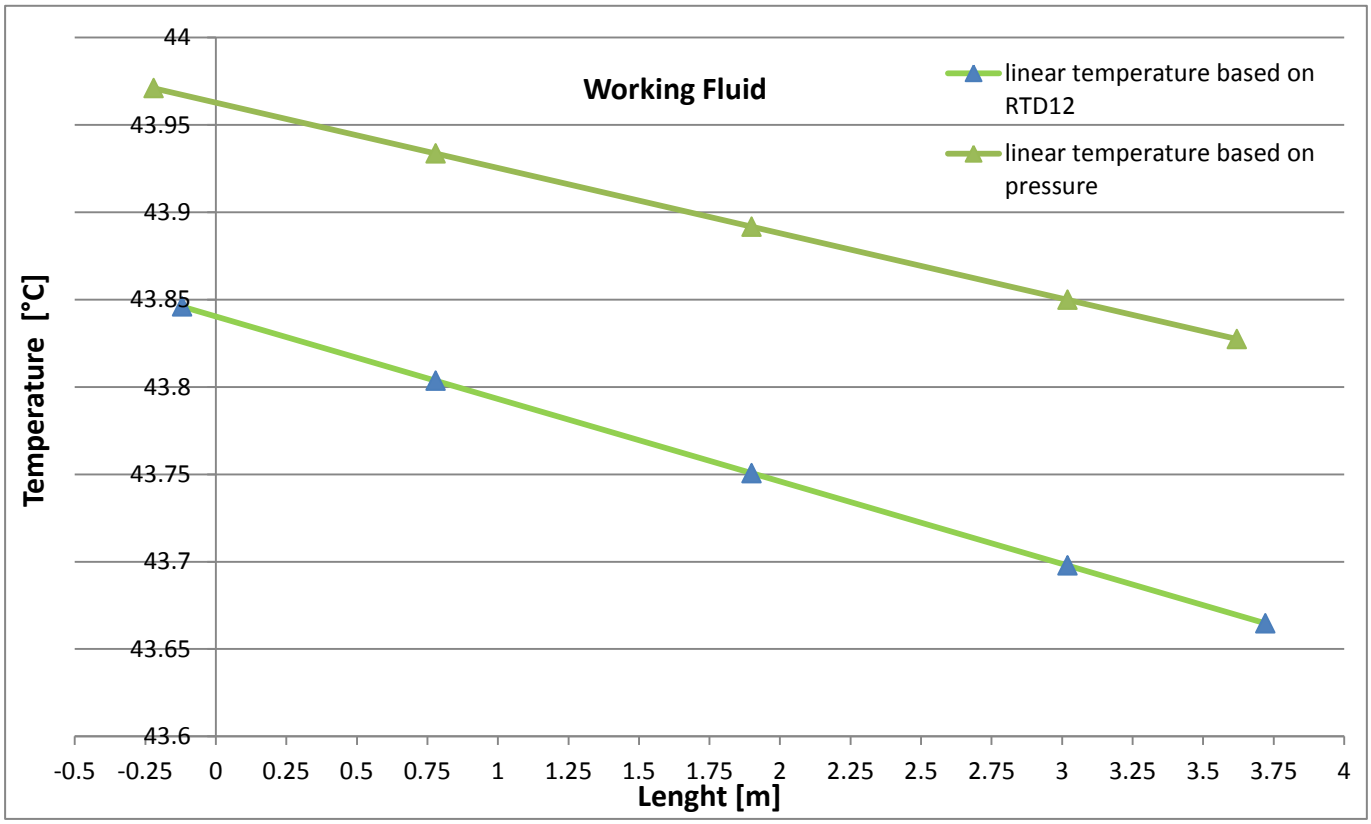

Figure 71: linear propane temperature based on RTD12 and AP5,6

A general overview between working and secondary fluid is represented in Figure 73:

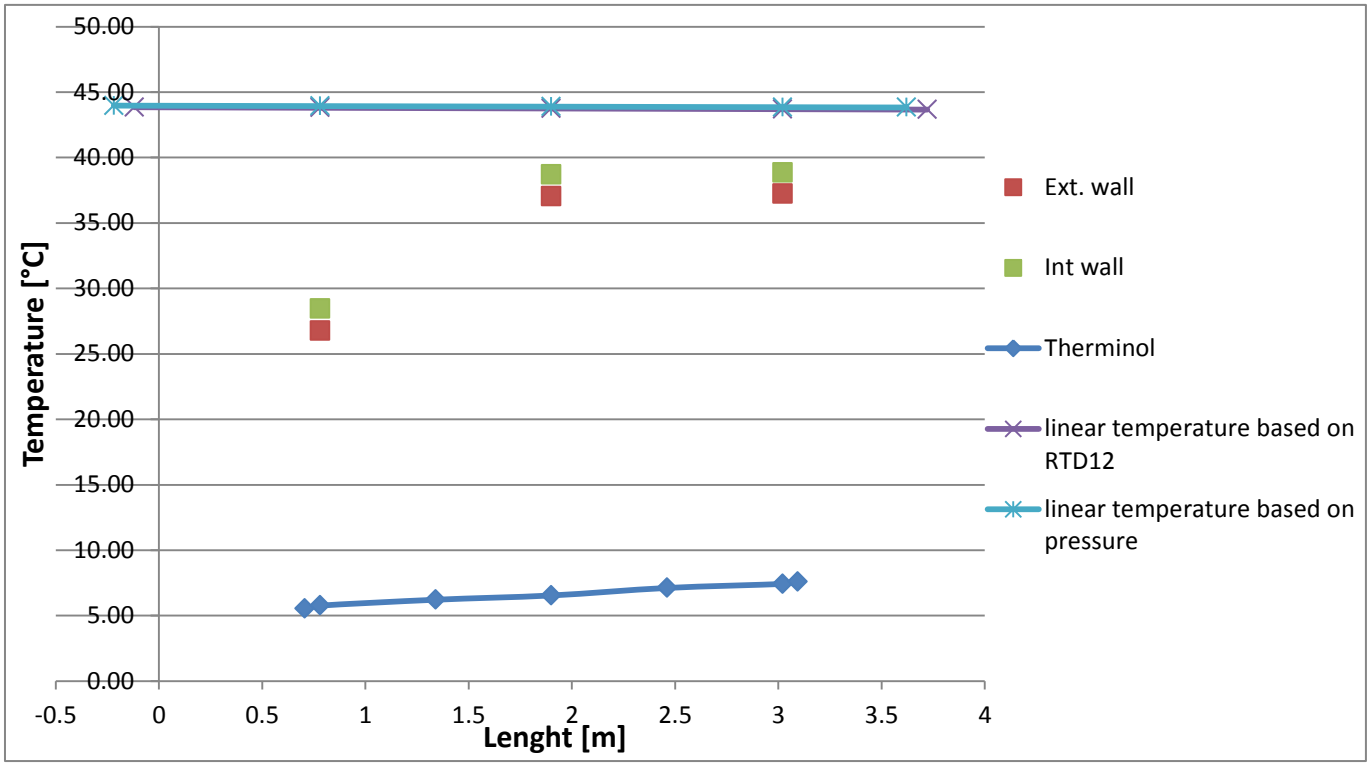

Figure 72: General overview in condensation of the temperature in the test section

Table 20: Comparison between experimental internal htc and predicted Cavallini et al., 2006 correlation [7] in function of the temperature determination of the propane inside the tube

n.measurement=18	Temperature determination of the working fluid					
	linear based on RTD12			linear based on AP5,6		
discrepancy % Cavallini et al. [7]	mean %	peak %	min %	mean %	peak %	min %
htc 2	5.5%	11.5%	0.2%	4.4%	-9.0%	-1.0%
htc 3	13.6%	24.2%	3.4%	7.7%	20.9%	0.7%
htc_2-3	17.0%	30.0%	5.9%	11.0%	27.0%	0.1%

A first overview reveals not huge differences between the two methods but just a higher mean discrepancy in the method based on RTD12 ;analysing the standard deviation of the results shown in Table 21, is possible to confirm this first impression.

Table 21: Standard deviation between the results of the methods involved in the calculation

n.measurement=18	Standard deviation
discrepancy % Cavallini et al. [7]	mean %
htc 2	0.7%
htc 3	4.1%
htc_2-3	4.2%

Considering the Table 21, the linear based on AP5,6 methods seems probably to give the most reliable results with a mean discrepancy of 4,4% for the alpha coefficient in the second section, 7,7% for the third section and 11% for the integral alpha coefficient showing a good reliability.
Is possible also to choose the other method, aware to the fact that the results from the two methods are slightly different of 4% on average.
Taking into account of this advice the next graphs are plotted considering the information from the pressure sensor.

The internal alpha coefficient in the second and third section gives good results like visible in Figure 74 that means that the results from these two sections are very reliable also for the 2-phase case.

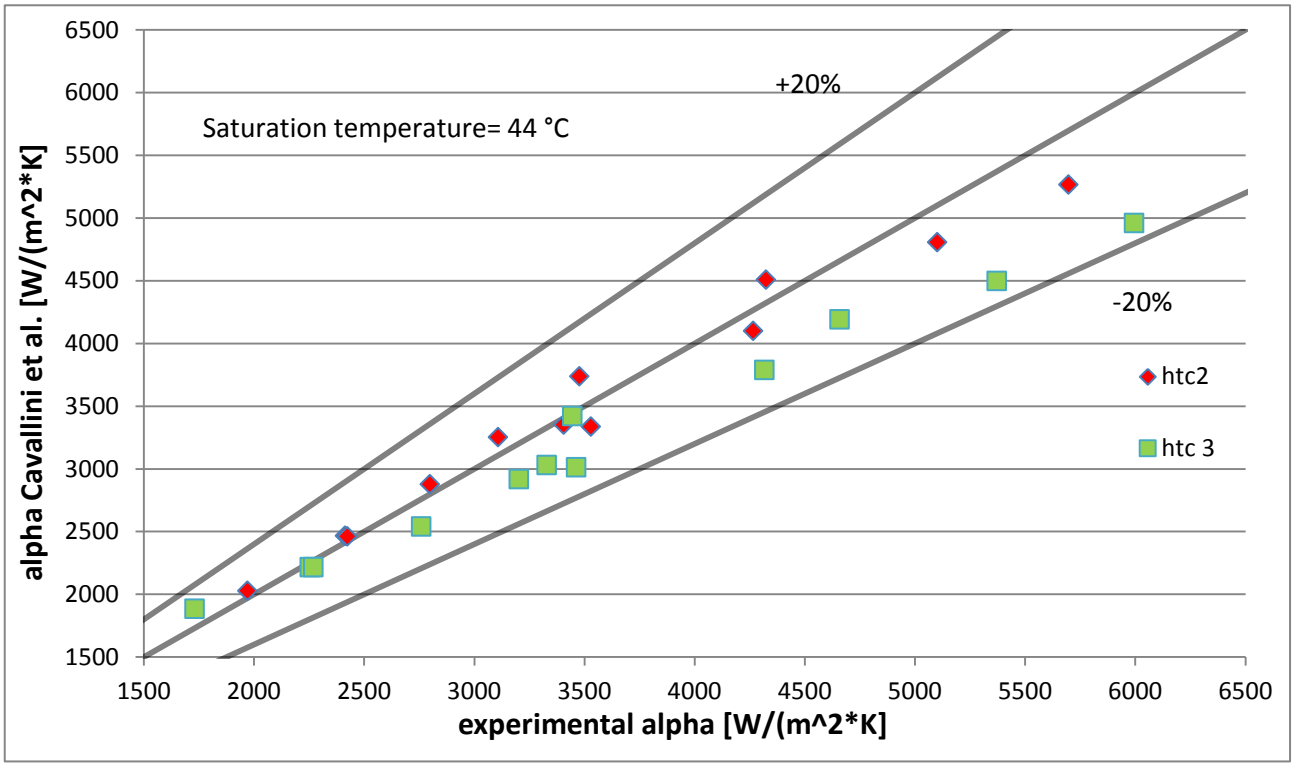

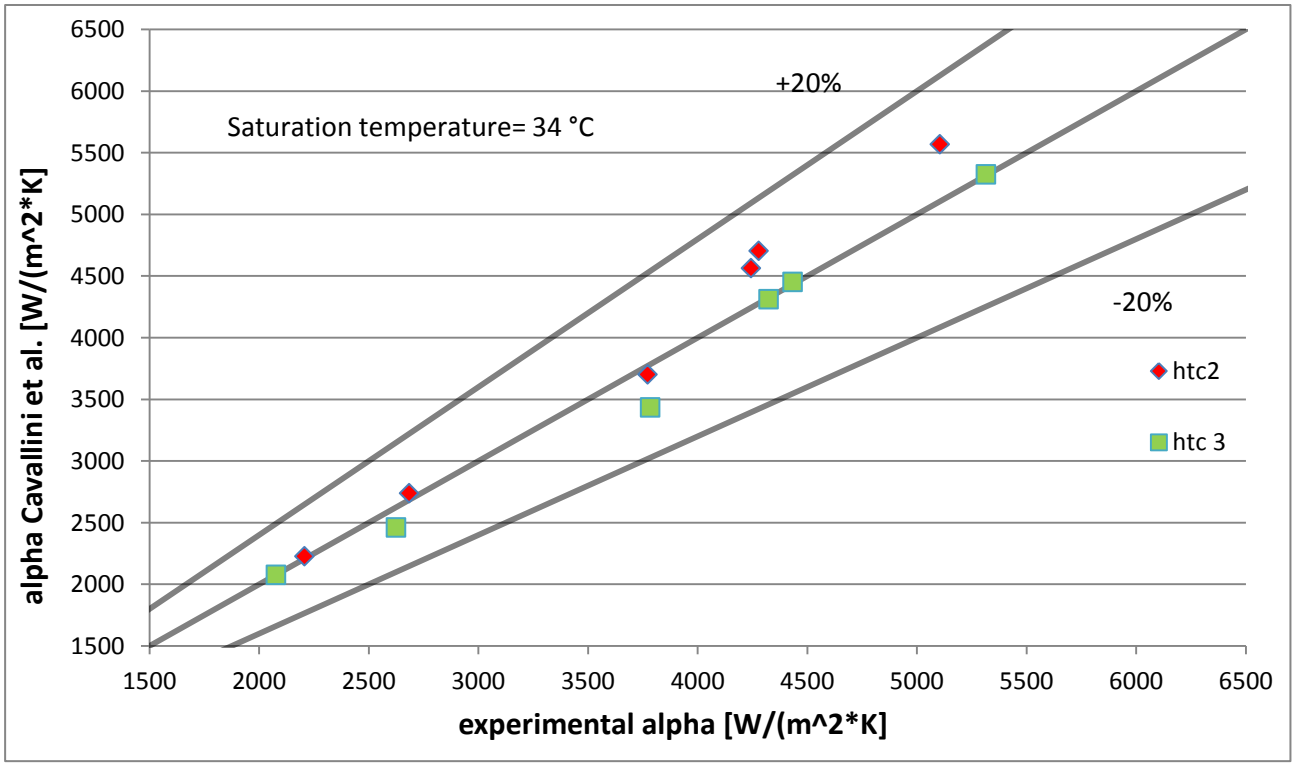

Figure 73: Comparison between Cavallini et al.,2006 correlation [7] and local experimental htc in the second and third section using the propane linear temperature based on AP5,6. All data are reported at approximately Tsat= 44°C in the first graph and Tsat= 34°C in the second.

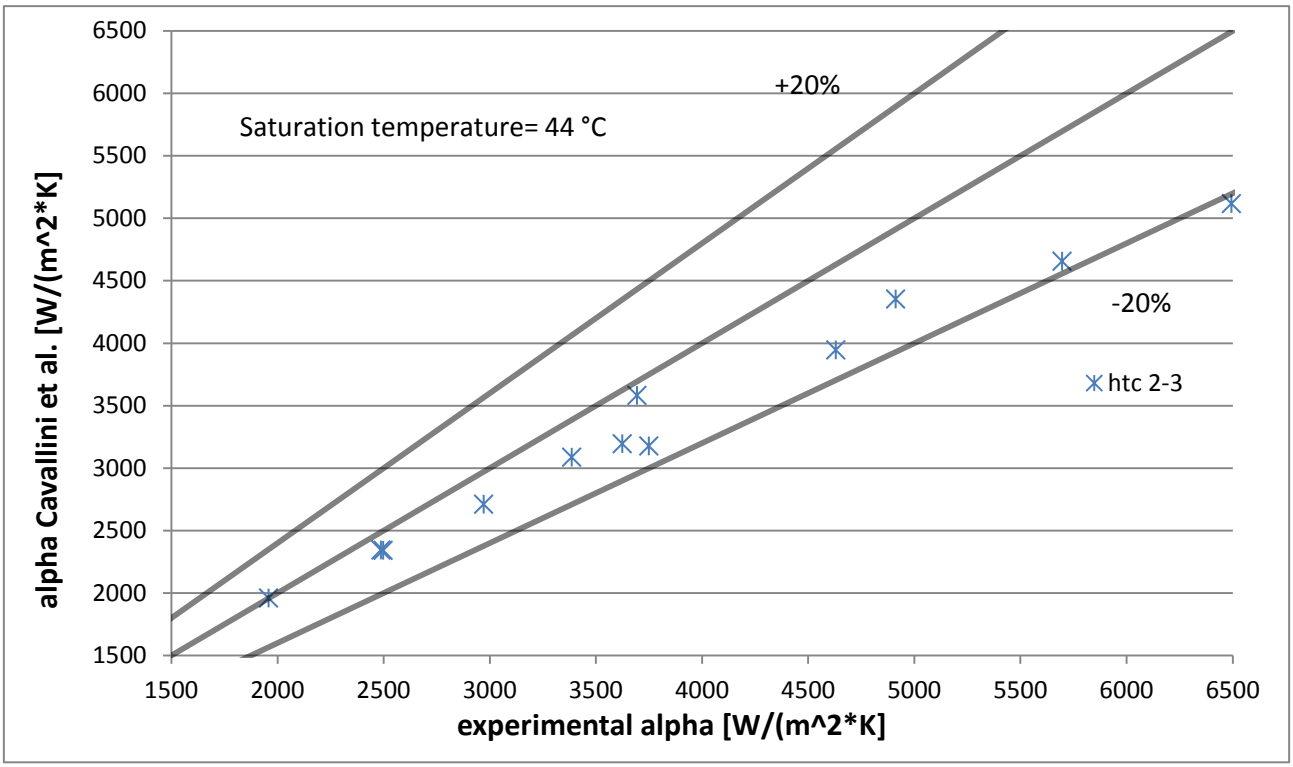

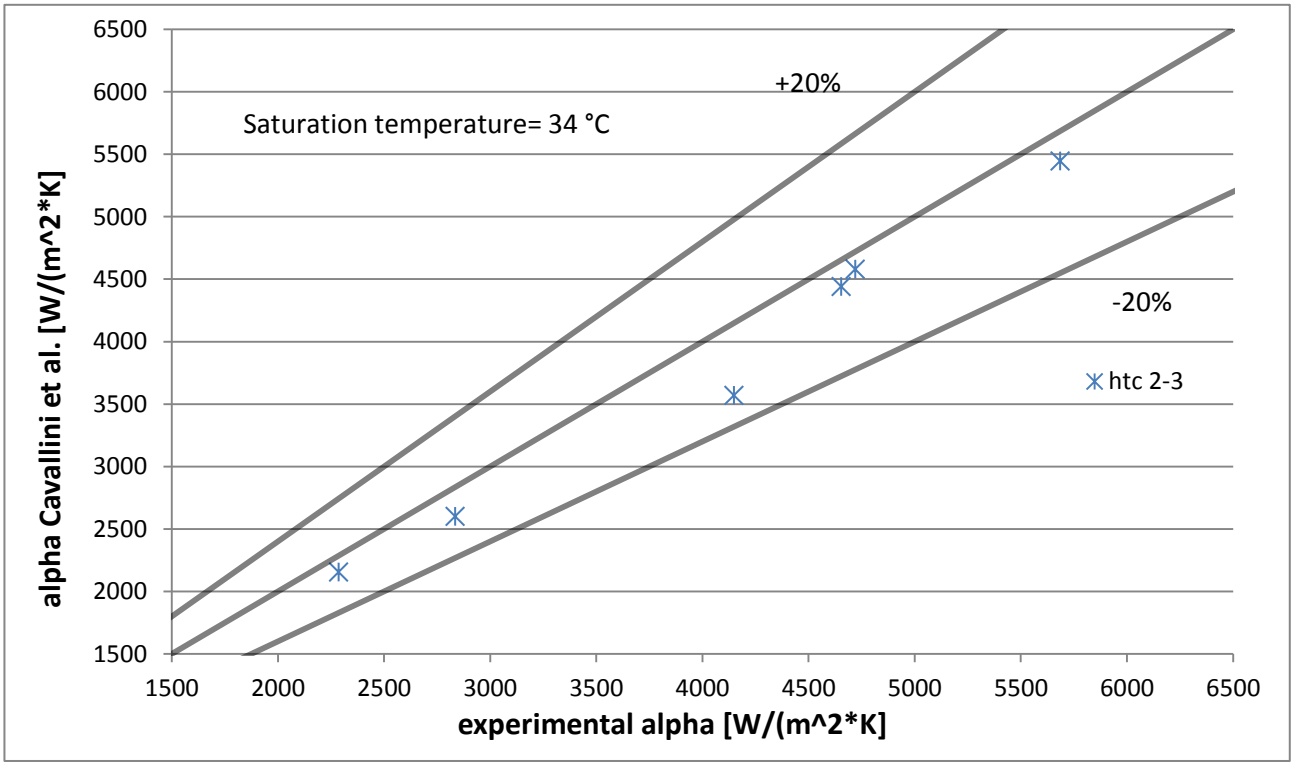

Figure 74: Comparison between Cavallini et al.,2006 correlation [7] and mean experimental htc between second and third section using the propane linear temperature based on AP5,6. All data are reported at approximately Tsat= 44°C in the first graph and Tsat= 34°C in the second.

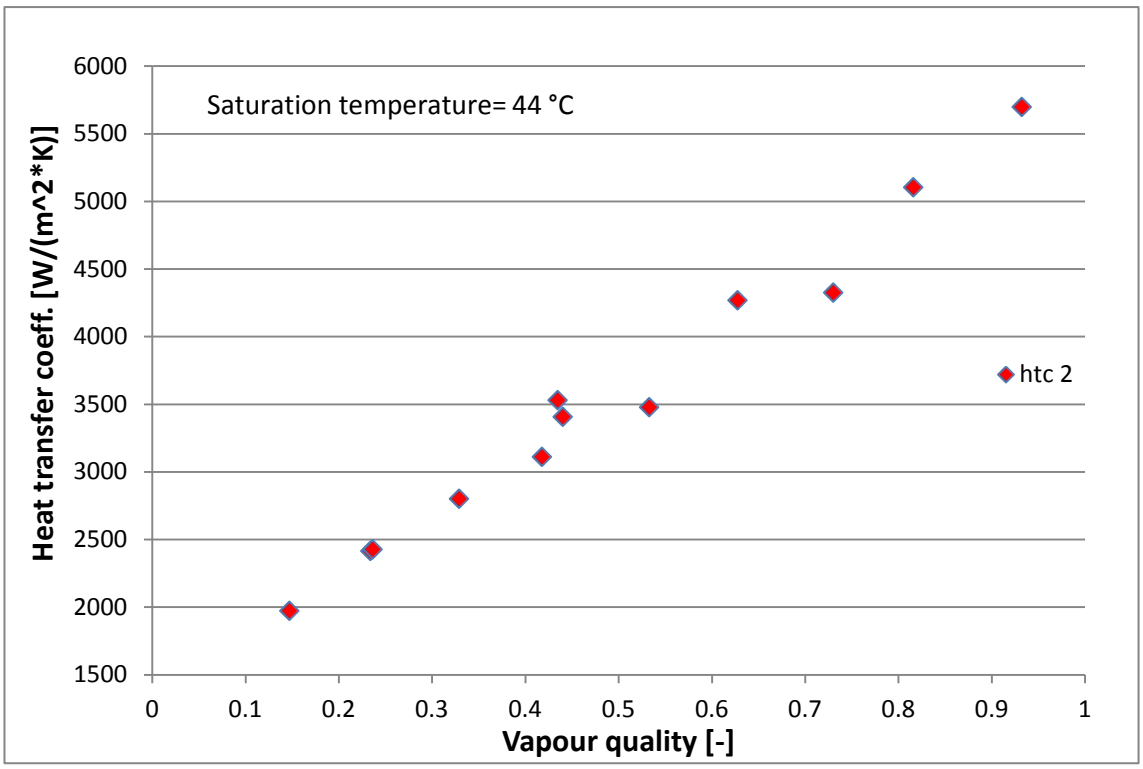

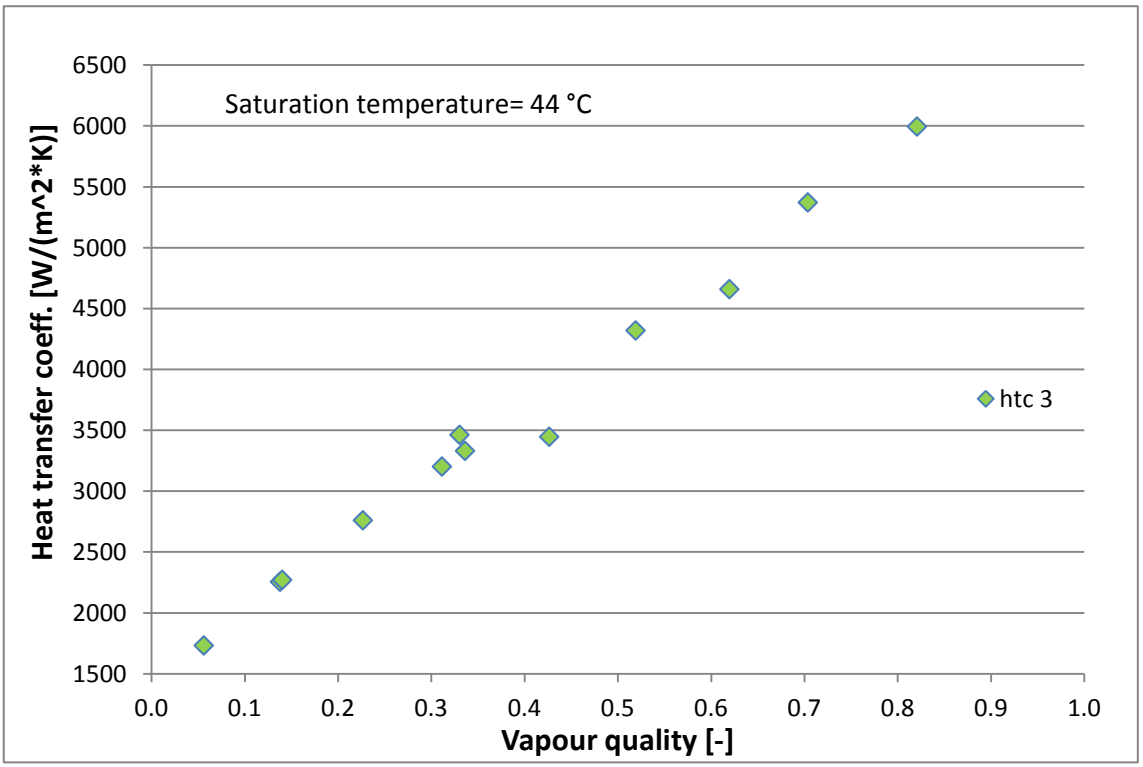

Figure 75: Experimental heat transfer coefficient vs. vapour quality. All data are reported at approximately Tsat.= 44°C

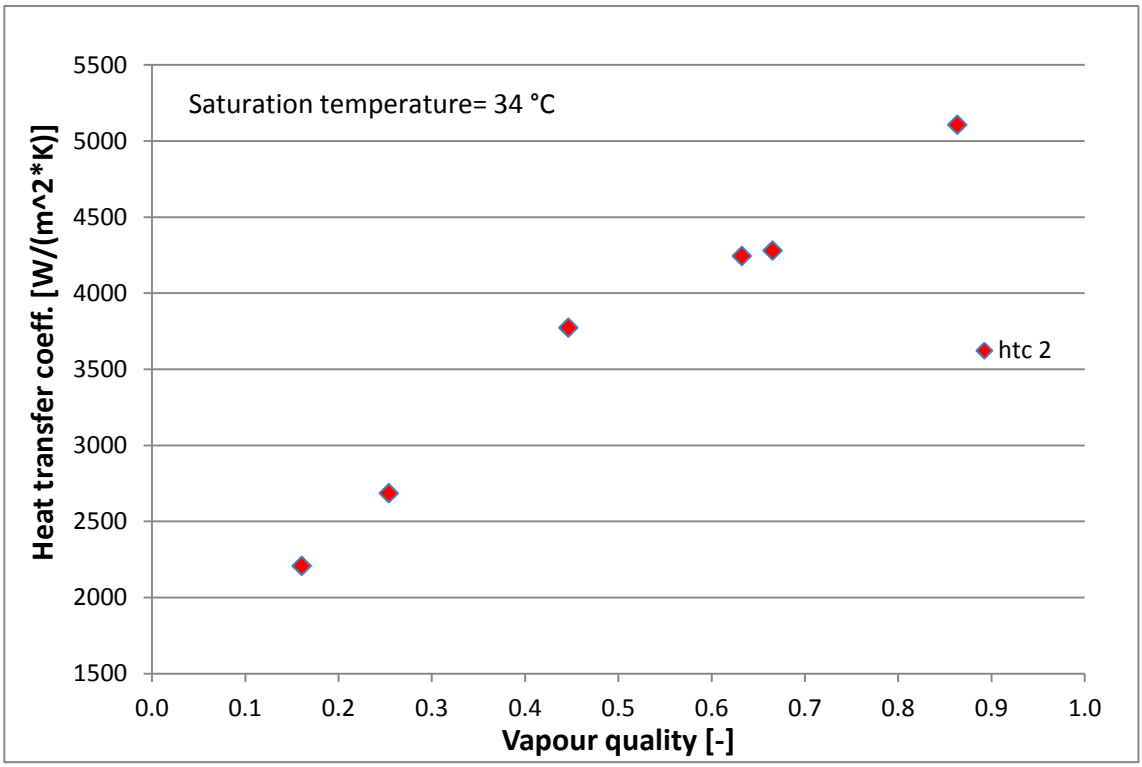

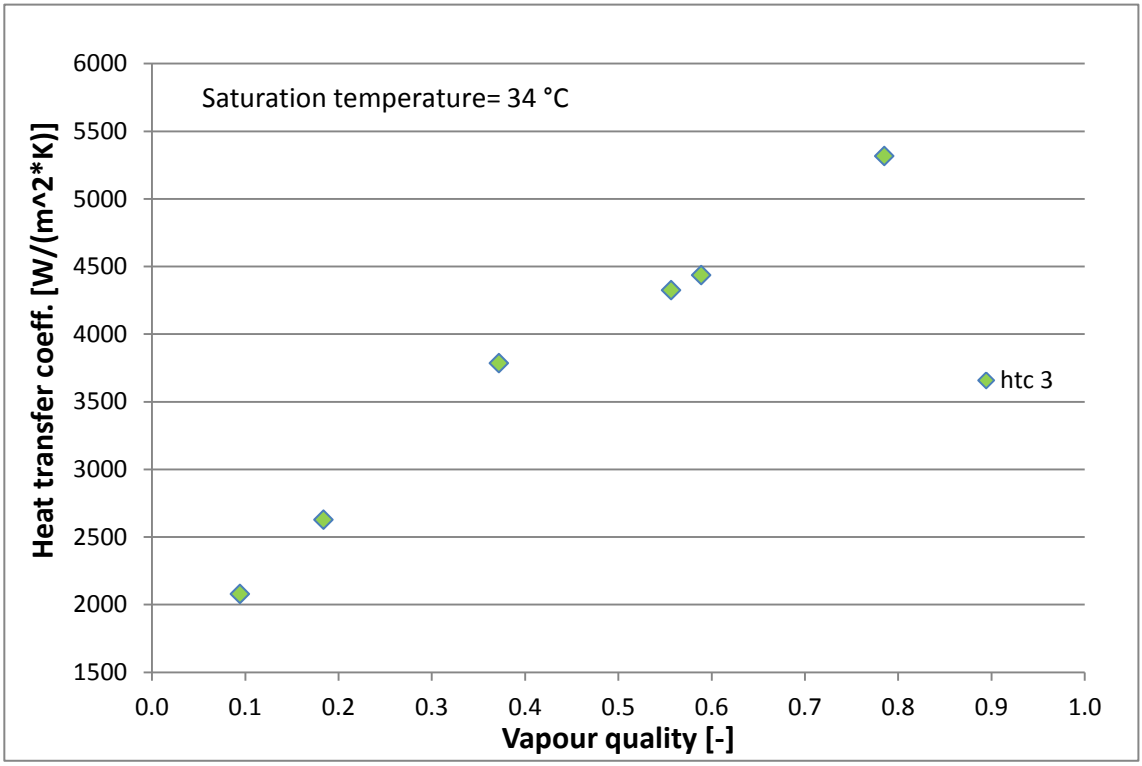

Figure 76: Experimental heat transfer coefficient vs. vapour quality. All data are reported at approximately Tsat.= 34°C

As seen in the Figure 76 and Figure 77, the heat transfer coefficient decrease with the decreasing of the vapour quality.

6.4.3 Flow pattern map

The 2-phase flow patterns inside horizontal tubes that is possible to observe are:

1) Stratified: the liquid flows due to the gravity to the lower part of the tube, completely separated from the gas part, that flows in the upper part of the tube

2) Slug and plug: the liquid flows with the formation of gas cavities.

3) Bubble: in this case, there are the formation of bubble, especially in the upper part of the tube

4) Annular: a liquid film flows along the internal wall of the tube

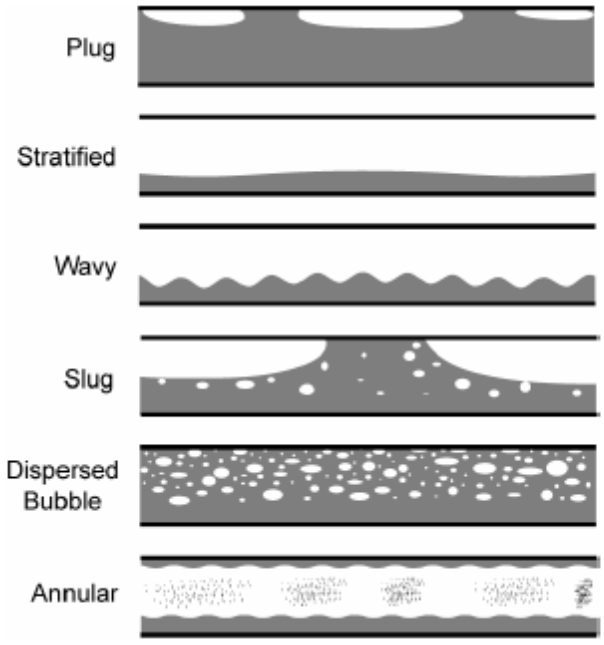

Figure 77: Different configurations for the 2-phase flow [13]

In literature there are some flow pattern map with the aim to extract the type flow of the working fluid.
Here, Breber et al. (1980) map [14] is choose, equipped with the dimensionless parameter descripted in the correlations 3.23 and 3.24.

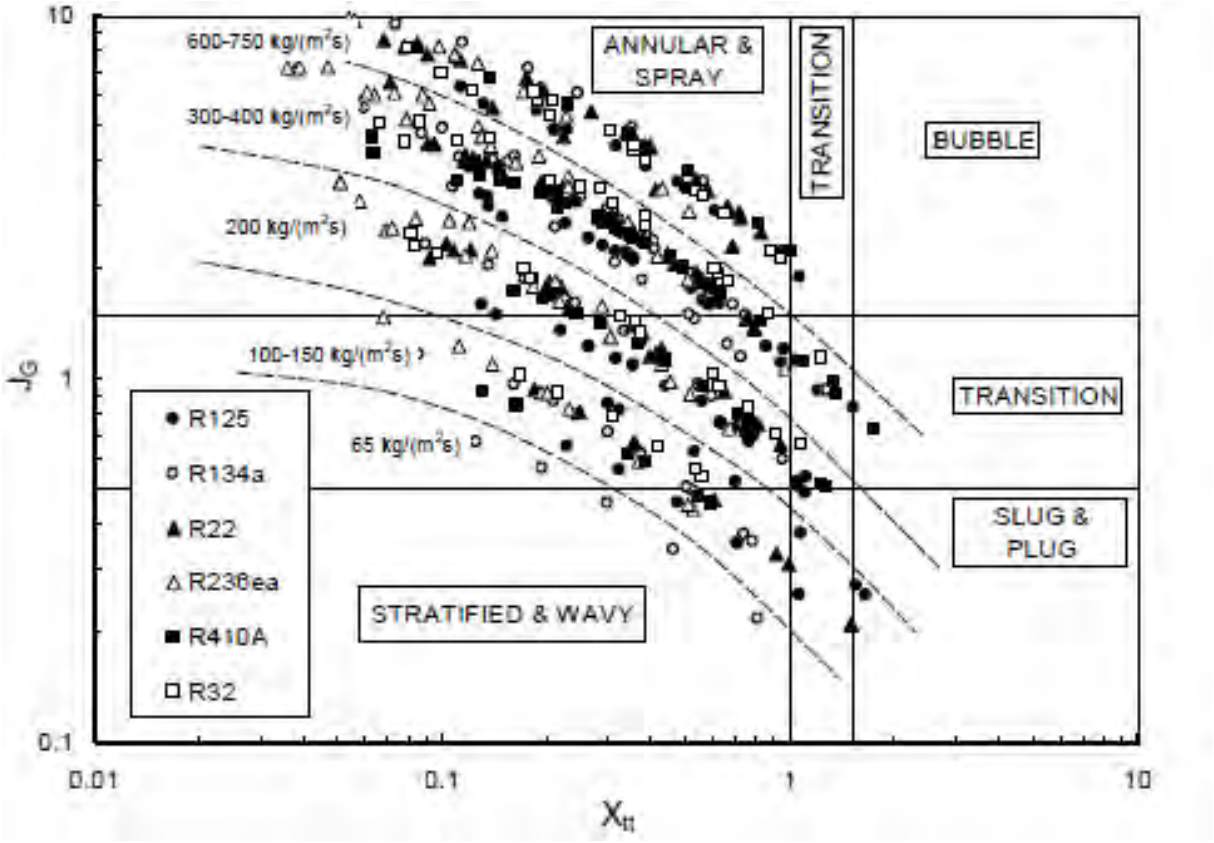

Figure 78: Example of Breber et al. (1980) map [14] for different kind of fluid and specific mass flow rate [15]

In the experimental measurements, with G=300 kg/(m^2s), the same map is reported with the experimental points in function of the Martinelli and dimensionless velocity of the gas parameters [7] (Figure 80).

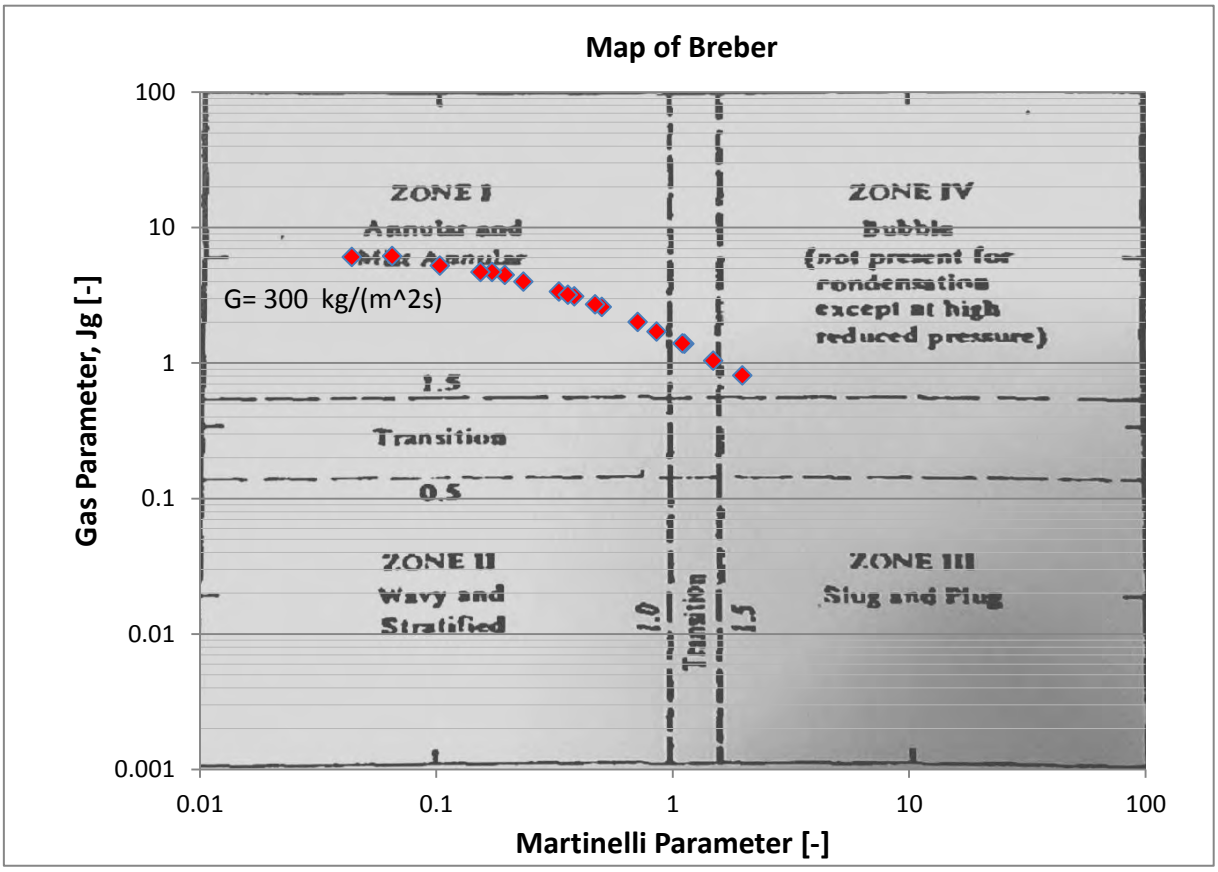

Figure 79: Experimental points represented on the Breber et al. (1980) map [14] in the second section (the graph [2] is implemented in the excel tool)

6.4.4 Pressure drop

Finally the comparison between the Separated flow models for flows inside plain tubes [10] explained in the chapter 3.4.2 and the experimental pressure drops obtained from the differential pressure sensor in the test section is illustrate in this part. The frictional parameter Δp_{frict} is the most influential parameter in the calculation and it is obtained from the two-phase multiplier and in this work the model of Friedel, 1979 [10] is used in order to obtain it.

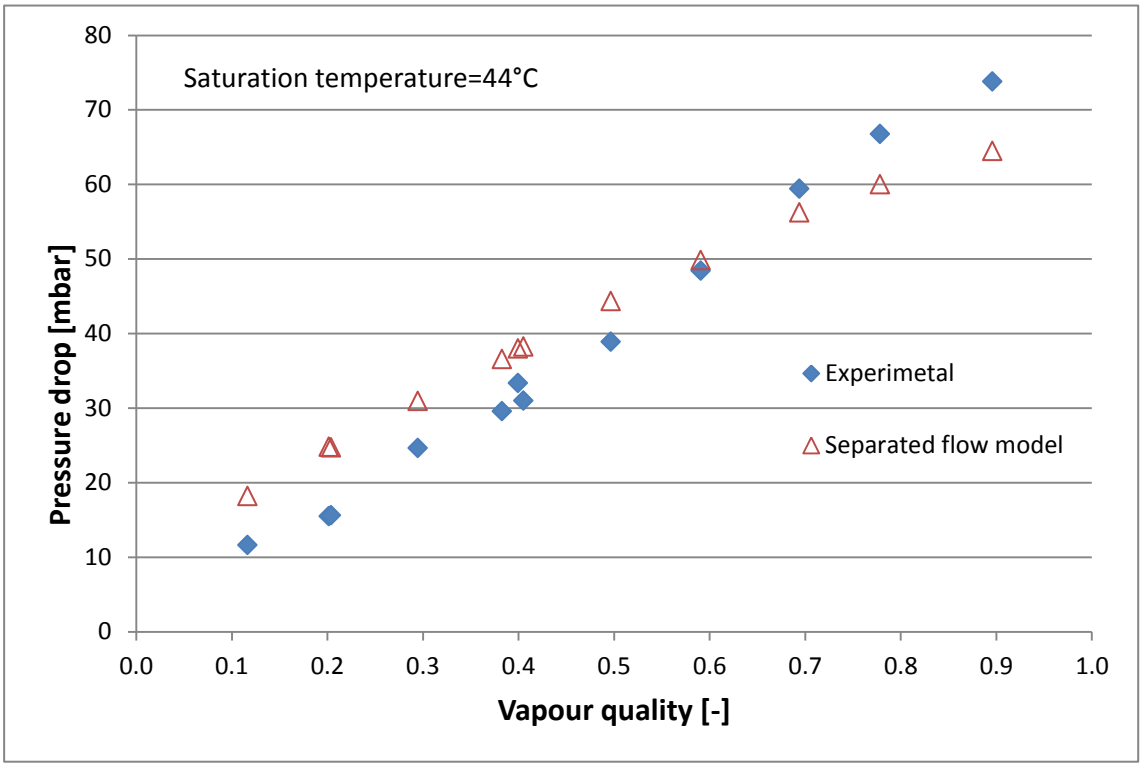

Figure 80: Pressure drops vs. mean value of the vapour quality, with approximately Tsat= 44°C

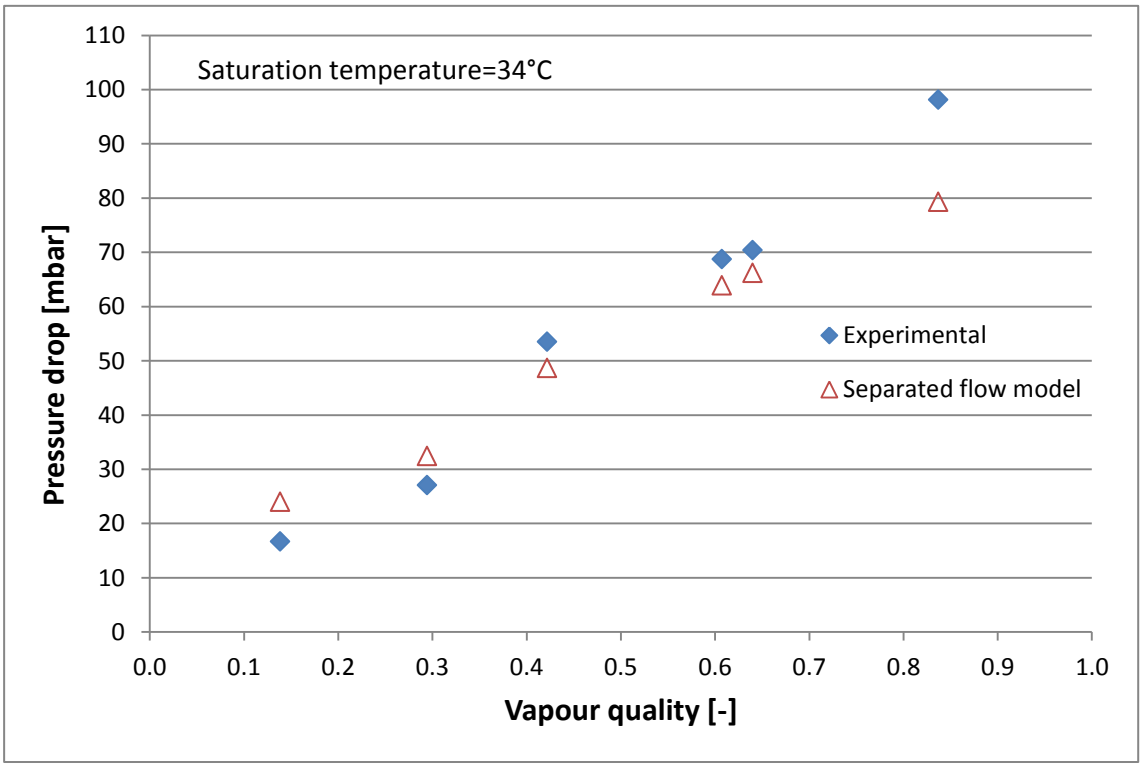

Figure 81: Pressure drops vs. mean value of the vapour quality, with approximately Tsat= 34°C

As seen in the Figure 81 and Figure 82, with a specific value of the vapour quality, the frictional parameter decrease with the increasing of the saturation pressure.
The comparison give a mean discrepancy for the measurements reported in Figure 81 of 19%, a peak of -37,7% and a minimum discrepancy of -2,8% and the measurements reported in Figure 82 of 15,8%, a peak of -30,4% and a minimum discrepancy of 6,4%.
The results shows an higher discrepancy compare to the single phase cases and it is due to the complexity of the 2-phase case and in particular the Friedel model [10] does not take into account the effect of the flow pattern inside the tube.

7 Conclusions

The commissioning of a test section for the experimental investigation of the internal heat transfer and pressure drop in a horizontal tube was carried out.
Several tests meant to prove the functioning of the test rig have been performed using propane as working fluid.
The aim of this work was to have a reliable and fast interface between the measurements extracted from the facility and the data analysing of these information; in order to solve this target, a new excel data sheet is built and adapted for different situations (single phase and 2-phase). This tool is equipped with the latest correlations about the heat transfer coefficient and pressure drops, which were compared with the experimental calculations (included in the data sheet).
About the results, only the first measurement section gives not reliable results about the local heat transfer coefficient due to the sub-pipes supplying the coolant in the shell side that are mounted in the proximity of the first measurement section; the reliable measurement sections are the second and the third and the Petukhov correlation is chosen as reference. Therefore, the test relatives to the pressure drops are in good agreement with the predicted values for the single phase cases with a mean discrepancy of 7,3% for liquid cooling and 8% for gas cooling and quite good results for the condensation case approximately of 17%, higher, due to the Friedel's model that does not take into account about the effect of the flow pattern throughout the tube. At the end of the work it is possible to assert that after several tests, the knowledge about the management of the cycle is clear and the results obtained from the data tool are in good agreement with the theoretical model and with the literature review. Therefore, after the results analysis it is possible to affirm that the data reduction excel file is able to work in the proper, clear and fast way and to offer a good interface in this stage of the project and also for the future steps of the experiment; for this reason, this study will be the base for the results of the new test section. In fact, in light of what has been proved in the tests, the shell side of the heat exchanger needs to be changed and actually a new test section is in the experimental stage; in order to avoid the problem of the inlet effect of the secondary fluid in the test section, the sub-pipes is moved far from the first and third measurement section.

8 References

[1] BP p.l.c.: BP Statistical Review of World Energy – June 2014; London 2014

[2] Hemmerling, K., Luke, A.: Inbetriebnahme einer Versuchsanlage zur Untersuchung des Wärmeübergangs von Kohlenwasserstoffen in horizontalen Rohren; Technische Thermodinamik, Universität Kassel; 2014

[3] Stefano Imprescia: Commissioning of a test section for the measurement of in-tube heat transfer coefficient, Technische Thermodinamik, Universität Kassel; 2014

[4] Jacob Fraden: Handbook of modern sensors; Second Edition

[5] Alberto Cavallini, Davide Del Col, Luca Doretti, Claudio Zilio: I fluidi frigorigeni, processi di sostituzione e nuove frontiere tecnologiche; Area Science Park, 2007

[6] Andrea Luke, Wido Stürwold: Literature review, Condensation of Hydrocarbons inside smooth and enhanced tubes; Technische Thermodinamik, Universität Kassel; 2011

[7] Alberto Cavallini, Davide Del Col, Luca Doretti, Marko Matkovic, Luisa Rossetto, Claudio Zilio: Condensation in Horizontal Smooth Tubes: A New Heat Transfer Model for Heat Exchanger Design; Heat Transfer Engineering, 27(8):31–38, 2006

[8] Bonacina, C.; Cavallini, A.; Mattarolo, L.: Trasmissione del Calore; Cleup Editore; Padova 1992

[9] Verein Deutscher Ingenieure: VDI-Heat Atlas; chapter L1.2, Springer; Berlin 2010

[10] John R. Thome: Engineering Data Book III; Director; Chapter 13: two-phase pressure drop, Laboratory of Heat and Mass Transfer (LTCM) Faculty of Engineering Science and Technology Swiss Federal Institute of Technology Lausanne (EPFL)

[11] Melkamu A. Woldesemayat, Afshin J. Ghajar: Comparison of void fraction correlations for different flow patterns in horizontal and upward inclined pipes; International Journal of Multiphase Flow 33 (2007) 347–370, School of Mechanical and Aerospace Engineering, Oklahoma State University, 2006

[12] Verein Deutscher Ingenieure: VDI-Heat Atlas, Springer; Berlin 2010

[13] A. J. Ghajar: Non-Boiling Heat Transfer in Gas-Liquid Flow in Pipes – a Tutorial; School of Mechanical and Aerospace Engineering Oklahoma State University 2005

[14] G. Breber, J.W. Palen, J. Taborek: Prediction of horizontal tubeside condensation of pure components using flow regime criteria; J. Heat Transfer, 102 (1980), pp. 471–476

[15] A. Cavallini, G. Censia, D. Del Col, L. Doretti, G.A. Longo, L. Rossetto: Experimental investigation on condensation heat transfer and pressure drop of new HFC refrigerants (R134a, R125, R32, R410A, R236ea) in a horizontal smooth tube; International Journal of Refrigeration, Volume 24, Issue 1, January 2001, Pages 73–87

9 Appendix

9.1 Filling amount

Before to start with the measurement, in this paragraph is reported the results about the filling procedure with the propane.

- **Propane bottle number 1:**

  Amount of propane introduced in the test rig: 2,5 kg

- **Propane bottle number 1.1:**

- Bottle weight with cap before to start with the filling: 43.1 kg.
  After filling:
- Bottle weight with cap: 39.6 kg

  Amount of propane introduced in the test rig: 3.5 kg

- **Propane bottle number 2:**

- Bottle weight without cap before to start with the filling: 63.6 kg
- Bottle weight without cap and with heat exchanger before to start with the filling: 91.8 kg
  After filling:
  Bottle weight without cap and with heat exchanger: 73.85 kg

  Amount of propane introduced in the test rig: 17.95 kg

- **Propane bottle number 2.1:**
  Bottle weight without cap before to start with the filling: 63.6 kg
  Bottle weight without cap and with heat exchanger before to start with the filling: 72.2 kg
  After filling:
  Bottle weight without cap and with heat exchanger: 68.2 kg

  Amount of propane introduced in the test rig: 4 kg

- **Propane bottle number 3:**

- Bottle weight with cap before to start with the filling: 65.1 kg.
- Bottle weight without cap before to start with the filling: 64.05 kg
- Bottle weight without cap and with heat exchanger before to start with the filling: 91.5 kg

  After filling:
- Bottle weight with cap: 53.6 kg
- Bottle weight without cap: 52.45 kg

Amount of propane introduced in the test rig: 11.5 kg

- **Propane bottle number 4:**

- Bottle weight with cap before to start with the filling: 65.05 kg.
- Bottle weight without cap before to start with the filling: 63.8 kg
- Bottle weight without cap and with heat exchanger before to start with the filling: 91.3 kg

  After filling:
- Bottle weight with cap: 41.1 kg

Amount of propane introduced in the test rig: 23.95 kg

- **Propane bottle number 5:**

- Bottle weight with cap before to start with the filling: 64.2 kg.
- Bottle weight without cap before to start with the filling: 63.05 kg
- Bottle weight without cap and with heat exchanger before to start with the filling: 90.5 kg

  After filling:
- Bottle weight with cap: 34.8 kg
- Bottle weight without cap: 33.7 kg

Amount of propane introduced in the test rig: 29.4 kg

Total amount of propane in the facility: 92.8 kg

After few test it was reduce to 92,8 kg-14,5 kg = 78,3 kg because the separator was too much full of liquid and this compromised the function of it.

9.2 PID of the entire facility